

**STRUCTURAL HEALTH MONITORING OF COMPOSITE
MATERIALS USING CARBON FIBER SENSORS**

BY
MOHAMMAD ABDULLAH SIDDIQUI

A Thesis Presented to the
DEANSHIP OF GRADUATE STUDIES

KING FAHD UNIVERSITY OF PETROLEUM & MINERALS

DHAHRAN, SAUDI ARABIA

In Partial Fulfillment of the
Requirements for the Degree of

MASTER OF SCIENCE

In
MECHANICAL ENGINEERING

DECEMBER 2016

KING FAHD UNIVERSITY OF PETROLEUM & MINERALS

DHAHRAN- 31216, SAUDI ARABIA

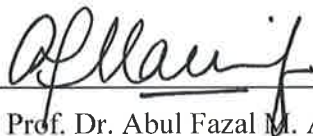
DEANSHIP OF GRADUATE STUDIES

This thesis, written by MOHAMMAD ABDULLAH SIDDIQUI under the direction of his thesis advisor and approved by his thesis committee, has been presented to and accepted by the Dean of Graduate Studies, in partial fulfillment of the requirements for the degree of MASTER OF SCIENCE in MECHANICAL ENGINEERING.



Dr. Salem Bashmal

Thesis Advisor



Prof. Dr. Abul Fazal M. Arif

Member



Dr. Jafar Albinmoussa

Member



Dr. Zuhair M. Asad Gasem

Department Chairman



311511

Dr. Salem A. Zummo

Dean of Graduate Studies





Dedicated to my mother, my father, my sisters and my teachers

ACKNOWLEDGEMENTS

Firstly, I would like to praise Allah, the Almighty, without whom it would have never been possible for me to complete my Masters. Also, my salutations be upon our beloved Prophet (P.B.U.H). I feel blessed and am very grateful to my parents and sisters who had always supported me and have been a source of comfort with their continuous appraisal and unwavering encouragement throughout my life.

I am much obliged to my advisor and my mentor Dr. Bashmal Salem for his unrelenting support and guidance. I highly regard him for his patience with me and for coping with my shortcomings. My sincere thanks to Prof. Dr. Abul Fazal M. Arif who kept me going persistently. I also highly appreciate Dr. Jafar Albinmoussa for giving me useful help and support regarding my thesis.

I would also like to thank everyone else who supported me with their help and advice throughout my study. Dr. Khurram Qureshi and Dr. Munir for being there whenever I needed help. Mr. Raashid Muhammad in Physics department for his support in the experimental setup. I am especially grateful and would like to express my appreciation to all the professors and technical staff in Mechanical Engineering department.

In the end, I would like to thank all my friends for being there for me through thick and thin. Thank you for the good memories and moral support during my study. I would like to especially thank Ahsan Javed, Mohsin Javed, Shahzada Pamir Aly and Taha Nasir for

all the wonderful time we had here and beyond and for make my stay enjoyable. This thesis would not have been possible if not for the selfless invaluable help and advice by Dr. Usama Siddiqui. Special thanks to the Stress analysis lab members: Abu Bakr Abba, Hafiz Kabir and Haris for the useful critique and the endless memorable days and nights spent. A big thank you also to Yasir Abdullah Siddiqui, Umair Yaqoub, Sajid Anwar and others.

TABLE OF CONTENTS

ACKNOWLEDGEMENTS	iv
LIST OF TABLES	ix
LIST OF FIGURES	x
THESIS ABSTRACT (ENGLISH)	xiv
THESIS ABSTRACT (ARABIC).....	xvi
CHAPTER 1 INTRODUCTION.....	1
1.1 Composite materials.....	2
1.2 Damages in composite materials	4
1.3 Structural Health Monitoring.....	7
1.4 Research Objectives of Current Work	11
1.5 Organization of the Thesis	12
CHAPTER 2 LITERATURE REVIEW.....	15
2.1 Related work on structural health monitoring.....	15
2.2 Carbon Fiber Sensors	18
CHAPTER 3 EXPERIMENTAL STUDY.....	27
3.1 Preparation of Carbon Fiber Sensor.....	28
3.2 Tensile test	32
3.3 Low Velocity Impact Test	36
3.4 Conclusion	42

CHAPTER 4 NUMERICAL MODELING	43
4.1 Silicon piezoresistive sensors	44
4.1.1 Methodology	44
4.1.2 Results and discussion	49
4.2 Computational model of carbon fiber sensor	56
4.2.1 Idealization and Assumptions	57
4.2.2 Geometric Model	57
4.2.3 Material Modeling	59
4.2.4 Loads and Boundary Conditions.....	60
CHAPTER 5 RESULTS AND DISCUSSION.....	61
5.1 Tensile tests.....	61
5.1.1 Effect of diameter on change in resistance	65
5.1.2 Effect of length of sensor on dR/R_0	71
5.1.3 Effect of Epoxy treatment on carbon fiber sensor	74
5.2 Impact test.....	74
5.3 Computational Results	81
5.3.1 Computational model of carbon fiber sensor.....	81
5.3.2 Model Validation using different piezoresistive coefficients	86
5.3.3 Application of carbon fiber sensor model.....	91
5. 4 Conclusion	95

CHAPTER 6 CONCLUSIONS AND RECOMMENDATIONS	97
6.1 Conclusions	97
6.2 Recommendations	99
REFERENCES.....	101
VITAE.....	108

LIST OF TABLES

Table 3-1 Preparation process of Carbon fiber sensor	31
Table 4-1 Material properties of Si sensor.....	48
Table 5-1 Max deflection and sensor's output	80
Table 5-2 Comparison of CFS and Si piezoresistive coefficients	84
Table 5-3 Piezoresistive coefficients of 1K, 3K, 6K and 12 K carbon fiber sensors.	86

LIST OF FIGURES

Figure 1-1 Delamination © Kolossos	5
Figure 1-2 Micro crack [4].....	5
Figure 2-1 Piezoelectric sensor	17
Figure 2-2 Equivalent circuit model for CFRPs in the tensile strain state [32].....	20
Figure 2-3 Discrepancy between the two-probe method and the four-probe method [34].	21
Figure 2-4 Carbon fiber sensor [43].....	22
Figure 2-5 U shaped carbon fiber sensors [44]	23
Figure 2-6 Fiber contact separation model to explain piezoresistivity in transverse direction[41].....	25
Figure 3-1 Carbon Fiber with springs on metallic bed.	29
Figure 3-2 Electrical connection of the carbon fiber sensor	30
Figure 3-3 INSTRON 3367 machine.....	33
Figure 3-4 UT71E Multimeter.	33
Figure 3-5 Acrylic grips.....	34
Figure 3-6 Carbon fiber sensor with grips in a tensile machine.	35
Figure 3-7 Machine used for low velocity impact tests: INSTRON 9250G.....	38
Figure 3-8 Dimensions of the impact test specimen	39
Figure 3-9 Good locations of the sensor	40
Figure 3-10 Composite plate with embedded sensor	41

Figure 4-1 2D model of the piezoresistive sensors on a plate.	45
Figure 4-2 3D Model of embedded microcantilever design.	46
Figure 4-3 Sensors placed on the surface of the microbeam	47
Figure 4-4 Displacement vector.....	49
Figure 4-5 Von Mises stress distribution.	50
Figure 4-6 Von Mises stresses and displacement of microcantilever with varying applied loads.	50
Figure 4-7 Comparison of analytical and computational results	51
Figure 4-8 Effect of thickness on von Mises stresses and deflection	52
Figure 4-9 Effect of thickness on voltage	52
Figure 4-10 Effect of length on Von Mises Stress and deflection.....	53
Figure 4-11 Effect of length on voltage.....	53
Figure 4-12 Effect of Width on Von Mises Stress and Displacement.....	54
Figure 4-13 Effect of width on output voltage.....	55
Figure 4-14 Effect of length of piezoresistors on Output Voltage.....	55
Figure 4-15 Geometric model of the sensor	58
Figure 5-1 Strain-Stress Plot of 1K with and without coating.....	62
Figure 5-2 Strain-Stress Plot of 3K with and without coating.....	62
Figure 5-3 Strain-Stress Plot of 6K with and without coating.....	63
Figure 5-4 Strain-Stress Plot of 12K with and without coating.....	63
Figure 5-5 Stress-Strain curves of all fibers with coating.....	64
Figure 5-6 Variation of load and change in resistance vs extension of 1K fiber.....	65

Figure 5-7 Comparison between analytical and experimental values of 1K	66
Figure 5-8 Plot of load and change in resistance vs extension of 3K fiber.	67
Figure 5-9 Comparison between analytical and experimental values of 3K	67
Figure 5-10 Variation of load and change in resistance vs extension of 6K fiber.....	68
Figure 5-11 Plot of load and relative change in resistance vs extension of 12K fibers....	68
Figure 5-12 Extension vs $\Delta R/R_o$ of all the fibers.....	69
Figure 5-13 Comparison of analytical and experimental results of 6K.....	71
Figure 5-14 Effect of length on $\Delta R/R_o$ of 1K samples.....	72
Figure 5-15 Effect of length on dR/R_o of 3K carbon fiber.....	73
Figure 5-16 Effect of length on dR/R_o of 6K carbon fiber sensor	73
Figure 5-17 Effect of epoxy treatment on carbon fiber sensor.	74
Figure 5-18 Deflection and energy curve for 5 J impact. Black curve: deflection. Red curve: energy.....	76
Figure 5-19 Plot of deflection vs time vs $\Delta R/R_o$ %	77
Figure 5-20 Deflection plots of all five impact tests.....	78
Figure 5-21 Carbon fiber sensor output for five different impact energies	79
Figure 5-22 impactor damage mark when using impact energy of 5J.....	80
Figure 5-23 Dent left from the strike using impact energy of 10J.....	81
Figure 5-24 Displacement Contours on the carbon fiber sensor.....	82
Figure 5-25 Left: Von Mises Stress. Right: Strain distribution.	82
Figure 5-26 Comparison of experiment and COMSOL results	83
Figure 5-27 Model validation of computational and experimental data for 1K 8cm	84

Figure 5-28 Model validation of computational and experimental data for 1K 4cm	85
Figure 5-29 Model validation using 1K parameters for (a) 1K Model, (b) 3K Model, (c) 6K Model, (d) 12K Model	87
Figure 5-30 Model Validation using 3K parameters for (a) 1K Model, (b) 3K Model, (c) 6K Model, (d) 12K Model	88
Figure 5-31 Model Validation using 6K parameters for (a) 1K Model, (b) 3K Model, (c) 6K Model, (d) 12K Model	89
Figure 5-32 Model Validation using 12K parameters for(a) 1K Model, (b) 3K Model, (c) 6K Model, (d) 12K Model	90
Figure 5-33 Geometric model of the cantilever and carbon fiber sensor	91
Figure 5-34 Displacement contours of the cantilever beam	92
Figure 5-35 Von Mises Stresses on the cantilever beam	93
Figure 5-36 Strain distribution on the cantilever beam	93
Figure 5-37 Comparison of COMSOL and analytical results of deflection of beam	94
Figure 5-38 Output of the carbon fiber sensor against applied force and deflection.....	95

ABSTRACT (ENGLISH)

NAME: Mohammad Abdullah Siddiqui
TITLE: Structural Health Monitoring of Composite Materials using Carbon Fiber Sensors
MAJOR FIELD: MECHANICAL ENGINEERING
DATE OF DEGREE: DECEMBER 2016

Structural health monitoring is being used in different engineering applications due to the economic benefits and the safety assurance that it may bring. It is crucial to the assessment of damages in structures by the use of any sensing elements. Since the method solely lies on detecting damage, various damage detection techniques are used, with each technique varying with the application. In recent years, composite materials have had an increased growth as an alternative to current materials like metallic alloys. This is due to their very high strength and stiffness as well as low weight and easy shaping. Moreover, carbon fibers also display linear piezoresistive properties, permitting their use as strain sensors similar to standard strain gauges. This allows them to be used as a sensor for various applications such as damage detection, stress analysis and monitoring of manufacturing processes and quality.

In this research, damage detection application of carbon fiber as a sensor is studied. The focus of this research is on structural health monitoring of composite structures using carbon fiber sensors. A multi-physics computational model is developed for simulation of effect of damage against composite structures. Carbon fiber sensors are developed to

perform reliable strain measurements. Both experimental and computational studies are carried out in order to understand the piezoresistivity of the carbon fiber sensors. A parametric study is conducted using experiments to find the effect of different parameters on the output of the carbon and to find an optimum set of parameters for the sensor. It was found that 3K carbon fibers had the largest change in resistance in low strain levels. Moreover, of the three different lengths used, the shortest lengths of carbon fibers were found to have relatively greater change in resistance. It was also found that changing the epoxy mixture ratio had no effect on the tensile behavior of the sensor. An impact test is conducted to evaluate the performance of carbon fibers when embedded in a composite plate subjected to low velocity impact. Five different impact energies were used to impact the composite plate and the sensor could follow the curve of deflection of the plate. The results show that carbon fiber sensor's output can successfully follow the deflection of the plate. 10 J of impact energy could damage the composite plates and was detected by the sensor. The value of the sensor at the damage can be set as a safety factor limit for damage detection. This study will allow researchers to predict the behavior of the carbon fiber sensor in real life and it will serve as a basis for designing a carbon fiber to be used in different applications as a sensor.

ABSTRACT (ARABIC)

ملخص الرسالة

الاسم: محمد عبد الله صديقي

عنوان الرسالة: مراقبة السلامة الهيكلية للمواد المركبة باستخدام الحساسات ذات الألياف الكربونية

التخصص: الهندسة الميكانيكية

تأريخ التخرج: 1438 هـ - (ديسمبر 2016 م)

تستخدم المراقبة الصحية الهيكلية في التطبيقات الهندسية المختلفة بسبب الفوائد الاقتصادية وضمان السلامة التي قد تجلبها. ومن الأهمية بمكان تقييم الأضرار في الهياكل باستخدام أي عناصر استشعار. وبما أن الأسلوب يكمن فقط في الكشف عن الضرر، تستخدم تقنيات مختلفة للكشف عن الضرر. وفي السنوات الأخيرة، شهدت المواد المركبة نموا متزايدا كبديل للمواد الحالية مثل السبائك المعدنية. ويرجع ذلك إلى قوة عالية جدا وصلابة وكذلك انخفاض الوزن وسهولة التشكيل. وعلاوة على ذلك، لدى ألياف الكربون خصائص مقاومة كهربائية خطية، مما يسمح باستخدامها كأجهزة استشعار لتكون مماثلة لأجهزة القياس القياسية. وهذا يسمح باستخدامها كمستشعر لمختلف التطبيقات مثل كشف الضرر، وتحليل الإجهاد ورصد عمليات التصنيع والجودة.

يهدف هذا البحث إلى دراسة عملية مراقبة سلامة الهياكل المكونة من مواد مركبة، وهذه العملية تتم باستخدام حساسات مكونة من ألياف الكربون. تم تطوير برنامج محاكاة تحسيسي لحساب الأضرار الناتجة في الهياكل المصنوعة من المواد المركبة. تم تطوير و تصنيع حساسات الياف الكربون. تم تطبيق بعض التجارب وإجراء بعض الدراسات التحسينية لفهم خاصية المقاومة الكهروميكانيكية للحساسات. تم إجراء دراسة تجريبية لفهم المتغيرات الخاصة بالحساسات بغرض إيجاد القيم المثلى للمتغيرات التي يجب إستخدامها في عملية مراقبة سلامة الهياكل. تم إجراء دراسة تجريبية لفهم الضرر الناتج من أحمال الصدم عندما يتم وضع الحساسات علي داخل الواح مستطيلة من مواد مركبة، وقد أثبتت نتائج هذه الدراسة أن الحساسات قادرة علي الكشف عن الانفصال والتشوه الناتج من أحمال الصدم. هذه الدراسة ستمكن الباحثين من توقع سلوك حساسات الياف الكربون، وكذلك تمثل الأساس لتصميم مثل الحساسات في المستقبل وإستخدامها في مختلف الأغراض.

CHAPTER 1

INTRODUCTION

Composite materials have several advantages over traditional materials that are commonly used in industry such as steel or aluminum. High strength to weight ratio, fatigue resistance and thermal conductivity are some of the favorable properties of composite materials. These advantages explain why different leading industry sectors are investing in composites in various applications such as pipes, aircrafts, tools, construction material, etc.

However, despite these advantages, composite materials are far from perfect. They suffer from major setbacks when it comes to specific types of damages. These composite materials are easily susceptible to damages that can cause variety of problems such as breakage of fiber matrix, cracking and delamination. Therefore, continued research is devoted to monitor these damages and detect them before they propagate further and cause unreparable damage. A great part of the research is aimed at investigating the applicability of the sensors that are used in the industry to monitor damages. Strain gages, fiber optic sensors, piezoelectric sensors and microelectromechanical systems(MEMS) are among

these sensors. The carbon fiber sensor (CFS), which has been recently attracting research interest, shows good promise in structural health monitoring. This sensor is made from carbon fiber material and uses its piezoresistive property to sense changes of strains in a structure which are caused by damages. Carbon fiber based materials possess excellent mechanical properties and show linear piezoresistive behavior which make them good candidate material for strain measurements. The sensor also offers some other advantages that are of interest such as material conformity and linear piezoresistivity.

Furthermore, limited research has been conducted on the sensing ability in CFs which shows the need for further research to understand and improve the performance of the CF sensor. This study will focus on understanding the behavior of carbon fiber sensor and investigating its mechanical and piezoresistive features. Performance of carbon fibers will be tested under different load conditions, hence, to gain better understanding towards the development of a reliable sensor that can be used to monitor damages in composite structures.

1.1 Composite materials

A composite material is a combination of two or more distinct materials at macroscopic level. Composite materials possess new properties that cannot be achieved by those of individual materials. Composite materials are different from alloys in that, each material keeps its own physical, chemical and mechanical properties whereas in alloys, the metals change physically into a new material with enhanced properties. Furthermore, metal is an

essential part of the alloy which is either combined with other metals or with non-metals while composites allow both materials to be non-metals.

Composite materials were one of the first technological advances by humans used thousands of years ago. Early examples include straw reinforced mud bricks, animal glue laminated wood by Egyptians and laminated metals to forge swords. Some recent examples include glass fibers reinforced polymers, metal composites, ceramic composites and concrete [1].

Composites have several advantages over traditional materials. For instance, composites are generally light weight when compared to metals. This property is greatly desired in applications where low weight is greatly needed, like in automobiles, aircrafts and some sports equipment. In such applications, low weight means less fuel consumption and lower CO₂ emission [2].

Composite materials such as carbon fiber reinforced polymers (CFRP) and Glass fiber reinforced polymers (GFRP) are used in pipes. They are chemically inert, and therefore, corrosion-free and they do not conduct static charges which metallic pipes are prone to. This is very important in pipes containing oil and other flammable liquids. Static charges in presence of high temperatures and flammable liquids or oxygen can lead to accidents such as fires or even explosions.

1.2 Damages in composite materials

Despite the advantages of composite materials, there are some problems that reduce their use for commercial applications. As multiphase materials, they exhibit anisotropic properties which means that their properties are directionally dependent. Therefore, additional parameters are needed to describe their behavior. This makes the structural analysis computationally and experimentally more complex and intensive.

A significant problem of composites is that they are easily prone to damage and are vulnerable to several types of damages that do not occur in metals. These include matrix cracking, fiber breakage, fiber-matrix and delamination between plies of layers of composites [3]. Delamination is when the plies in laminated composites get debonded. This is mainly caused by crack in matrix materials, imperfect bonding, and separation of adjoining plies and broken fibers. Some of the defects may originate during manufacturing process while the in-service loading such as foreign body impact or fatigue may also induce others.



Figure 1-1 Delamination ©Kolossos.

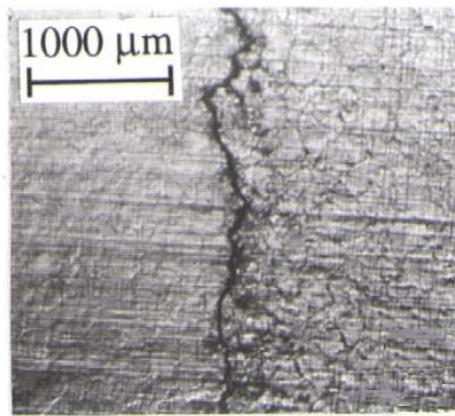


Figure 1-2 Micro crack [4].

Furthermore, a major problem in composite materials is their susceptibility to impact damage. This is due to lack of reinforcement in the direction perpendicular to the plane of the composites. When a structure is impacted by a high-energy impact, a small penetration

on the composite is observed. However, when energy level of the impact is low or medium, the matrix of the composite cracks and this will induce delamination.

In view of the damages that can occur in composite materials, structures made with composites are constantly inspected for damage such as oil pipes for leakages. However, not all structures can be inspected fully because firstly, there are structures which are simply too large to inspect completely, for example, an aircraft or a long pipeline. Secondly, there are places on a structure that are hard to reach for inspection like top of a tall tower or locations that would require structure to be disassembled.

During the lifecycle of a structure, damages due to impact of foreign objects is common. For instance, Mechanical damage can occur during handling, installation and service of the composite pipes. Due to the laminate structure of composite materials, their behavior to impacts is different to the metallic structures. The modes of damage in composite structures due to impact can be categorized as matrix cracking, fiber breakage and/or delamination [5].

Generally low velocity impact, which are of low to medium energies and the range depends on the material and its dimensions, cause a global structural response, and often results in internal cracking and delamination, while at higher energy levels can cause penetration and excessive local shear damage [6].

The impact damage can be caused by several reasons such as dropped tool, damage due to mishandling and in-service impacts. Composite materials are prone to low energy

impacts that can be observed with the effect of delamination in the plies and can be indirectly responsible for the failure. Delamination reduces elastic moduli, strength, durability and damage tolerance [5]. Low velocity impacts can also cause matrix cracking which may not be visible on the surface of impact but on the internal or bottom surface, due to the flexibility of the laminate. Matrix cracking occurs in a plane perpendicular direction to the laminate and is referred to as a tensile crack. In thicker laminates, matrix cracking is near the top surface and characterized as the shear crack. To ensure reliability, good impact properties against low and intermediate velocity impacts are essential.

Moreover, the micro failure modes commonly observed in composite laminates are fiber breakage, fiber micro buckling and matrix crushing, transverse matrix cracking, transverse matrix crushing, debonding at the fiber-matrix interface and delamination.

1.3 Structural Health Monitoring

To eliminate the failure modes due to loading conditions, there is a need for a reliable method for inspection in composite structures. Monitoring systems is important for early damage detection in critical structures such as aircraft, where damage can easily propagate and cause catastrophic failure. In pipes, for example, damage due to cracks can cause leakages resulting in loss of precious oil and chemical liquids. Conventional non-destructive testing (NDT) methods like thermography, X-rays, ultrasonic, and eddy current methods can be used for damage detection in composite structures [7]. The downside of these NDT methods is that they are labor-extensive and time consuming especially if the

structure is very large. They also require heavy and complicated equipment. Meanwhile, some structures need to be disassembled so the inspection area becomes accessible, which leads to increase in maintenance costs.

Among the techniques used in NDT, the most common one is the ultrasonic inspection [8]. A two-dimensional map of the structure is produced using the reflected waves. Defects occur in composite structures, such as disbondings and delaminations can very easily detected. However ultrasonic inspection has some limitations; surface on which damage is inflicted must be accessible so the probe can be placed there. Some of the common inaccessible locations are high altitude structures, very close network of pipes resulting in hard to reach places and structures that are buried in the ground. Another disadvantage is that ultrasonic method requires a skilled and trained operator for interpretation of the results. Additionally, the method cannot detect flaws that are oriented parallel to the wave propagation.

Structural health monitoring (SHM) is defined as, “The process of implementing a damage identification strategy for aerospace, civil and mechanical engineering infrastructure is referred to as structural health monitoring [7].” The main feature of SHM over NDT is that SHM provides an online and real time damage detection that can be performed via in-situ sensors. The potential benefits of SHM include reducing lifecycle costs, improving reliability and safety and helping design of composite materials. Some of the SHM methods are acoustic emission, lamb waves, active vibration-based methods and strain-based method [9]. Some novel methods are embedding a network of sensors between

the layers of composite material so that diagnosis can be done automatically [10]. Despite the potential advantages of this method, it is very costly and time consuming as the sensors must be embedded during the manufacturing phase of the composite material.

Strain gages are also one of the most common sensors used in SHM. Information from strain can be used to detect the static and dynamic deformation the structure and assist in evaluation of the amount of damage [11, 12].

Piezoelectric sensors are frequently used for measuring low or high frequency vibrations, such as Lamb waves or acoustic emission [13]. Compared with conventional acoustic probes, e.g., wedge or comb Lamb wave transducers, piezoelectric sensors are more desired for SHM in view of their weights, sizes and costs. With direct piezoelectric effect, which is when strains applied can induce voltage, the sensors in a stress field can generate charge response and vice versa, an external electric field applied to the sensors can result in an induced strain field through inverse piezoelectric effect. Consequently, piezoelectric sensors can be employed both as actuators and sensors [14].

Microelectromechanical systems (MEMS) are devices that have both mechanical and electrical components and are used in a variety of ways. They can be used both as a sensor or actuator. As an emerging technology, they are increasingly being used in numerous applications such as in micro-pumps, micro-mirror controllers, filters, resonators and accelerometers [15]. Since silicon is piezoresistive, its resistance changes with applied strains. This property makes it useful in application where there is a change in strains or

bending. It is commonly used in microelectromechanical systems (MEMS) in applications such as accelerators, pressure sensors and other applications.

Among the structures used in the schematic of MEMS devices, microbeams are the most common. Several micrometers in size, they are very effective and therefore they have applications in MEMS industry. Microbeams are used in micro-switches as switching elements, microscope probes and as band-pass filters. Two frequently occurring types of microbeams are cantilever or double-clamped microbeams. While cantilever is fixed in one end, double-clamped microbeam is fixed in both ends. Microcantilever beams are preferred due to their fast response time, easy fabrication, compact size and high sensitivity.

Present microcantilever sensors are fabricated with piezoresistor on top of the microcantilever. The piezoresistor are usually made from doped single-crystalline silicon or a polysilicon and the microcantilever from silicon dioxide or silicon nitride. This design results in microcantilever having good piezoresistivity and high sensitivity. On the other hand, this requires additional steps in fabrication process and additional cost and manufacturing time will be incurred [16].

1.4 Research Objectives of Current Work

The objectives of the thesis study are listed below.

- Examine the use of carbon-fiber as sensor for structural health monitoring of fiber reinforced polymeric composite structures subject to several types of loads such as the low velocity impact loads.
- To develop a multi-physics computational model to simulate behavior of the developed carbon fiber sensor under static uniaxial loading.
- To design and optimize of the carbon-fiber sensing device configuration for low velocity impact loads.
- Characterization and performance evaluation of the designed carbon fiber sensor will be performed.

1.5 Organization of the Thesis

In this section, the organization of the thesis and the methodology that will be followed to achieve the thesis objectives are discussed. In chapter 2, the literature review is presented. Recent work on structural health monitoring and the sensors used for the monitoring are discussed. Focus is on recent research on carbon fiber sensors.

Chapter 3 is dedicated to experimental study in which the preparation of carbon fiber sensor as well as experimental setup is discussed. The equipment used and the samples prepared are detailed.

In chapter 4, the numerical modeling performed in the research is introduced. Modeling of silicon piezoresistive sensors is discussed followed by results and discussion. Computational model of the carbon fiber sensor is discussed next. A computational model of an application of the carbon fiber in a beam is also presented.

Chapter 5 focuses on the results and discussion of the thesis. Both experimental and numerical results are presented. In the experimental part, the tensile test results are presented where a parametric study is done. This is followed by discussion on impact test results. The results of numerical model are discussed next where a parametric study is performed on a carbon fiber sensor and its piezoresistive coefficients are obtained. The results of the application of the carbon fiber sensor are discussed.

Finally, the major conclusions from this study with some recommendations for future directions are presented in chapter 6.

The main goal is to develop a carbon fiber sensor that can detect strain and test its performance using tensile tests and impact loads. The proposed work includes both numerical and experimental tasks essential to design and characterize the carbon fiber sensor. A numerical model will be developed to investigate the effect of various parameters such as size, location and material properties. The advantage of numerical model is that these parameters can be found without performing many experiments thus saving valuable time. To validate the numerical model, experiments are performed on carbon fibers to examine their performance in real time. The experiments will allow us to assess the accuracy of the carbon fiber in detecting damages caused by various loads. Necessary pre-treatment, preparation and installation techniques are studied to make them useful for the industry.

The following points will be used in the methodology:

- To develop a carbon fiber into a sensor that is capable of detecting strains based on the study of methods used in literature and to list the proper procedures used in developing this sensor. This will help future researchers conducting study in this sensor as a reference to develop this sensor.
- To develop a numerical model to study the behavior of carbon fiber sensor and perform a parametric study to understand the effect of various parameters like

length, diameter and treatment. This will give us the ability to test it without performing many repetitive experiments.

- Design and setup of an experiment for using carbon fiber sensor. The experimental setup should allow us to find out whether the sensor is capable of detecting damage. The experiments would give us information such as the output range of carbon fiber and the breaking point of the sensor, etc.
- Test the capability of carbon fibers to detect impact loadings. Low velocity impact causes significant damage to structures. The indication of these damages might be visible on the surface but the severity of the damage is barely visible. The purpose of this study is to investigate the capability of CF sensor to monitor the response of the structure due to these disturbances. The sensor will be embedded on surfaces of composite plates which will be used for impact damage. The experiment will help in determining the factors that affect the performance of the sensor in detecting impact damage.

CHAPTER 2

LITERATURE REVIEW

This thesis research is concerned with strain measurements in composite materials using carbon fibers. It is, therefore, essential to shed light on the current structural health monitoring techniques with special focus on those used in composite materials. Then, the relevant reported studies on carbon fibers and their properties are presented and discussed.

2.1 Related work on structural health monitoring

There have been several studies on SHM using various sensors. The studies include experimental, numerical and analytical which discuss damage detection using the sensors and how various techniques can be used to use more than one sensor for finding the location for the damage. In situ sensing systems placed in or around a structure can provide real-time evaluation of its performance. The use of SHM were commonly used in civil engineering applications, such as in roads, bridges, and dams, but now is finding applications in other engineering environments, such as naval, pipeline and aerospace engineering [17].

Fiber optic sensors (FOS) are competitive candidates for SHM applications because of their unique advantages of light weight, long life cycle, low power utilization, EMI(electromagnetic inductance) immunity, compatibility with optical data transmission and processing [18]. According to the sensing range, FOSs can be categorized into local and distributed sensors. The most-commonly used local FOSs are interferometric sensors, such as Mach-Zehnder, Michelson and Fabry-Perot FOSs. These sensors can measure strains and deformations at local sites by detecting the phase shifts of relative optical waves [19].

Fiber optics has received intensive attention during the past decade due to advantages such as immunity to electromagnetic interference, high resolution, long distance sensing and sensor networking [20]. Advancement in micro-technology has led to development of novel micro-structured fiber optic sensors which have shown promise in terms of faster response, smaller size and higher sensitivity [21]. Some applications of these new sensors are in strain pressure measurements [22]. However, these sensors still face some challenges such as high installation costs, expensive and bulky test equipment for testing and high susceptibility to physical damage [23].

Moreover, several studies focus on investigating the SHM processes by combining numerical and experimental studies in the analysis. Moselhi et al. discussed the applicability of FEM software in SHM [24]. Data from a case study were used to update the developed finite element and evaluate how damages on a structural element can be detected.

Lead zirconium titanate ceramics (PZT) wafers and polyvinylidene fluoride (PVDF) films are the two common piezoelectric elements. A PZT sensor is shown in Figure 2-1.

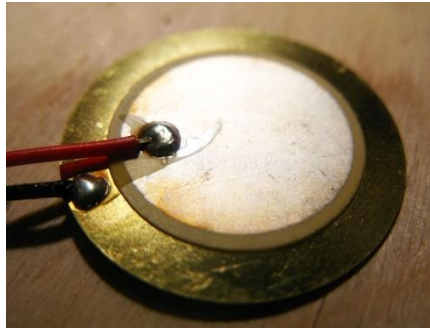


Figure 2-1 Piezoelectric sensor © Yakut.

PZT wafers with high piezoelectric constant possess both excellent sensitivities as sensors and strong driving abilities as actuators, whereas the wafers are quite brittle due to ceramic inherent nature. In contrast, PVDF films have the advantages of high flexibility, low mass and cost and high internal damping. However, because of the poor inverse piezoelectric properties and large compliance, PVDF films are usually preferred to be sensors. To overcome the disadvantage of high brittleness of PZT wafers, piezoelectric composites, such as piezoelectric rubbers and piezoelectric paints, have been developed [25].

Strain gages are also used in SHM because they can sense strains and vibration-based damages. Strain information can be used to detect how much deformation the structure went or is going through which can be used to find the amount of damage [11]. Several parameters such as temperature, carrier material and gage length affect the sensing ability

of the strain gages were discussed and it was found that the dimensions of the strain gages play an important part in their application [26].

The advantages of these types of gauges are that they are simple to install, low cost and have proved to be successful though years of use in industry. However, metal foils also have a very limited strain range, and because these gages are adhered to the surface they are susceptible to damage. Furthermore, more wires must be routed across or through the structure to carry the required signal to the monitoring unit [12].

2.2 Carbon Fiber Sensors

Piezoresistive materials attract the attention of researchers to investigate their capability to act as strain sensors. Intensive research was conducted on a variety of materials in different applications. A comprehensive review of recent development on smart fabric sensors can be found in [27]. The potential of using newly developed smart materials in damage detection is obvious. Carbon fiber based materials possess excellent mechanical properties and show linear piezoresistive behavior which make them good candidate material for strain measurements.

One of the early research studies to shed light on the piezoresistivity of carbon fibers was performed by Wang and Chung [28]. It was observed that electrical resistance of carbon fiber epoxy matrix composite changed with applied strain. Wang and Chung, investigated the piezoresistive behavior of short carbon fibers and epoxy resin composite, and showed that resin with short fibers have better response than that with long fibers [29].

Wang et al., illustrated that the piezoresistive behavior of carbon fibers and other similar graphite fibers can be utilized in sensing [30]. The piezoresistive behavior of carbon fibers is tested under different conditions: single bare fiber, in polymer composite and in cement composites. It was shown that bare carbon fiber is not piezoresistive while embedding short fibers in cement would give maximum gauge factor.

S. Blazewicz et al. studied the piezoresistivity of single carbon fiber and graphite fibers that have different microstructure parameters and heat treatment [31]. The study showed that piezoresistivity of carbon fibers is highly dependent on the crystallite sizes and treatment method which might lead to positive or negative piezoresistivity. The relationship between gauge factor and strain levels to structural parameters are presented.

In the work of Huang and Yang, the electrical sensing properties of carbon fiber reinforced plastic(CFRP) strips under tension were studied [32]. The study observed that microfibers are not completely straight or arranged in parallel, and the fibers are connected in transverse direction as shown in Figure 2-2. Under the application of tension load, the fibers are more concentrated in the transverse direction than when they are stress free. thus, there is induced non-linearity when some fibers are not aligned properly or break individually. The CFRP strips were only tested in low level strains, up to $1000 \mu\text{m/m}$, while the response in high level strains was not studied.

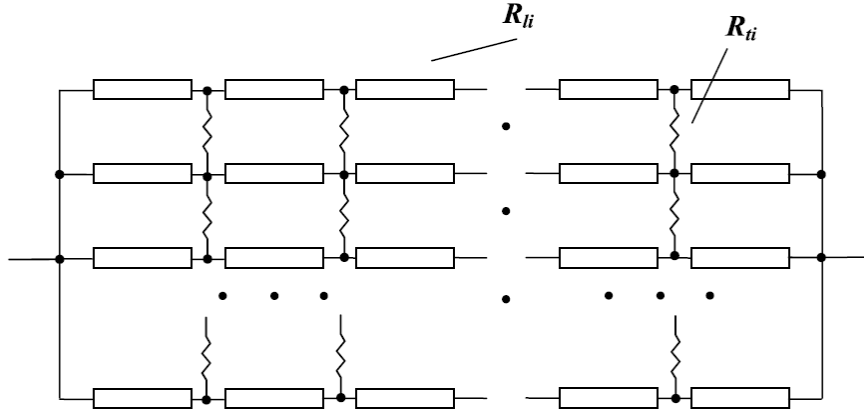


Figure 2-2 Equivalent circuit model for CFRPs in the tensile strain state [32].

Chung provides a comprehensive review on structure property relationships of continuous carbon fiber polymer-matrix composite [33]. Among the many properties listed, the effect of strain on the electrical resistivity is emphasized. Brief theory is presented and many experimental studies were cited and reviewed.

Todoroki and Yoshida discussed the monitoring of damages in CFRP composites by measuring several quantities, like potential change, electrical resistance change and eddy current [34]. The self-sensing capability of carbon fibers in the composite could provide precise measurement by observing the variation in its electrical resistance.

However, there are some inherent problems in the resistance measurement of CFRP. For example, the variation of electrical resistance in CFRP composite is highly sensitive to several parameters. Measurements from different studies showed some contradictory results when measured using different probe configurations. Schulte and baron [35] and other researchers [36, 37, 38] have reported that, using two probe method, electrical

resistance of CFRP laminate in the fiber direction increase with applied tensile load in the fiber direction. . However Chung obtained completely contrary results [39]. They used four probe method to measure precise electric resistance change in the fiber direction during tensile loading. Their results showed negative piezoresistance (negative gage factor). The difference in the results is shown in Figure 2-3.

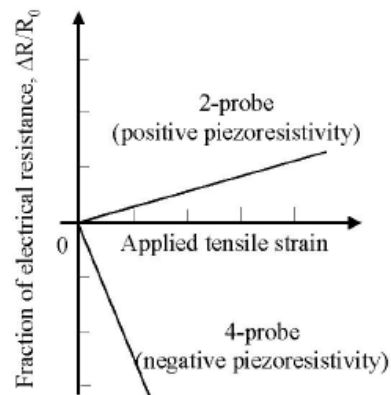


Figure 2-3 Discrepancy between the two-probe method and the four-probe method [34].

It was later found after further studies by the researchers that the carbon electrodes that were used for the electrical contact had low reliability and was the cause of the negative piezoresistivity [40]. In carbon paste, electrical contact is attained only at several discrete points with the carbon paste electrodes causing a complicated electrical current path in the specimen. When silver paste was used, positive piezoresistivity was obtained. Additional tests were performed by the authors themselves and they confirmed that poor electrical contact in four probe method was reason of negative piezoresistivity [41].

In their work, the authors investigate the sensing ability of commercially available carbon fibers [42]. Different configurations were tested to find the influence of relatively

high strain levels laminate micro-cracks on CF resistance. Micro-cracks were detected using carbon fibers which shows the potential to use them as a sensor for composite materials.

In a subsequent study, they have characterized the piezoresistivity of carbon fiber used as sensor in two industrial applications: CT scanner and pressure vessels [43]. The carbon fiber sensor developed is depicted in Figure 2-4.

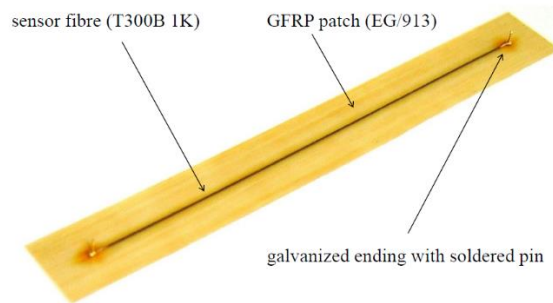


Figure 2-4 Carbon fiber sensor [43].

For CT scanner application, the authors applied the carbon fiber sensor into a carbon fiber reinforced plastic(CFRP) table of a computer tomography (CT) scanner [44]. Unlike metallic materials, carbon fiber is a nonmetal and does not interfere with X-rays. The metal wiring cannot be present in the table because they will interfere with the X-rays; therefore, U-shaped carbon fiber sensors were used as can be seen in Figure 2-5. The slope of the beam was found using integral strain measurement method.

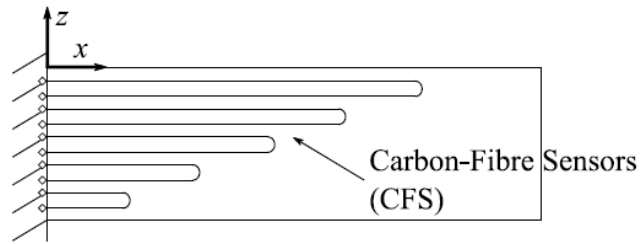


Figure 2-5 U shaped carbon fiber sensors [44].

Further analytical and numerical analyses were performed by the authors in order to monitor crack density using carbon fiber sensor [45]. They also carried out experiments on Glass Fiber reinforced polymer specimens and pressure vessels. Analytical and numerical analyses were performed and good correlation was shown between crack density strain measured by carbon fiber sensor.

Recently, Goldfeld et al. investigated the feasibility of intelligent textile-reinforced concrete embedded with carbon fibers to add strength and sense damage at the same time [46]. Cracks were detected and, it was shown that electrical readings can detect wetting of cracked elements which can be used to monitor leakages.

Based on the integral strain measurement property of carbon fiber, Matzies et al. proposed to use a triaxial arrangement of the sensors, where a mesh is created that can measure two-dimensional strain field [47]. The authors presented the theoretical background of this phenomenon, performed numerical study and an experiment to validate their results.

A simple resistance based sensor was proposed by Hou and Hayes who used two-probe approach to detect damage and its locations [48]. However, the experimental results showed that sensor was only able to measure area of approximately 1 mm making it only useable for precise damage location measurement. The sensor was able to detect damage from fiber fracture, but impact damage detection was more difficult.

Yang et al. studied the behavior of carbon fiber reinforced plastics(CFRPs) that are reinforced with carbon fibers of different types of moduli [49]. Effect of temperature on the resistance was observed and it was concluded that CFRP can be used as a temperature sensor. However, changes in electrical resistance would be affected by applied strains but this effect was not considered.

A study was presented by Huang and Wu, in which low level strains were measured using long carbon fibers [50]. Static and dynamic uniaxial tensions were applied to the steel specimen which has CF sensors embedded to it. Static and dynamic response measured using carbon fiber sensors were compared to those obtained from regular strain gauges.

More recently, A long-gauge carbon fiber line sensor was introduced for structural health monitoring and was implemented by Saifeldeen et al, in conjunction with an auxiliary carbon fiber line sensor to compensate for errors in readings [51]. The lengths of the sensors were 50 cm. The authors show that this technique of using two sensors reduces error and shows good linearity under low strain levels. However, the effect of length of the

sensor was not studied. The study was based on experiments and no computational model was developed. Moreover, the study illustrates that post-tensioning of the sensor can significantly enhance the linearity and cyclic ability of the sensor.

In the work of Todoroki et al. the large discrepancies in measured piezoresistivity even in simple tensile loading cases was discussed [41]. It was shown that the irregularities in the piezoresistivity readings are caused by fiber contacts in transverse direction which is depicted in Figure 2-6. The contacts between the fibers cannot be predicted and thus leads to difficulties in modeling the piezoresistivity analytically. However, they only performed tests in CFRP strips while the behaviour of carbon fiber tows was not studied.

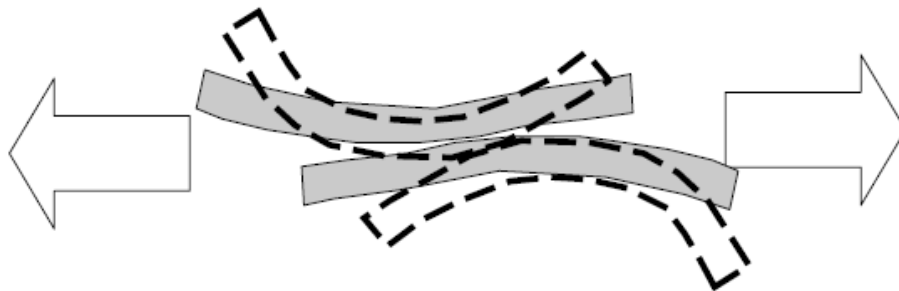


Figure 2-6 Fiber contact separation model to explain piezoresistivity in transverse direction[41].

Todoroki et al. extended their work to examine the anisotropy of piezoresistivity in unidirectional single-ply CFRP subject to multiaxial loading. The unsymmetrical piezoresistivity matrix is calculated using the measured piezoresistivity [52]. It was concluded that negative piezoresistivity was mainly caused by fiber misalignment and sparse electrical contact at electrodes.

Carbon fiber sensor can be used with different patch materials like Glass fiber reinforced plastic (GFRP) and Carbon fiber reinforced plastic (CFRP). Commercially available carbon fiber, Ex-PAN fiber T300B, have excellent linear piezoresistive behavior among other characteristics [43]. Micro crack detection using the CFS showed that CFSs have good applications in damage monitoring and lifetime prediction of damaged structures. They are excellent sensors in detecting delamination in multidirectional reinforced laminates and offer to unique features for fracture mechanics which are; detection of matrix cracks and measurement of strain levels. However, improvement still needs to be made in the effect of influence of temperature on the sensors' performance.

CHAPTER 3

EXPERIMENTAL STUDY

As mentioned in the previous chapter, the literature review has shown the need for further research on carbon fiber sensors for structural health monitoring purposes. Moreover, recent papers have shown that carbon fibers sensors hold good promise in damage detection.

The purpose of the experiment is to develop a sensor from carbon fibers and perform tensile tests to characterize the behavior of the sensor. Then, impact test is conducted on a composite plate in which carbon fiber sensors were embedded to monitor the damage. Furthermore, the results from experimental tests will be used to validate the developed numerical model for the sensor.

This chapter is divided into sections that represent different parts in the experimental work; namely the preparation of the sensor, the tensile tests, and the impact test on composite plates with carbon fiber sensors

3.1 Preparation of Carbon Fiber Sensor

The type of carbon fibers used in the current research were carbon fiber tow or rovings which were based on a commercially available Toray T300b. Toray is one of the leading manufacturer of carbon fiber composite materials. The choice of Toray T300b was based on its performance in literature [42, 43, 51, 53] Each roving contains a bundle of long strand of fibers. The name of the product indicates the number of filaments it has. So, the 1K means that it has one thousand filaments in one strand and 3K has three thousand filaments in one strand. For the current work, carbon fiber tows with 1K, 3K, 6K and 12K filaments were used to conduct the experiments.

Carbon fiber cannot be directly used as a sensor in its natural form because it is not piezoresistive in its natural form. The change in resistance observed is solely due to the change in dimensions (area and length). To induce piezoresistivity, the fibers have to go through a preparation process that will enhance its piezoresistivity [30]. This process includes the following phases:

- Pre-curing
 - To stabilize carbon fiber
 - Connect electrical wires for measuring electrical signals
- Curing
 - Impregnate by an epoxy resin
 - Curing process 180 °C for 90 minutes in a furnace

- Embedding

- For electrical insulation

- Depends on patch type and material used.

In the pre-curing stage, the purpose is to stabilize the carbon fibers and make sure all the individual filaments are aligned together and facing the same direction. This is attained by attaching the ends of the carbon fiber yarn to springs which are fixed on a bed made from metallic strips as shown in Figure 3-1.



Figure 3-1 Carbon Fiber with springs on metallic bed.

Moreover, the spring elements provide a slight tension on the fibers to ensure that fibers remain straight during the application of the epoxy and heat treatment. Multiple beds were prepared to develop several carbon fibers at the same time. The beds along with protruding springs have a total length of 20 cm.

The next step is the preparation of electrical connections. For this purpose, two short electrical wires were wrapped around the carbon fiber near the end points. Half of the electrical wire is wrapped and the other half is left free as shown in Figure 3-2. The length between the electrical connections is called the effective length of the sensor.

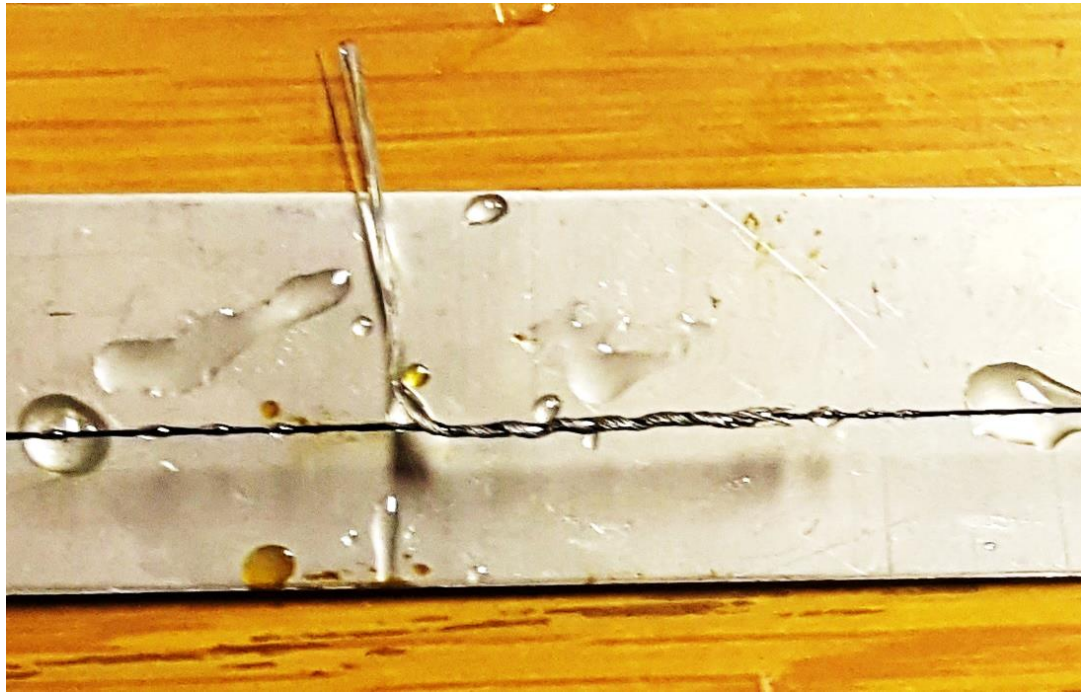


Figure 3-2 Electrical connection of the carbon fiber sensor.

After the electrical connections are made, the epoxy resin was applied. The epoxy coating is applied using EP301 which is a two-component epoxy resin adhesive. It has a liquid watery consistency and allows very thin adhesive layer. The carbon fiber is cured at 180 °C in a furnace for 90 mins.

Once the sensor is cured, the extra length after the electrical connections was cut for sensors used in the impact test. For the samples that were used for the tensile testing, the

excess length was not removed because that additional length was used to attach fixation patches which would help secure the sensor in the tensile machine grips.

The sensor is now ready to be embedded inside a composite structure or attached to the surface of the structure. For this research, the latter approach was used due to its simplicity and because it serves the purpose for damage detection on the surface of the plate due to impact load. To embedment of the sensor inside a composite material has to be performed in the manufacturing stage of that material in order to place the sensor between the layers of the composite.

To glue the sensor to the composite, several glues were tested and most of them fail to stick to fiber glass composites. The glue that worked with fiberglass plates was Devcon© epoxy. The glue required half an hour preparation time and an hour to cure properly.

The breakdown of the total time it takes to prepare one sensor is listed in Table 3-1. It can be realized from the table that the whole process of preparation takes 115 minutes.

Table 3-1 Preparation process of Carbon fiber sensor.

No.	Process	Time taken
1	Fixing the carbon fiber into the bed with the springs	10 mins
2	Preparing electrical connections of the carbon fiber	5 mins
3	Preparing epoxy resin for the sensor	5 mins
4	Applying epoxy coating on the carbon fiber	5 mins
5	Curing the carbon fiber sensor	90mins
	TOTAL TIME	115 mins

3.2 Tensile test

The principle behind piezoresistive sensor is that its resistance changes when mechanical strain is applied. In order to correlate the resistance with the strains, tensile tests were conducted to observe the variation in electrical resistance with applied strains. This would give valuable information that allows characterization of the sensor. Also, the maximum allowable stress or load can be identified. The tensile tests of the carbon fiber sensors were conducted with various specifications such as length, diameter and treatment of the sensor. This allowed us to characterize the effect of each parameter and gain better understanding of its effects on sensors performance. Thus, the parametric study consisted of three main parameters;

- i) Length
- ii) Width
- iii) Treatment/Epoxy Ratio.

The tensile tests were carried out on INSTRON 3367 machine, Figure 3-3. The machine can bear a maximum load of 30 kN, minimum extension speed of 0.005 mm/min and total vertical test space of 1193 mm [54]. The machine has a built-in extensometer that allows to the calculation of stresses and strains automatically and obtain the stress-strain curves.

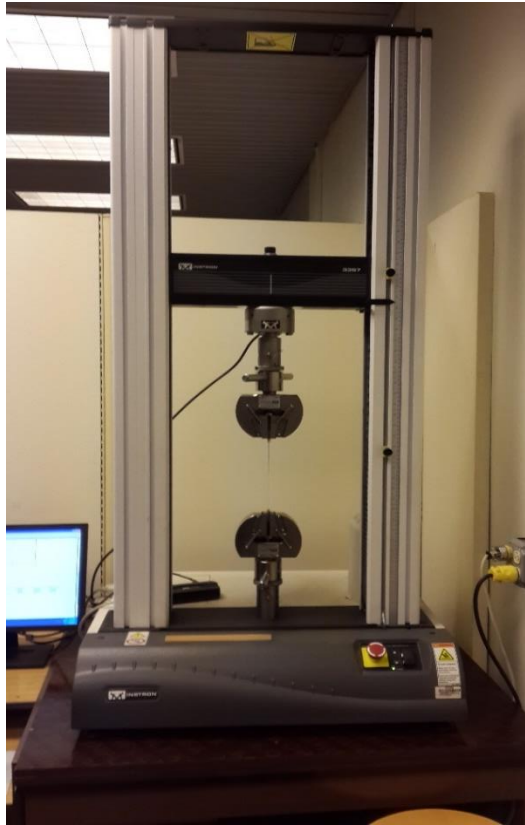


Figure 3-3 INSTRON 3367 machine.



Figure 3-4 UT71E Multimeter.

For the measurement of resistance, a datalogging multimeter UNI-T UT71E was used, shown in Figure 3-4. This multimeter was selected due its ability to record real-time data, measure low resistances with resolution up to 0.01, portability and affordability.

To perform the tensile test on carbon fibers, carbon fiber sensor is mounted by installing grips on the specimen's ends to prevent slippage. The grips were prepared by using two acrylic pieces bonded together with a strong adhesive as shown in Figure 3-5.

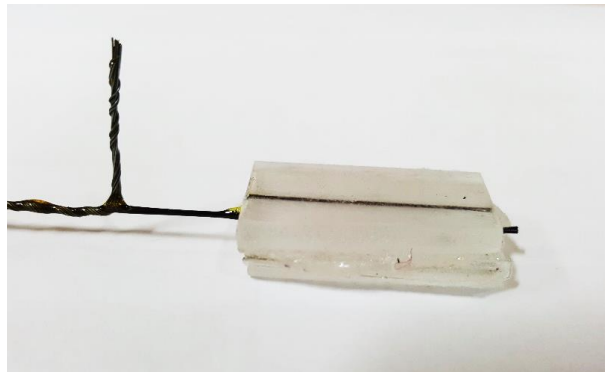


Figure 3-5 Acrylic grips.



Figure 3-6 Carbon fiber sensor with grips in a tensile machine.

Before starting the experiment, it is necessary to make sure that the sensor is tightly secured by the grips of the machine. This avoids any slippage which would cause erroneous results. The rate of extension on the tensile machine was set to 1 mm/min which is slow enough to properly record the strains versus stresses. However, it was found from literature [55] that T300 fibers can be regarded as strain rate insensitive material so the rate of extension does not have significant effect on stress development.

The multimeter is connected to the electrical connections of the sensor and is further connected to a PC for data recording. The data is recorded in time which can then be tallied with the data from the tensile machine to plot graphs of change in resistance versus change in strains.

3.3 Low Velocity Impact Test

The goal of this study is to detect various damages using the carbon fiber sensor. Low velocity impact damage is one of the major damages concerning composites and requires further research. The tensile tests were performed to get the relationship between the resistance and strain level of the sensor which facilitated the use of the sensor in detecting low velocity impact.

In this study, the information collected from previous tests was used to characterize the damage inflicted on a composite plate. A composite plate was impacted and the carbon fiber sensor was placed near the area of impact, where the maximum strains were induced. Consequently, the strains induced by the impact caused a change in resistance which was measured by the ohmmeter. The strains are induced in the axis perpendicular to the area of the plate. The displacement recorded by the machine is the displacement along this axis. Once change in resistance is obtained, it can be plotted versus displacement to observe how resistance varies with displacement. By performing the experiment at different impact energies, the sensor's response at different energy levels and the limits which would cause failure in the composite plate could be evaluated. The resistance output at this energy is

recorded and set as threshold which indicates the failure point of the plate. Thus, whenever the output of the sensor is close to this value, there is a risk of breaking in the plate.

The machine used for the impact test is “INSTRON Dynatup 9250G”. The machine consists of specimen holder and a striker that consists of impactor and its holder. Weights can be added and removed to vary the level of energy needed. There are different fixtures to hold samples with different shapes such as pipes or plates. The impactor is of hemispherical shape of diameter of 12.7 mm. The maximum impact energy that can be measured is up to 1603 J with maximum load weight of 80.5 kg. The maximum impact load speed that can be reached is 20 m/s.

A photocell device is used by the machine is used to calculate the impact velocity. It is in the path of the striker before it hits the plates. The force is measured from the moment the impactor hits the plate and moves through the plate's thickness. By the integration of the force-time signal, the energy is calculated. Data acquisition system is used to record both energy-time and force-time information. only the first impact is of interest because repeated impacts may cause excessive damage therefore to avoid this situation, pneumatically actuated rebound arrestors are used that can spring up and separate the impactor from the plates after the initial impact. The impactor machine is shown in Figure 3-7.



Figure 3-7 Machine used for low velocity impact tests: INSTRON 9250G.

Using this apparatus, from low-velocity impact tests, many different properties can be found such as impact velocity, total deflection, maximum force, total energy absorbed, failure load point, total load point, and deflection at maximum load.

The composite plates used were made from fiber glass, manufactured by ‘Arabian Glass Factory’. The plate, shown in Figure 3-8, was cut into 13 cm x 13 cm smaller plates

that could be placed in the fixture of the impact testing. In the fixture, the effective open area that is exposed is 11 cm x 11 cm while the remaining area is used to clamp the plate.

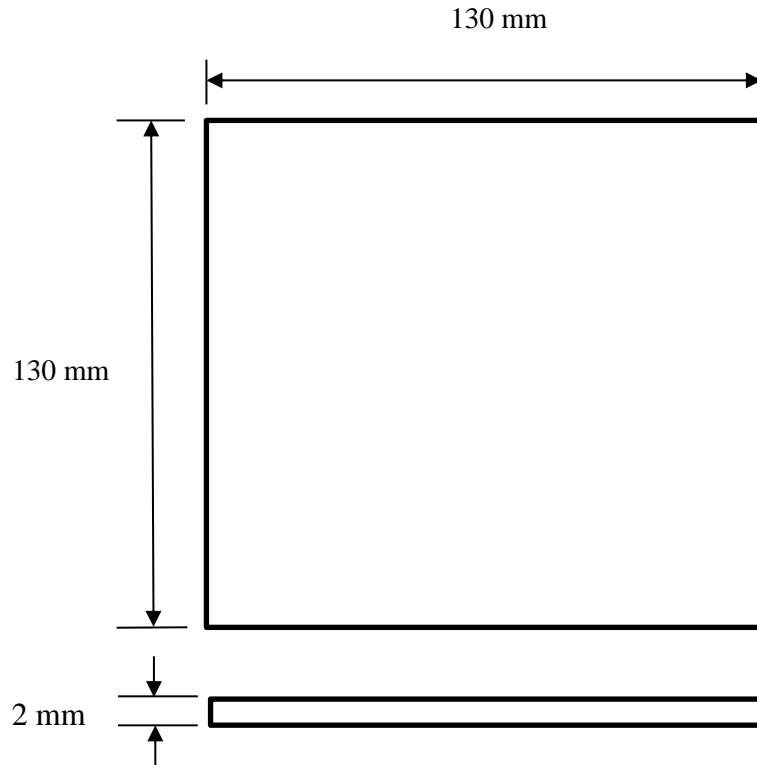


Figure 3-8 Dimensions of the impact test specimen.

The plates need to be embedded with carbon fiber sensors in order to detect the impact damage. There are many possible configurations for placing the sensors on the plates. The location of the sensors will affect their ability to detect damage and, hence, it is important to find out the optimum configuration of the sensors. When impacted at the center, it is obvious that the maximum displacement occurs at the center; the displacement slowly fades moving away from the center with the sides or edges of the plate having zero

displacement. Since carbon fiber sensors detect strains, it is recommended to place the sensor in a position that will have the most strains. This can be done by placing one end of the sensor near the edge and the other end close to the center. By doing so, maximum strain can be sensed which will be transduced into resistance. Figure 3-9 shows some of the possible locations for the placement of sensor.

While one sensor is sufficient to detect the damage, previous works in the literature show that carbon fiber sensors are not immune to temperature effects and the resistance values change with temperature [43]. In actual applications of this sensor, this will affect the sensor's performance. One way to combat this temperature effect is to use four sensors in a wheatstone bridge connection. This configuration cancels out the change in resistance due to temperature.

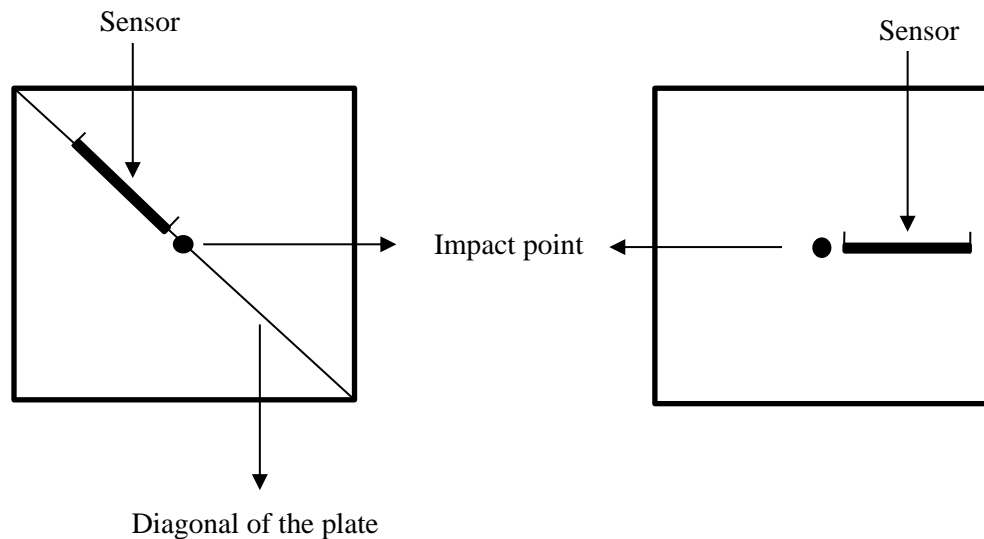


Figure 3-9 Good locations of the sensor.

To prepare the plates for the impact loads, sensor must be embedded into the plates on the desired locations. Also, sensor was placed on the surface of the plate. To glue the sensors, epoxy glue was used to stick the sensor onto the plate. Pressure was applied to make sure the sensor is stuck tightly on the plate. After that, the glue was allowed to cure for one hour.



Figure 3-10 Composite plate with embedded sensor.

Then, to perform the impact test, the plate was carefully placed on the fixture of the impact machine with the sensor side of the plate on the opposite side so that it is not facing the impactor. The electrical connections were made to the multimeter allowing live feed of the resistance values and enabling the recording of data. Figure 3-10 shows the plate with embedded sensor.

3.4 Conclusion

This chapter gives details regarding the experimental work conducted on carbon fiber sensor and the processes involved during its fabrication. Setup and details of the tensile tests of carbon fibers was mentioned. Then, the setup of low velocity impact test on the composite material using carbon fiber sensor was presented and detailed. The results and findings of the experimental work will be discussed in a subsequent section along with the parametric study.

CHAPTER 4

NUMERICAL MODELING

One of the objectives of this research is to develop a computational model that can be used to evaluate the performance of carbon fiber sensors under various loadings and conditions. The model can save valuable time and resources that spent in performing many repetitive experiments. Therefore, numerical models are helpful to future researchers conducting study in this sensor.

Before developing the computational model of the carbon fiber sensor, it is necessary to establish an approach to illustrate the validity of the model. Unfortunately, no existing computational models of carbon fibers as sensors was found in the literature to validate the model. Since carbon fibers are piezoresistive by nature, the development of the model starts with general piezoresistive computational models that can be validated easily by considering any of the well-known piezoresistive materials. For instance, there are many models of silicon which is a piezoresistive material. Therefore, the material properties of the piezoresistive silicon were used as the basis of the study of modeling piezoresistivity.

4.1 Silicon piezoresistive sensors

This model focuses on simulation and characterization of a microcantilever embedded with four piezoresistors. The piezoresistors consist of p-type silicon material and microbeam is made of silicon. The embedded piezoresistors are connected in a Wheatstone bridge which gives output in terms of voltage, which can be easily measured. Characterization was performed to observe the effect of the geometrical aspects of the microbeam. Hence, geometry of the microbeam was varied, namely, the length, thickness and width of the microcantilever.

4.1.1 Methodology

The 3D model of the silicon piezoresistors was built by first studying a 2D model of wheatstone bridge connection of piezoresistors based on an example in ANSYS user documentation. The 2D model was modified and studied to observe sensor outputs by varying the forces applied on the model. Figure 4-1 shows the 2D model that was built and studied.

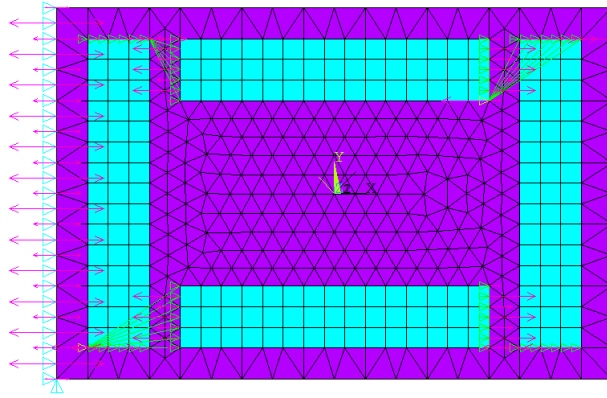


Figure 4-1 2D model of the piezoresistive sensors on a plate.

Silicon was chosen because it is an existing piezoresistive material and studying it will provide a good insight into piezoresistive behavior which will be helpful in predicting piezoresistive properties of carbon fiber. Tension forces were applied to the 2D model and the resulting output of the sensors were studied. The results were verified with analytical values. The model was then further modified into a rectangular microbeam with embedded piezoresistors.

The design of the cantilever is based on a simple rectangular microbeam with embedded piezoresistors as shown in Figure 4-2. The dimensions of the microcantilever are 1000 μm in length (l), 200 μm in width (w) and 200 μm also in thickness (t). The effect of varying these dimensions was observed by changing these parameters one at a time. The simulations were performed using the multiphysics finite element software ANSYS.

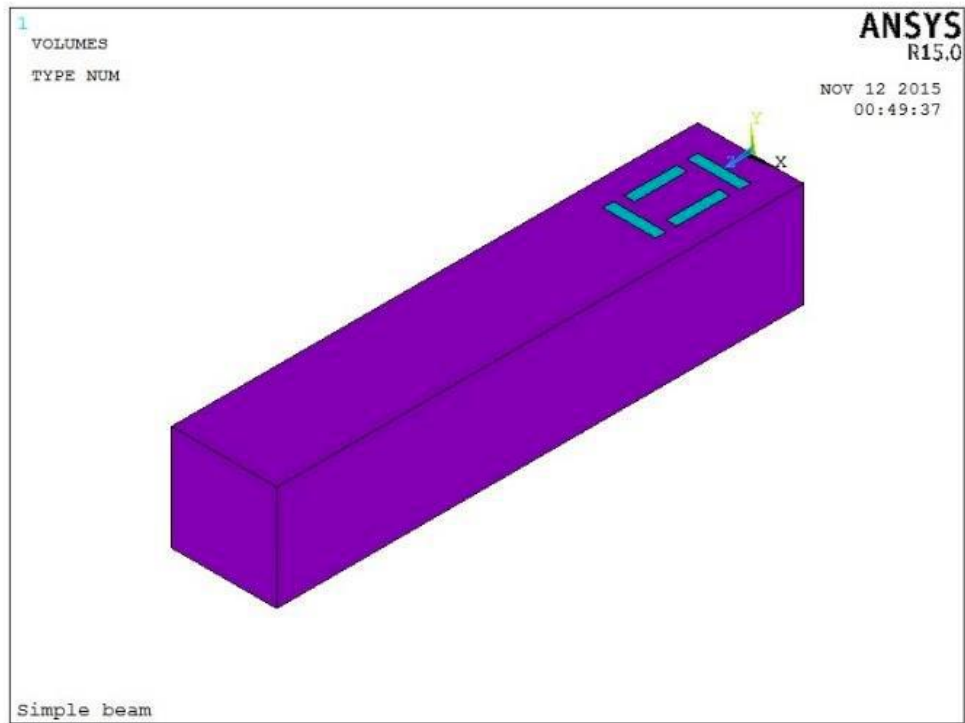


Figure 4-2 3D Model of embedded microcantilever design.

The piezoresistors are connected in a Wheatstone bridge setup and embedded in the cantilever beam. Initially, the sensors were placed at the surface of the microbeam as shown in Figure 4-3.

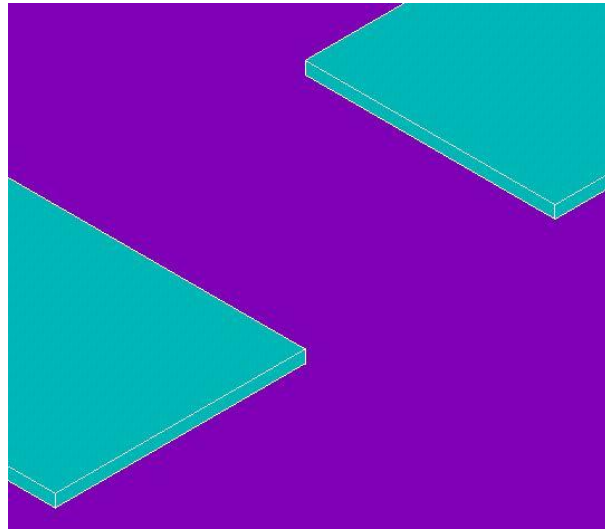


Figure 4-3 Sensors placed on the surface of the microbeam.

This caused problems because the junction of the sensor and microbeam experienced localized high stress concentration regions which caused large fluctuation of the voltage output of the piezoresistors [56]. It was found that stress concentration regions can be avoided by embedding the sensors into the microbeam. The piezoresistors were modeled using the element SOLID 226 which is a 3-D 20 nodes coupled field solid. For the microbeam, SOLID 186 was selected which is a 3-D 20 nodes structural solid element. Free meshing was performed separately for the piezoresistors and the microcantilever. A summary of material properties used ANSYS is provided in Table 4-1

Table 4-1 Material properties of Si sensor.

Parameter	Value
Young's Modulus(MPa)	165×10^3
Poisson's ratio	0.25
Piezoresistive Coefficient (MPa^{-1})	$\Pi_{11} : 6.60 \times 10^{-5}$ $\Pi_{12} : -1.10 \times 10^{-5}$ $\Pi_{44} : 138.1 \times 10^{-5}$

The voltage output of the sensor is calculated using the following equation:

$$V_{out} = V_s \left| \frac{\Delta R}{R} \right|$$

where $\left| \frac{\Delta R}{R} \right|$ is the relative change of piezoresistance and it is calculated as:

$$\left| \frac{\Delta R}{R} \right| = \pi_l T_l + \pi_t T_t + \pi_s T_s$$

where T is the stress caused. π is the piezoresistive coefficient. The subscripts l denotes longitudinal, t denotes transversal and s denotes shearing. After simplifying, the final equation of output voltage in terms of stress is

$$V_{out} = V_s \frac{\pi_{44}}{2} T$$

4.1.2 Results and discussion

The microbeam was fixed at the end close to the piezoresistors and a constant load was applied at the free end, which resulted in the bending of the beam. The displacement contours of the beam are shown in Figure 4-4 which shows that the maximum displacement occurs at the free end.

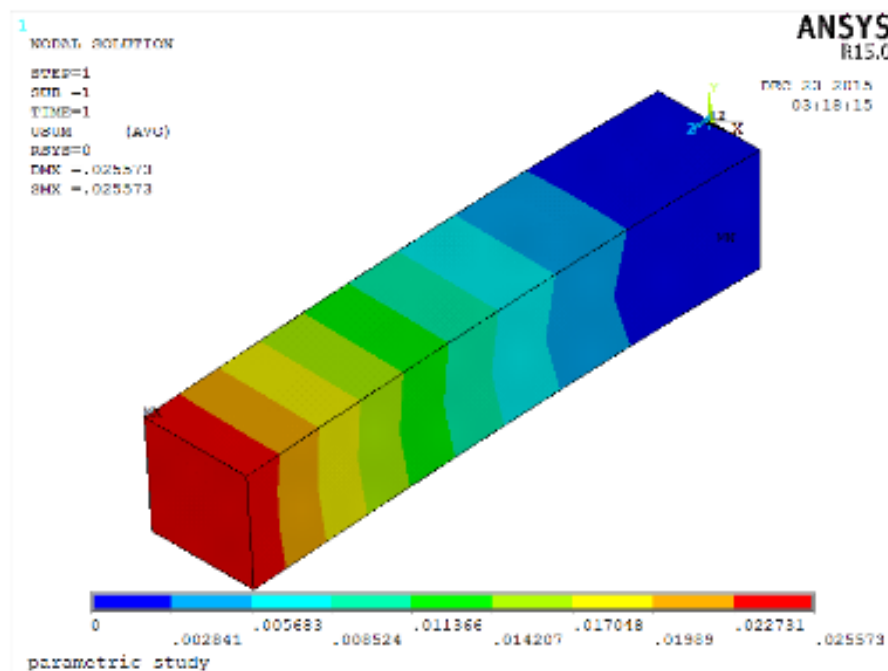


Figure 4-4 Displacement vector.

When force is applied at the free end, the microcantilever will bend with maximum displacement occurring at the free end and maximum stresses is develop near the fixed end as shown in Figure 4-5. The piezoresistors are embedded at this fixed end so the developed strain in the microcantilever can be sensed.

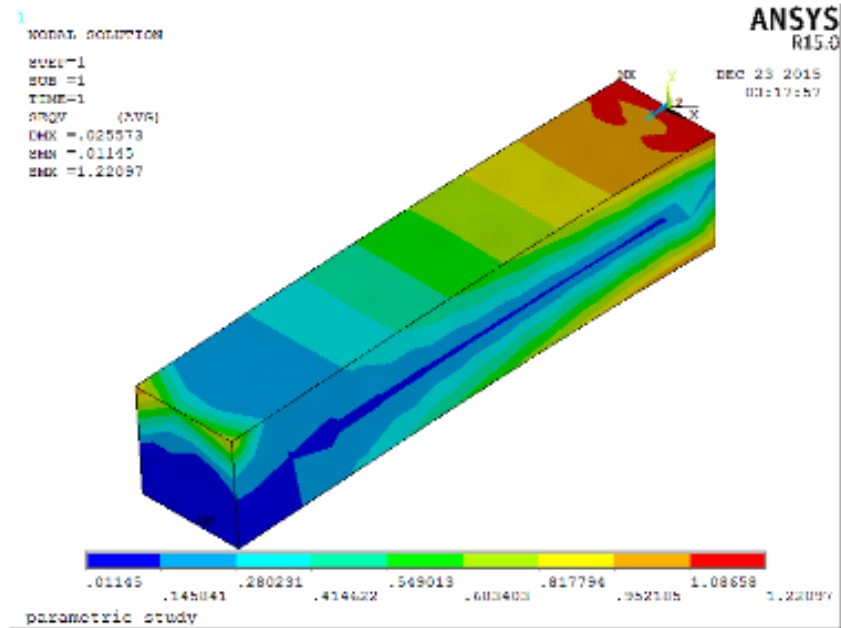


Figure 4-5 Von Mises stress distribution.

The variation of von Mises stress and displacement of the microcantilever with change in applied force is shown in Figure 4-6.

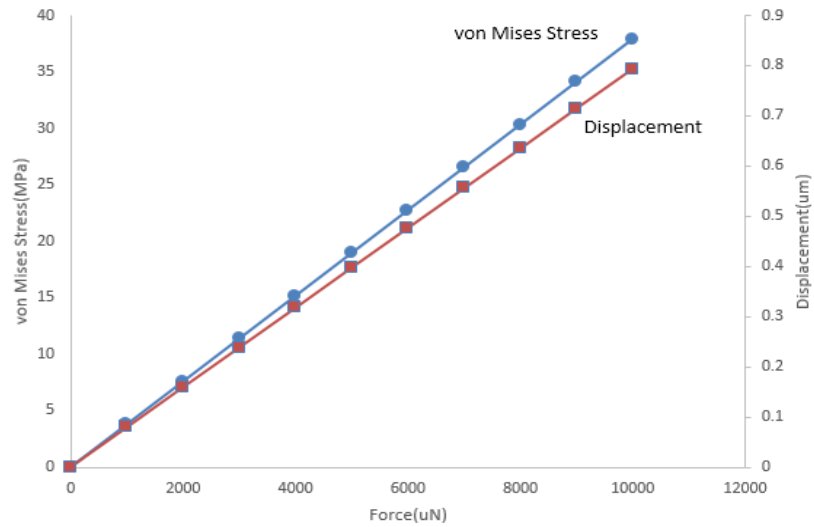


Figure 4-6 Von Mises stresses and displacement of microcantilever with varying applied loads.

It is shown that the relationship between von Mises stress and displacement with applied load is linear which agrees with analytical results. The values of output of the sensor obtained from ANSYS were compared with values using analytical formulas described previously. The comparison is shown in Figure 4-7.

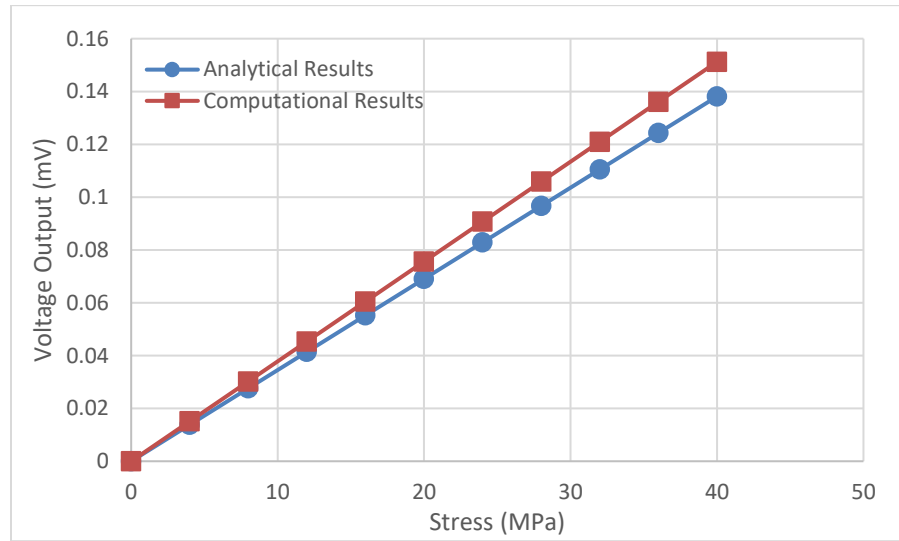


Figure 4-7 Comparison of analytical and computational results.

The first geometrical parameter that will be studied is the thickness of the microcantilever and its effect on von Mises stresses, displacement and the output voltage of the Wheatstone bridge. It was observed, as shown in Figure 4-8 and Figure 4-9, that increase in thickness cause von Mises stress and the deflection to decrease. Accordingly, less stresses at the fixed end will result in less voltage output. The results agree with the those in [56].

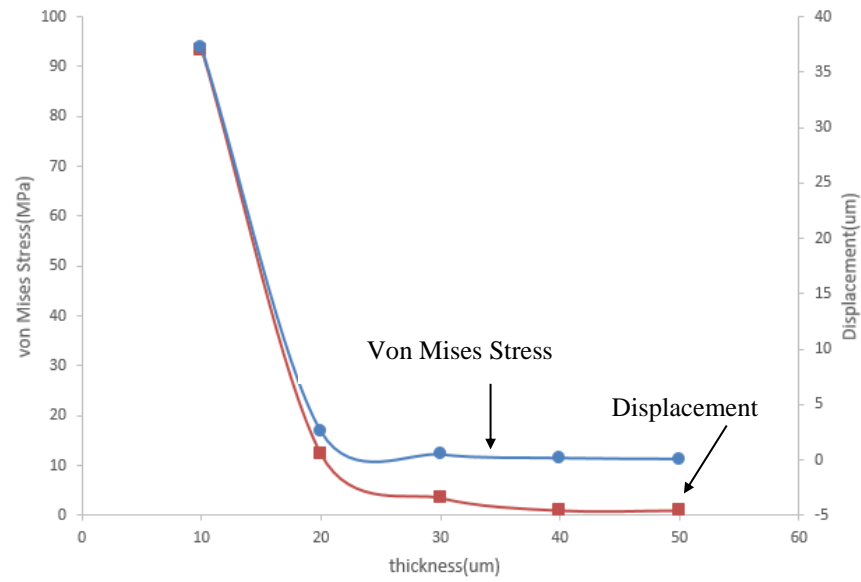


Figure 4-8 Effect of thickness on von Mises stresses and deflection.

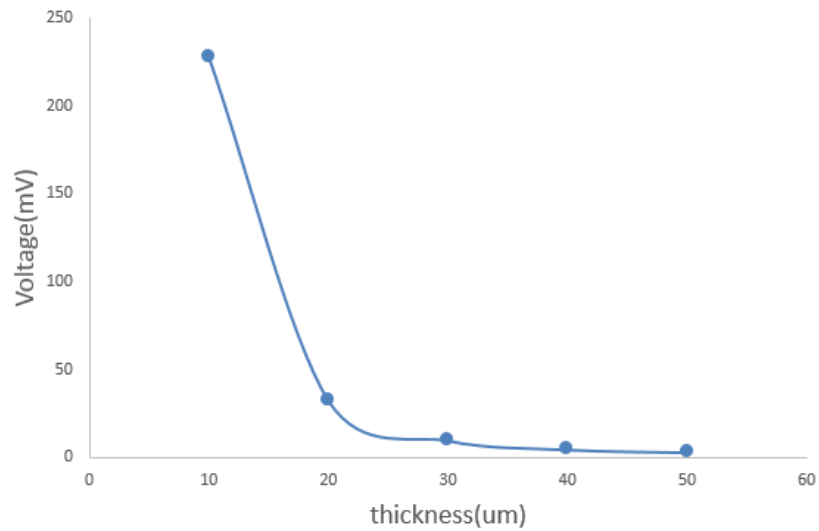


Figure 4-9 Effect of thickness on voltage.

The effect of the second geometrical factor which is the length of the microcantilever as shown in Figure 4-10. It is observed that the increase in length causes increase in both von Mises stresses and deflection in linear fashion. This is because increase in length will

cause more bending to occur at the same amount of force. The increase in bending will cause more stress to be developed at the fixed end. Therefore, the increase in stresses at the fixed end will cause the increase in output voltage as shown in Figure 4-11.

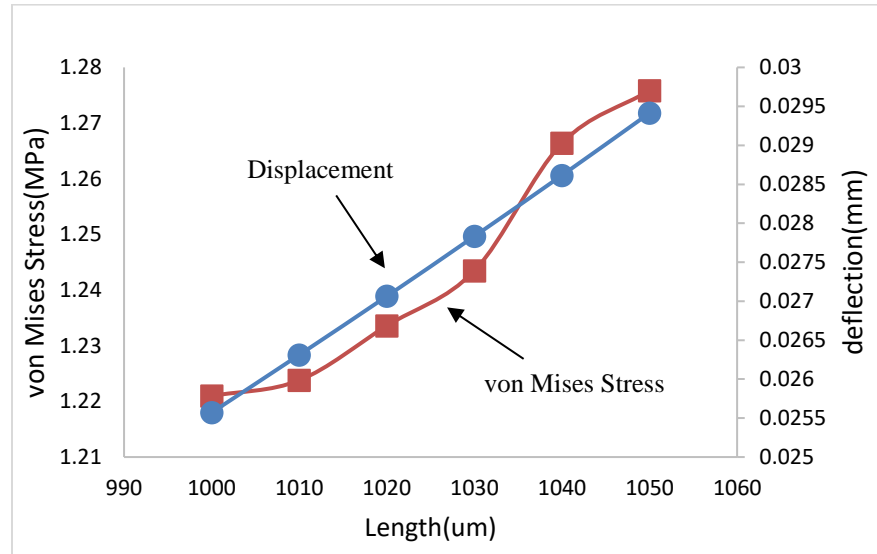


Figure 4-10 Effect of length on Von Mises Stress and deflection.

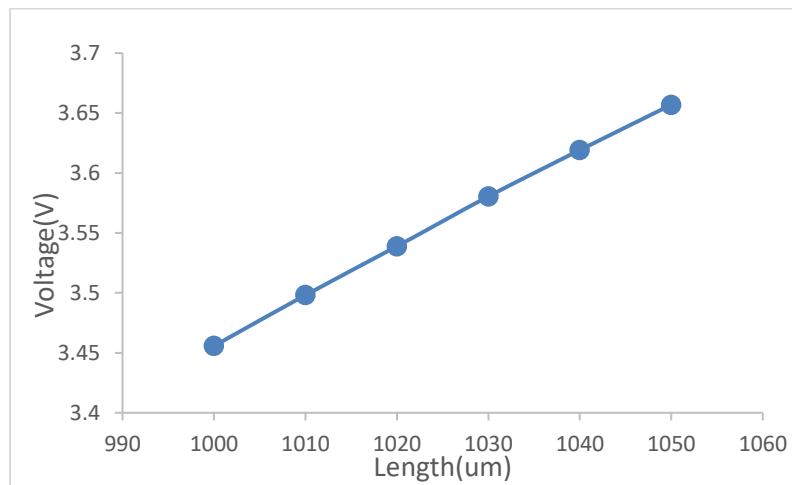


Figure 4-11 Effect of length on voltage.

Effect of width is investigated and the results show that as the width increases, both the von Mises stresses and deflection of the microcantilever decrease. The decrease in the stresses causes decreasing trend in output voltage. The results are shown in Figure 4-12.

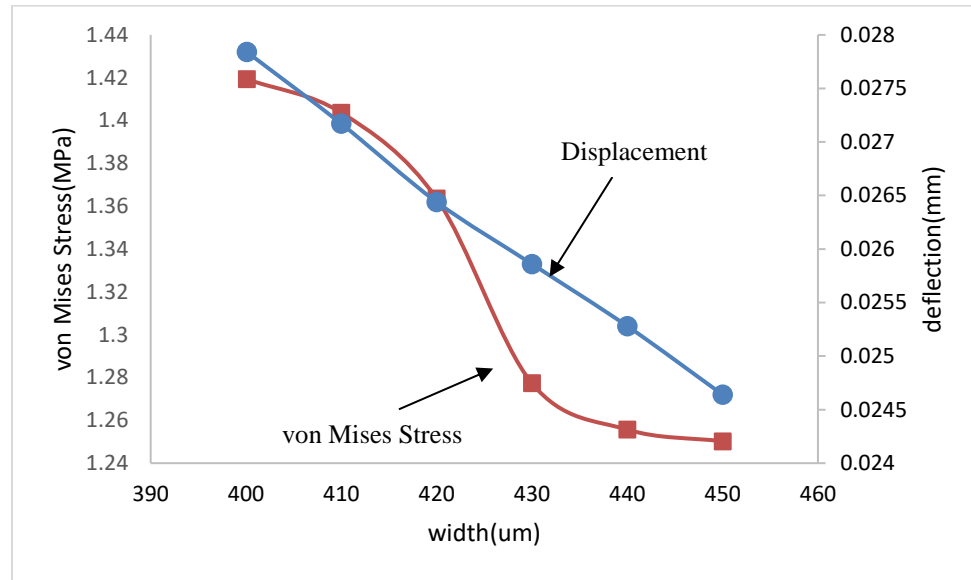


Figure 4-12 Effect of Width on Von Mises Stress and Displacement.

This decrease in stresses and deflection is observed because as the width increases, the microbeam becomes more difficult to bend and the same amount of force will produce less bending as the width increases. Thus, the decrease in stresses and displacement will lead to decrease in voltage output as shown in Figure 4-13.

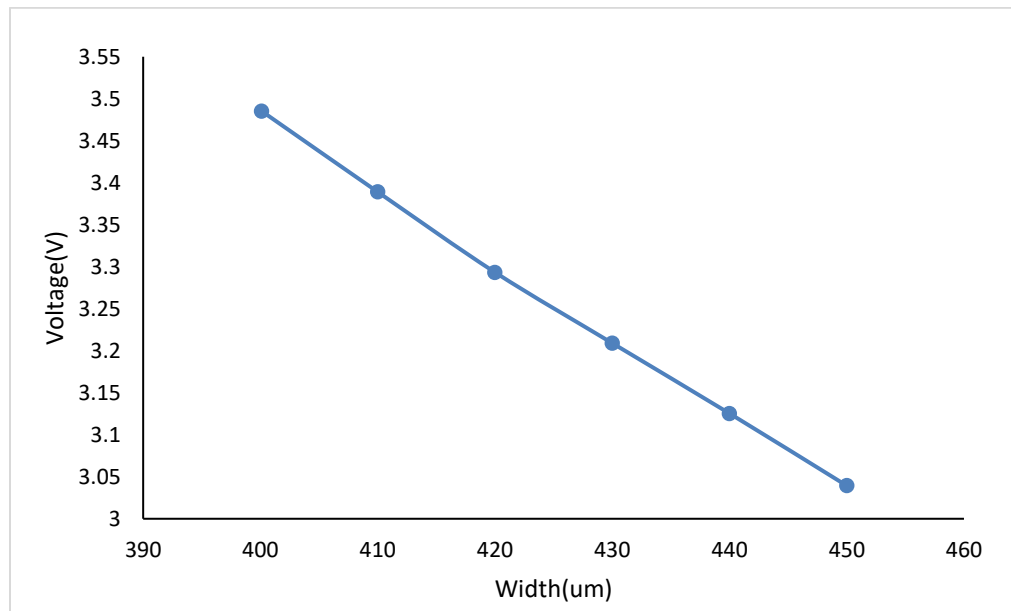


Figure 4-13 Effect of width on output voltage.

Finally, the effect of length of the piezoresistors which were embedded on the microbeam is observed and is plotted in Figure 4-14 where it is seen that the voltage gradually drops as the length of the piezoresistors is increased.

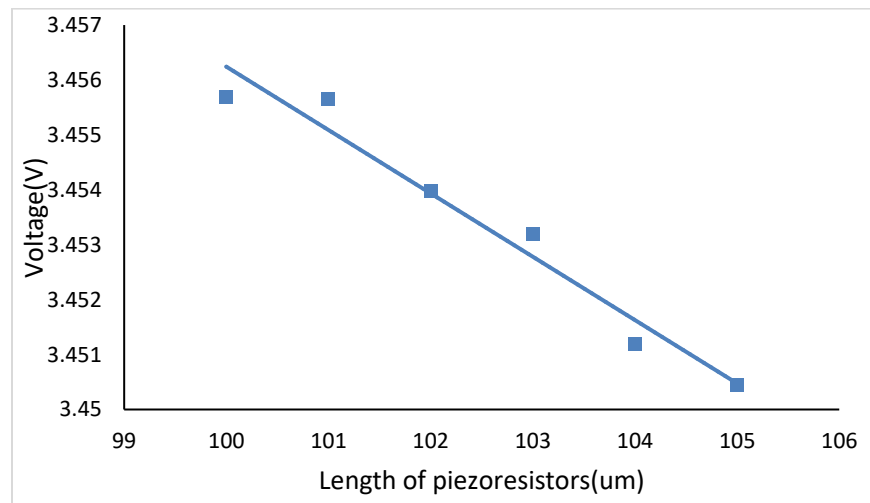


Figure 4-14 Effect of length of piezoresistors on Output Voltage.

Characterization of an embedded microcantilever beam using finite element method was highlighted. Geometrical variations were made in the microcantilever beam and the results: von Mises stresses, deflection of the beam and output voltage, were calculated and their trends were observed. It was illustrated that thickness of the microcantilever caused the most change in results.

It can be concluded from this study that the proposed model for piezoresistive sensors embedded in the microcantilever gave satisfactory results and could detect all the changes that were performed in the study. This demonstrates the validity of the model and allow its use in more complicated applications.

4.2 Computational model of carbon fiber sensor

The computational model of the carbon fiber sensor was developed in COMSOL platform. The carbon fiber sensor required changing the governing equations of piezoresistivity and including differential equations into the model. The COMSOL platform can accommodate user defined equations in its computational tool which is required for current analysis.

In the following sections, the COMSOL model of the carbon fiber sensor is introduced. The basic characteristics and parameters of the computational model will be discussed.

4.2.1 Idealization and Assumptions

The model developed in COMSOL was 3-D in shape with some idealization. The following are some of the idealization and assumptions that were made in the development of the model.

- Each tow or strand of carbon fiber contains thousand small filaments each of 7 μm . Instead of modeling thousands of small filaments, which would be computationally prohibitive, each strand is modeled as a single whole fiber.
- The material is assumed to be homogenous and orthotropic. This is a valid assumption because the property of the carbon fiber is same throughout the material.
- The effect of epoxy coating is included in the material properties. Its effect is properly estimated and added to the effective properties of the material.
- The copper wires were not considered in the model. The electrical connections are assumed to be at the ends of the fiber so the voltage is measured from one end to the other. In the experiments, the wires were attached to the ends to find the resistances. In both cases, the gage length is distance between the two connections.

4.2.2 Geometric Model

In this study, carbon fiber sensor has been modeled and the model has been calibrated using experimental data. The dimensions of the model have been taken to match those from experiments. Since various experiments were performed, the parameters in the numerical model were altered to fit the experimental results.

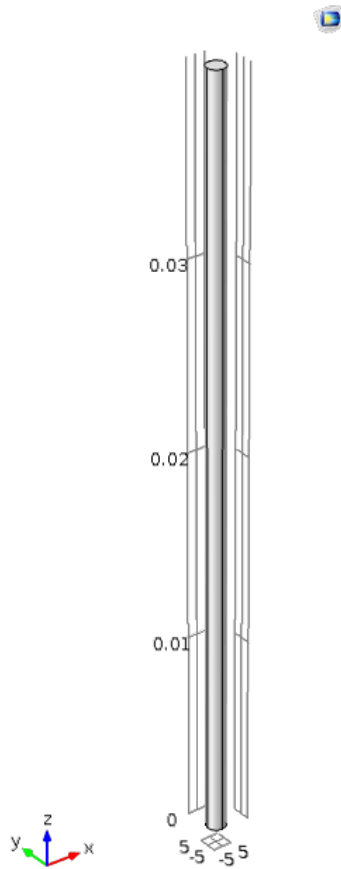


Figure 4-15 Geometric model of the sensor.

The dimensions of the sensor can be varied to the desired values. The size shown in the Figure 4-15 is of a sensor of length 40 mm and diameter of 1 mm. The parameters that changed were the force on the sensor, the diameter and the length of the sensor.

4.2.3 Material Modeling

Carbon fibers are anisotropic materials, meaning they have different material properties in different directions. the carbon fibers are considered to be transversely isotropic which is a subset of orthotropic materials. Transversely isotropic materials are those that have material properties re higher in the direction of the fiber and lower in the transverse direction. The material used in the model is considered to be impregnated with epoxy resin.

The relationship between strains and stresses is defined by only five independent constants for transversely isotropic materials. The matrix relating strains to stresses is given as:

$$\begin{bmatrix} \epsilon_{xx} \\ \epsilon_{yy} \\ \epsilon_{zz} \\ \epsilon_{yz} \\ \epsilon_{zx} \\ \epsilon_{xy} \end{bmatrix} = \begin{bmatrix} \frac{1}{E_x} & -\frac{\nu_{yx}}{E_x} & -\frac{\nu_{xy}}{E_x} & 0 & 0 & 0 \\ -\frac{\nu_{xy}}{E_x} & \frac{1}{E_x} & -\frac{\nu_{zy}}{E_x} & 0 & 0 & 0 \\ -\frac{\nu_{xy}}{E_x} & -\frac{\nu_{yz}}{E_x} & \frac{1}{E_x} & 0 & 0 & 0 \\ 0 & 0 & 0 & \frac{1}{2G_{yz}} & 0 & 0 \\ 0 & 0 & 0 & 0 & \frac{1}{2G_{xy}} & 0 \\ 0 & 0 & 0 & 0 & 0 & \frac{1}{2G_{xy}} \end{bmatrix} \begin{bmatrix} \sigma_{xx} \\ \sigma_{yy} \\ \sigma_{zz} \\ \sigma_{yz} \\ \sigma_{zx} \\ \sigma_{xy} \end{bmatrix} \quad (3.1)$$

where the five independent constants are E_x and E_y are x and y components of elastic modulus, ν_{yx} and ν_{zy} are shear components of Poisson ratio and G_{xy} is the component of shear modulus.

The piezoresistive matrix which represents the relationship between changes in resistivity and applied strains is:

$$\begin{bmatrix} \Delta_1 \\ \Delta_2 \\ \Delta_3 \\ \Delta_4 \\ \Delta_5 \\ \Delta_6 \end{bmatrix} = \begin{bmatrix} \Pi_{11} & \Pi_{12} & \Pi_{12} & 0 & 0 & 0 \\ \Pi_{12} & \Pi_{11} & \Pi_{12} & 0 & 0 & 0 \\ \Pi_{12} & \Pi_{12} & \Pi_{11} & 0 & 0 & 0 \\ 0 & 0 & 0 & \Pi_{44} & 0 & 0 \\ 0 & 0 & 0 & 0 & \Pi_{44} & 0 \\ 0 & 0 & 0 & 0 & 0 & \Pi_{44} \end{bmatrix} \begin{bmatrix} T_1 \\ T_2 \\ T_3 \\ T_4 \\ T_5 \\ T_6 \end{bmatrix} \quad (3.2)$$

where Δ vector is the change in resistivity, Π is the piezoresistive matrix and T is the applied strain matrix.

4.2.4 Loads and Boundary Conditions

The loads and boundary conditions of a tensile test were simple to apply. The bottom cross sectional area was constrained in all directions while axial force was applied to the other end to apply stretching to the sensor. The force applied was constant but different magnitudes of the force were applied to obtain relation between change in resistance and change in strains due to the applied forces.

CHAPTER 5

RESULTS AND DISCUSSION

In this section, results of the experiment and the computational model will be presented and detailed discussion is presented. Various experiments were performed to test the carbon fiber sensor and a parametric study was also carried out to study the effect of parameters that influence the sensors signals. The purpose of the experiments is to study the relation between strains and change in resistance and what parameters have significant effect on the performance. The experiments were carried out in form of different studies hence, the subsections of this chapter will deal with each study.

5.1 Tensile tests

For the tensile experiments on the carbon fibers, tests were first conducted to observe the stress-strain behaviour of the carbon fiber material. This will also indicate the fracture point at which the sensor would break. Based on this information, the strain levels at which the carbon fibers operate can be estimated.

For each of the four carbon fiber tows, tensile tests were performed with and without the epoxy coating, to observe how the epoxy affects the stress-strain curves. Results of 1K, 3K, 6K and 12K are shown below.

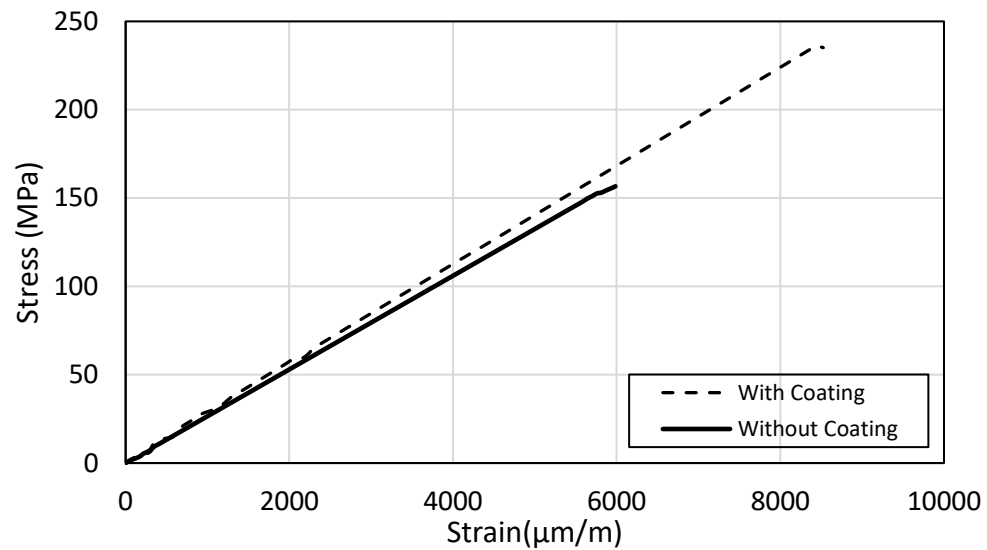


Figure 5-1 Strain-Stress Plot of 1K with and without coating.

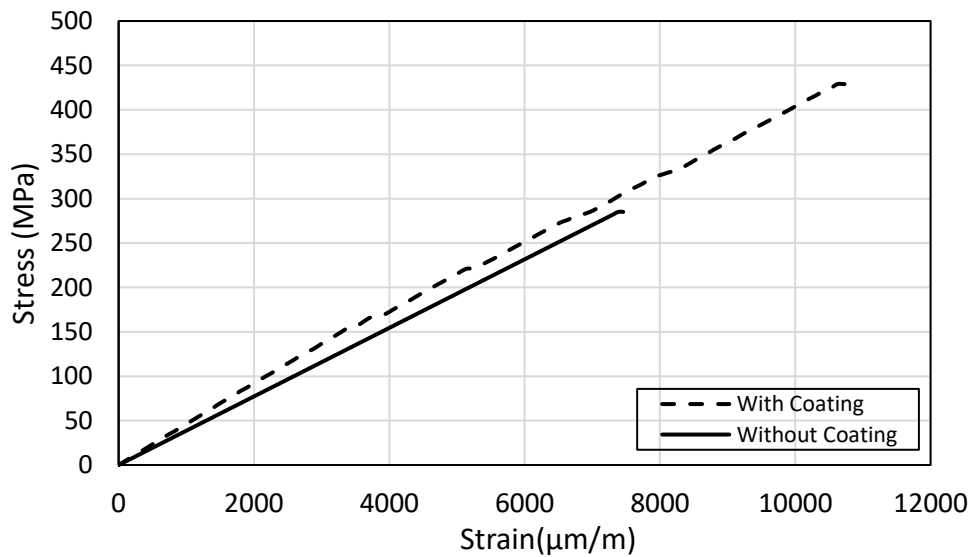


Figure 5-2 Strain-Stress Plot of 3K with and without coating.

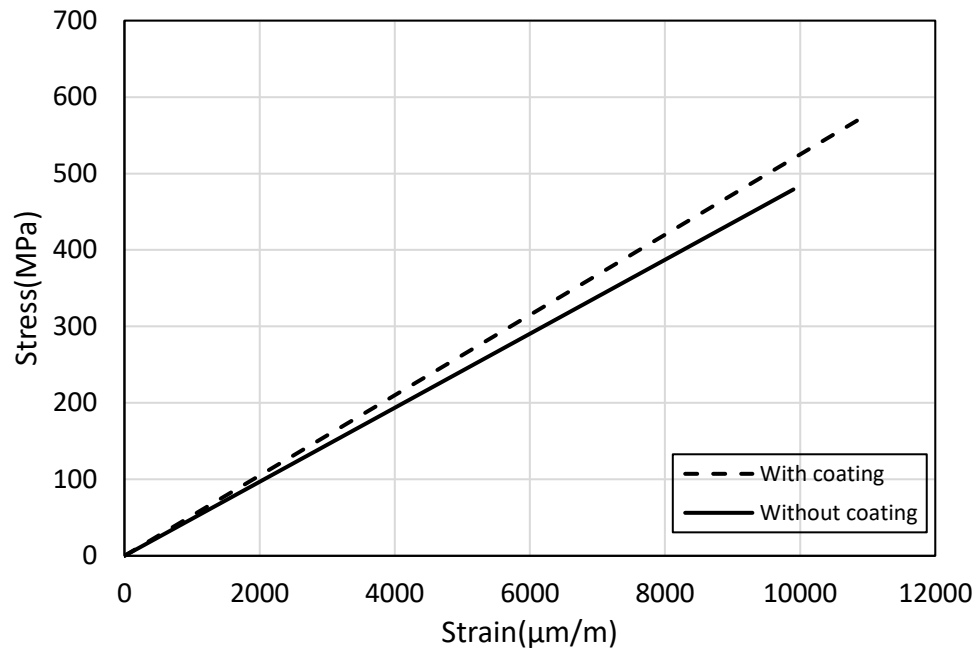


Figure 5-3 Strain-Stress Plot of 6K with and without coating.

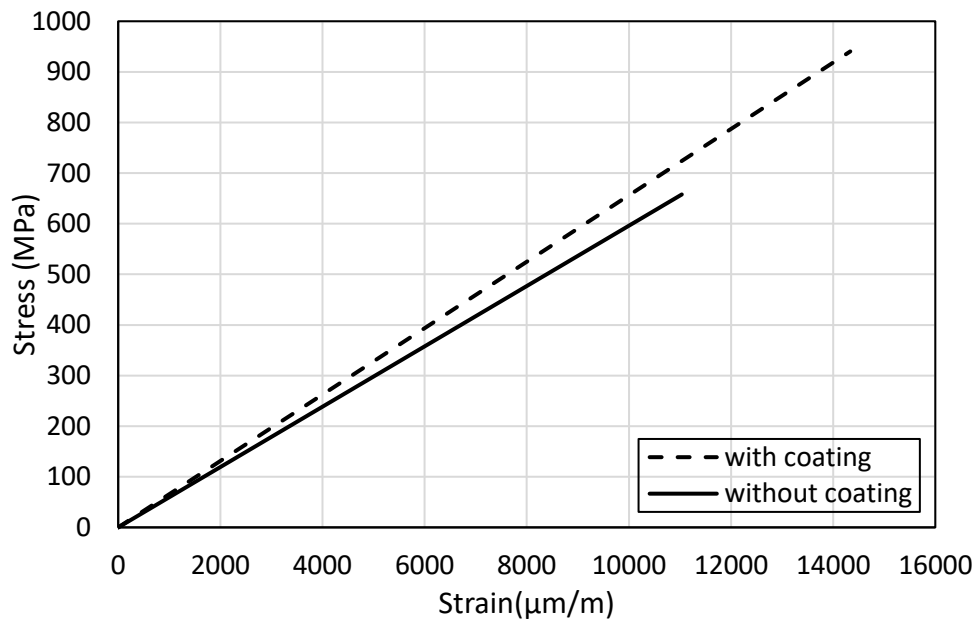


Figure 5-4 Strain-Stress Plot of 12K with and without coating.

It can be observed from the above graphs that coating increases the strength of the carbon fiber and makes them able to withstand higher stresses. Figure 5-5 shows the combined plots of all the fibers with coating. As the number of fibers increase, the stress needed to break the fibers rises. It can also be noted that the fibers can have maximum strain level of up to 15,000 $\mu\text{m}/\text{m}$ for 12K fibers.

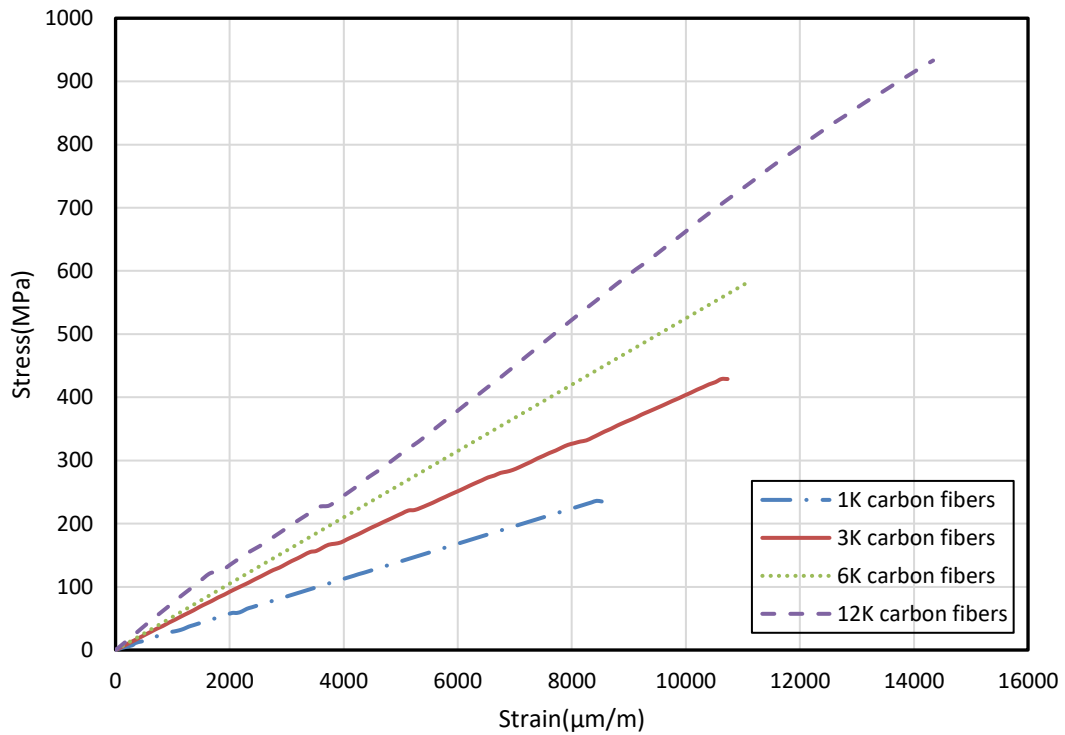


Figure 5-5 Stress-Strain curves of all fibers with coating.

5.1.1 Effect of diameter on change in resistance

In this study, the effect of diameter of the carbon fiber sensor is observed. Four samples were tested: 1K, 3K, 6K and 12K fibers. The other parameters such as length and epoxy treatment was kept constant so purely the response to diameter can be observed.

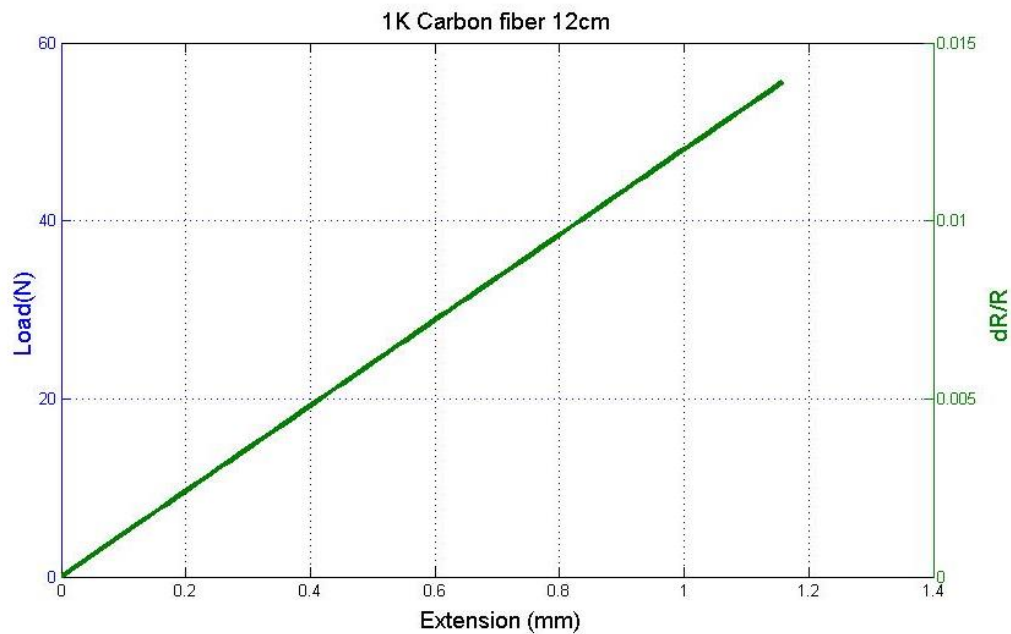


Figure 5-6 Variation of load and change in resistance vs extension of 1K fiber.

The results, shown in Figure 5-6, show that 1K carbon fiber sensor can detect loads up to 60 N. The relationship between changes in resistance/initial resistance versus extension is linear. Because of the relatively low number of fibers, this sensor can withstand a load only up to 60 N. It was observed that 1K had the least relative change in resistance among all the fibers. The least relative change in resistance is due to the fact that 1K, being the sample containing the least amount of fibers, is very fragile thus it breaks easily.

The experimental results were verified with the analytical values calculated using analytical formula ($R = \rho L/A$). The result is shown in Figure 5-7 where it can be observed that experimental values are slightly lower than the calculated ones. The lower values of the experiment are attributed to the increase in piezoresistance of the fibers. It is seen that mostly the change in resistance is due to change in dimensions. The results are consistent with the findings of Blazweick et al. who observed that values obtained from experiment are lower than those estimated analytically using the linear equation the governs variations of resistance due to change in geometrical parameters [31].

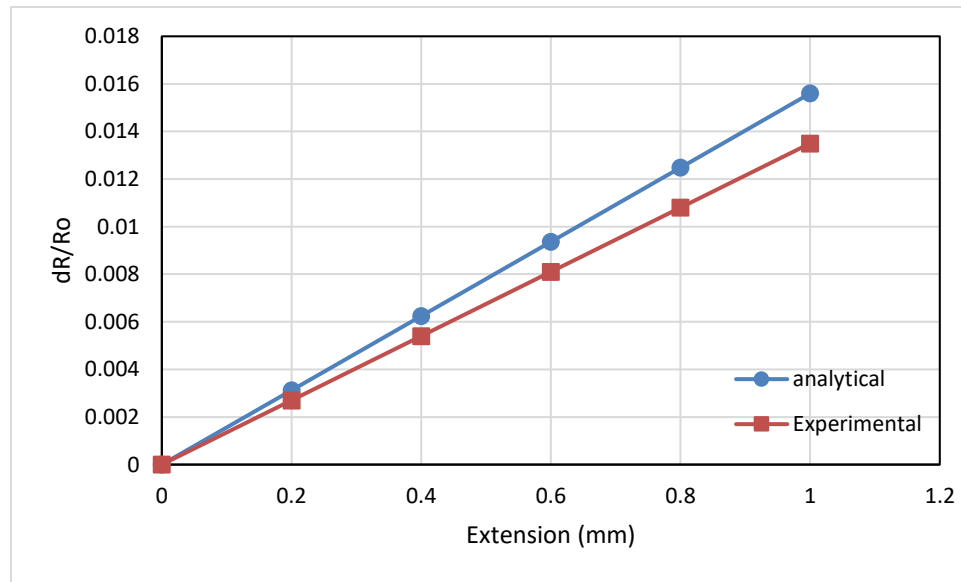


Figure 5-7 Comparison between analytical and experimental values of 1K.

Similarly, graph of 3K in is shown in Figure 5-8, 6K in Figure 5-10 and 12K in Figure 5-11 individually followed by Figure 5-12 in which all graphs are combined.



Figure 5-8 Plot of load and change in resistance vs extension of 3K fiber.

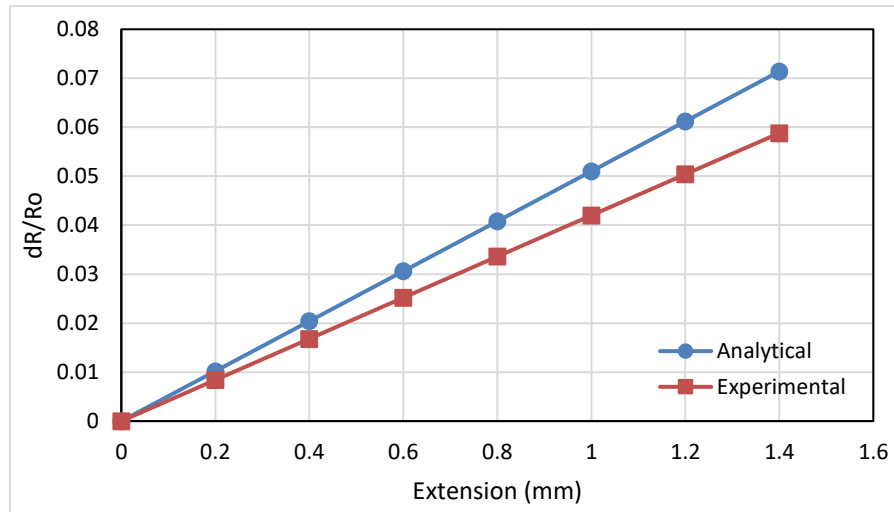


Figure 5-9 Comparison between analytical and experimental values of 3K.

The experimental results of 3K carbon fibers were verified with analytical values and are shown in Figure 5-9. It is observed that experimental values are lower than the analytical one as seen in 1K.

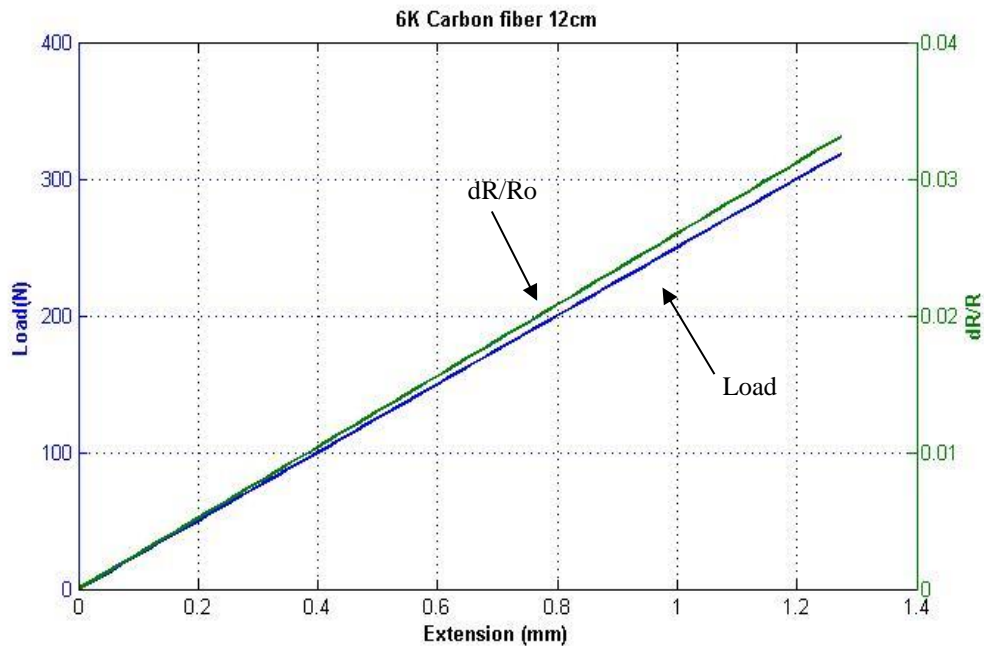


Figure 5-10 Variation of load and change in resistance vs extension of 6K fiber.

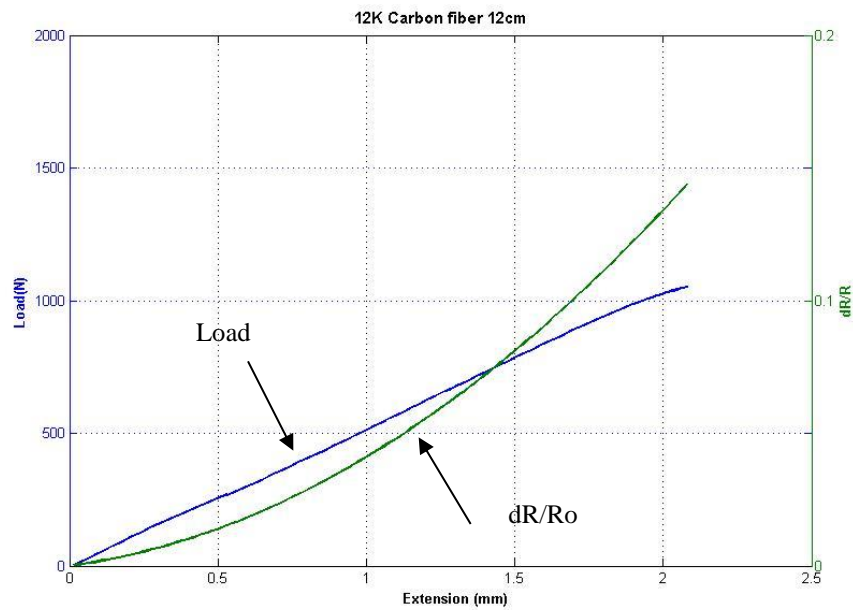


Figure 5-11 Plot of load and relative change in resistance vs extension of 12K fibers.

In the plot of 12K carbon fibers, the load versus extension is linear. However, the variation of resistance exhibit nonlinear pattern. The nonlinearity may be attributed to

wrinkling or slippage due to high number of fibers. However, the main cause of nonlinearity is that the fibers may not be properly treated with epoxy resin. This would lead to transverse resistance and result in nonlinear trend. This nonlinear fashion was also observed in results reported in literature in [34, 51].

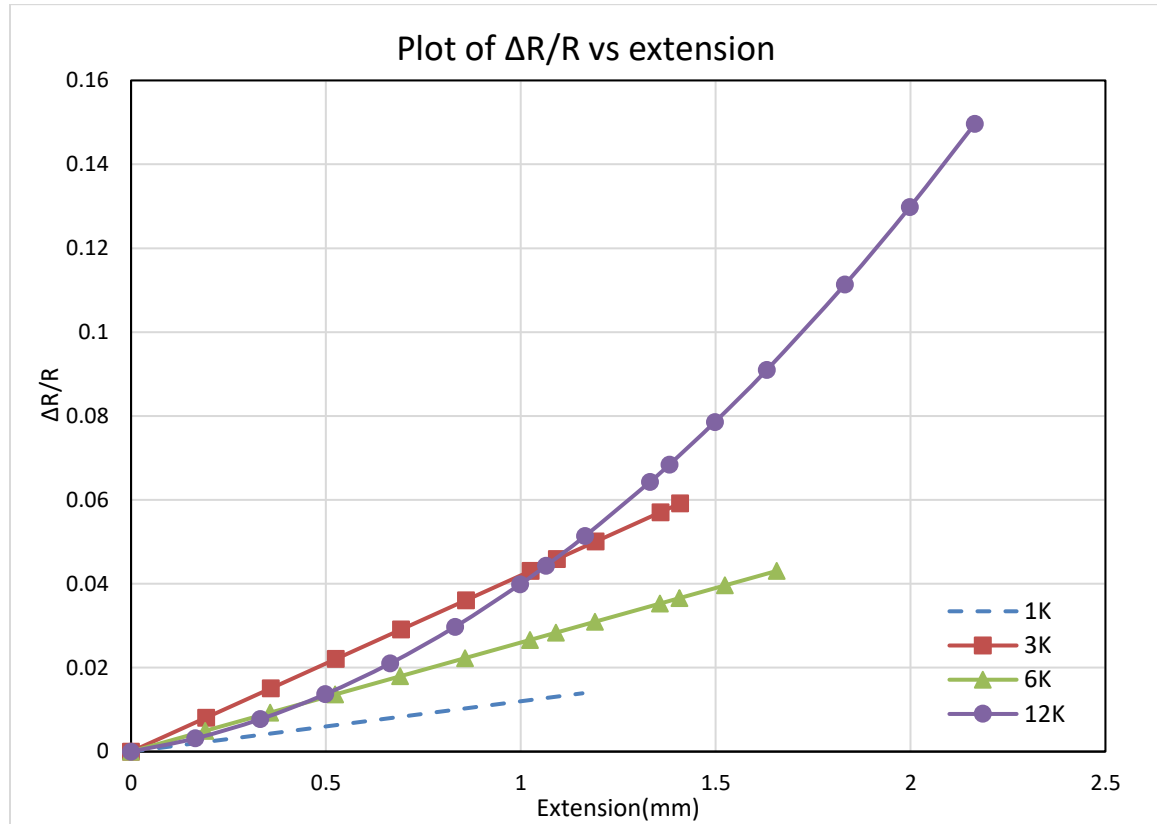


Figure 5-12 Extension vs $\Delta R/R_o$ of all the fibers.

Figure 5-12 shows the relative change in resistance of all the fibers in one plot. It is observed that 1K fiber has the least relative change in resistance. 6K and 12K display almost similar behavior up to 0.6 mm but it is observed that 12K shows non-linear behavior after 0.42mm extension. Therefore, 12K fibers can be used as linear sensor if the strain level is relatively low [51].

From the plots, it is seen that 6K carbon fibers display less resistance than expected. These experimental results of 6K were verified with analytical results to find an explanation to the results. The results are shown in Figure 5-13 where it is observed that the experimental results are very low compared to the analytical results. Here, a greater difference is observed than the difference in Figure 5-7. This indicates that the change in resistance is not linear due to change in dimensions and there is contribution from other factors. It is expected that the effect of transverse resistance in the piezoresistivity is significant when the number of fibers is more than 3K. Fibers with large number of filaments (6K and above) start to exhibit nonlinear behavior. However, the fibers of 6K filament are relatively weak and cannot withstand higher load; otherwise, it would have nonlinear trend similar the 12K fibers. Therefore, the 1K and 3K exhibit linear trend and can be used for low level strain applications. The 6K is not recommended because it does not provide higher strain range and the resistance variation is lower than 3K fibers. The 12K fibers have the highest range of strains, stresses and resistance variation but nonlinearity has to be taken into account.

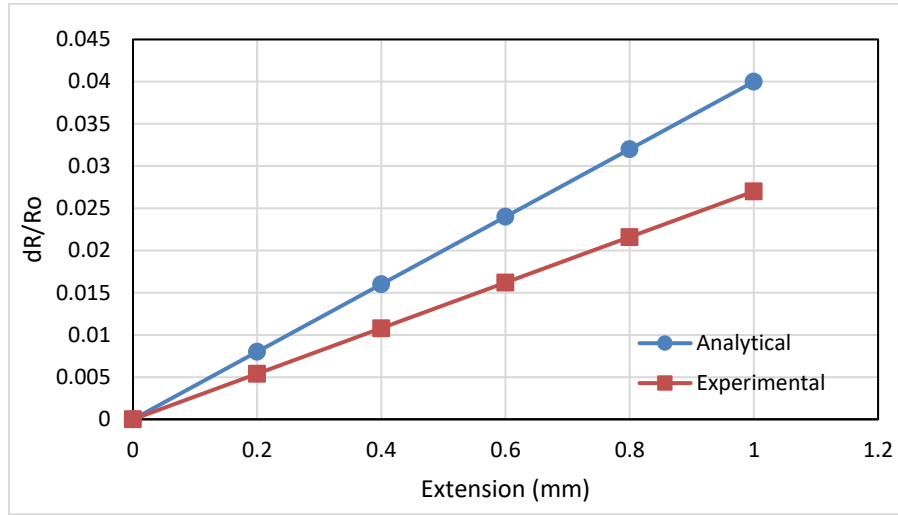


Figure 5-13 Comparison of analytical and experimental results of 6K.

5.1.2 Effect of length of sensor on dR/Ro

In this study, lengths of the sensors are varied and results are observed for change. Three type of fibers were considered: 1K, 3K and 6K while each type was cut into lengths of 4, 8 and 12 cm. Sample of 12K carbon fiber was not included as it displayed nonlinear results. The other parameters such as diameter and epoxy treatment was kept constant so purely the response to length can be observed.

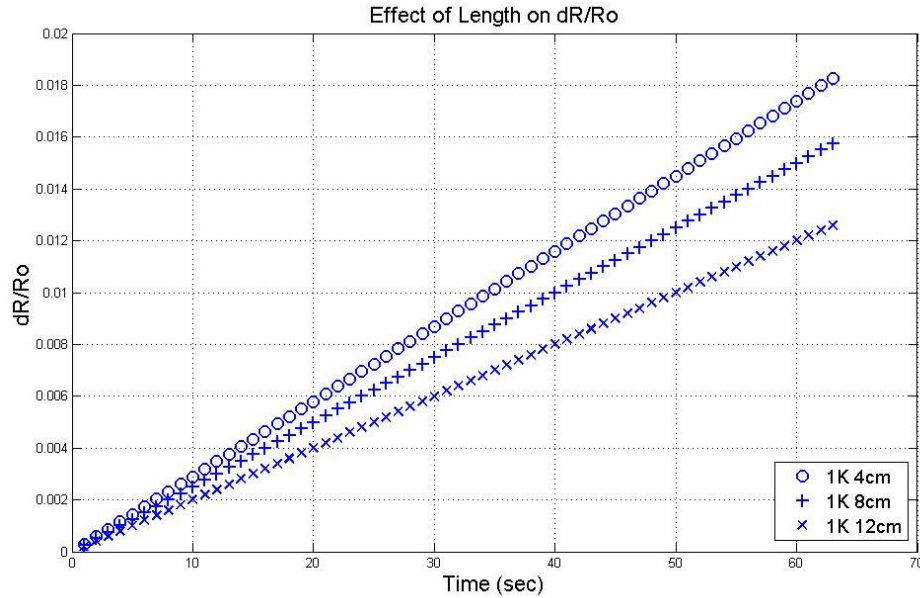


Figure 5-14 Effect of length on $\Delta R/R_0$ of 1K samples.

The plot in Figure 5-14 represents the change in resistance vs time for the 1K sample. It is observed that as the length increases, the change in resistance decreases slightly meaning the more length of the sensor, the less sensitive it is to change in strains.

This phenomenon is due to the fact that the resistance value increases with length because of the well-known formula ($R = \rho L/A$) which states that the resistance is directly proportional to the length. The calculated resistance using the formula of 12 cm is 39.15Ω and of 4 cm is 13.05Ω . The 12cm sample has more resistance than the 4cm sample. The change in resistance formula used is $\Delta R/R_0$ where the change in resistance is divided by the initial resistance. If the initial resistance is large, the term $\Delta R/R_0$ will be small because initial resistance term is in the denominator. Hence, it can be deduced that as length increase, the resistance will increase and thus $\Delta R/R_0$ will decrease.

The same effect can be observed on the 3K and the 6K carbon fiber sensors, in Figure 5-15 and Figure 5-16 respectively, thus proving the phenomenon is not effected by change in diameter.

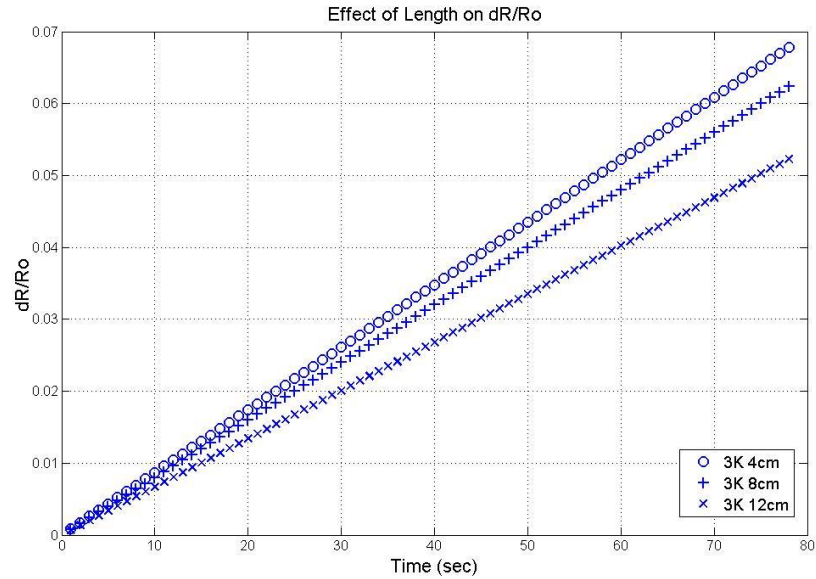


Figure 5-15 Effect of length on dR/Ro of 3K carbon fiber.

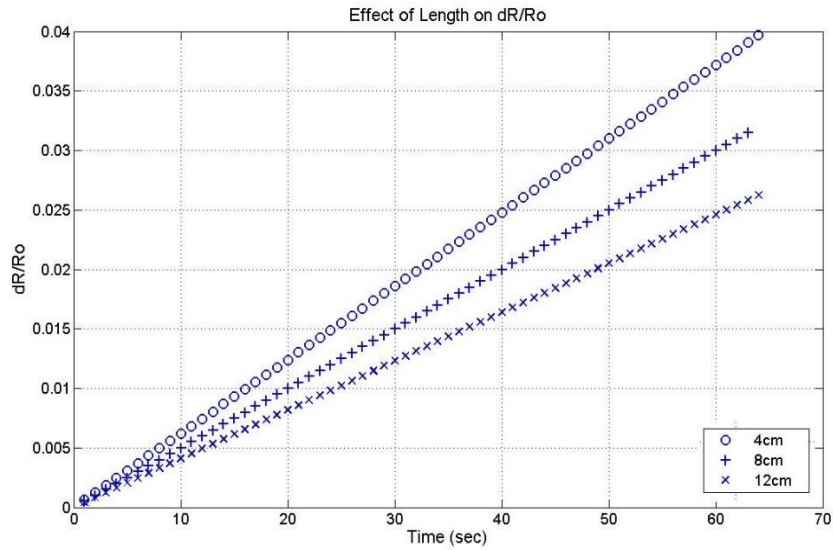


Figure 5-16 Effect of length on dR/Ro of 6K carbon fiber sensor.

5.1.3 Effect of Epoxy treatment on carbon fiber sensor

For this study, it was desired to observe the effect of epoxy treatment of the carbon fiber sensor. The mixture used for treatment contains 5-parts epoxy resin and 1-part hardener. Only one fiber diameter can be used to test the effect of treatment and for that 3K sample was chosen because it displayed the best results when tested in section 5.1.1. The other parameters such as length and diameter was kept constant so purely the response to epoxy treatment can be observed. Figure 5-17 shows the results of the study where “5/1” refers to 5-parts epoxy resin and 1-part hardener. It can be observed that changing the ratio of epoxy and hardener has insignificant effect on the response of the sensor.

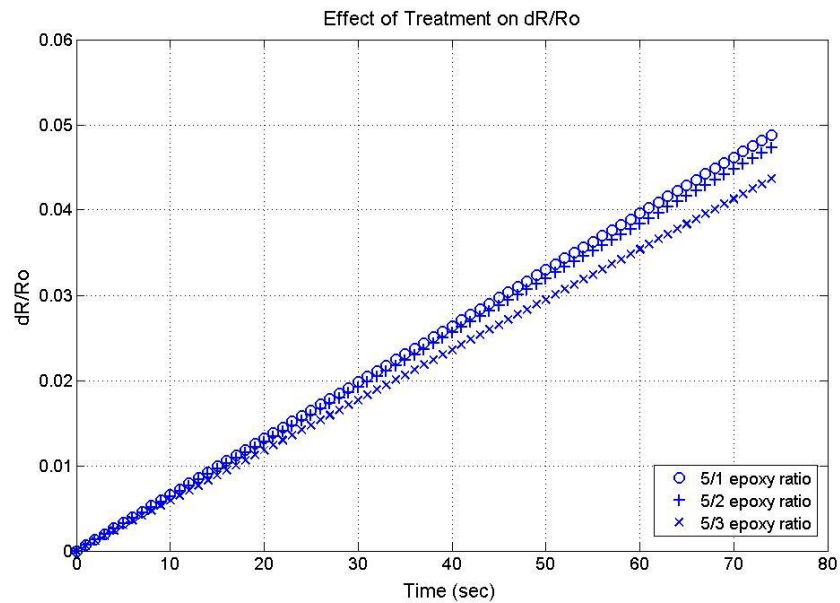


Figure 5-17 Effect of epoxy treatment on carbon fiber sensor.

5.2 Impact test

After studying the behavior of the sensors subjected to tensile testing, the task here is to observe the performance of the sensor due to an impact test. As discussed in the literature, low velocity impact damage is one of the major defects in composite materials and, therefore, it is essential to examine the performance of the sensor under impact loads. Particularly, impact force causes strains/deflection on the structures which can be measured by the embedded carbon fiber sensor in terms of change in resistance.

Impact tests were carried out on composite plates embedded with one carbon fiber sensor as shown in Figure 3-10. Experiments were repeated with different values of impact energies to observe how sensor's output varies with different magnitudes of impact force on the plate. Five different values of impact energies were chosen: 5J, 6J, 7J, 8J and 10J. with one of them such that a visible damage is observed on the plate. Sensor's output when the damage occurs is recorded and this value is correlated with the strain measurements. The measured values can be used to characterize the sensor so that it would be known that damage has been inflicted on the structure.

Figure 5-18 illustrates the plot of deflection and energy plotted against time when the impactor was set to fall with impact energy of 5 J. The graph reaches its maximum value at the point of maximum deflection where impact energy is also maximum. The energy curve eventually settles down after its maximum point while the deflection decreases after the maximum point. The value of the impact energy curve at the end shows the amount of impact energy absorbed by the plate. It can be observed that maximum energy is close to

not 5J but 4.25 J because some energy is changed into internal energy and that impact energy absorbed by the plate is 3.5 J.

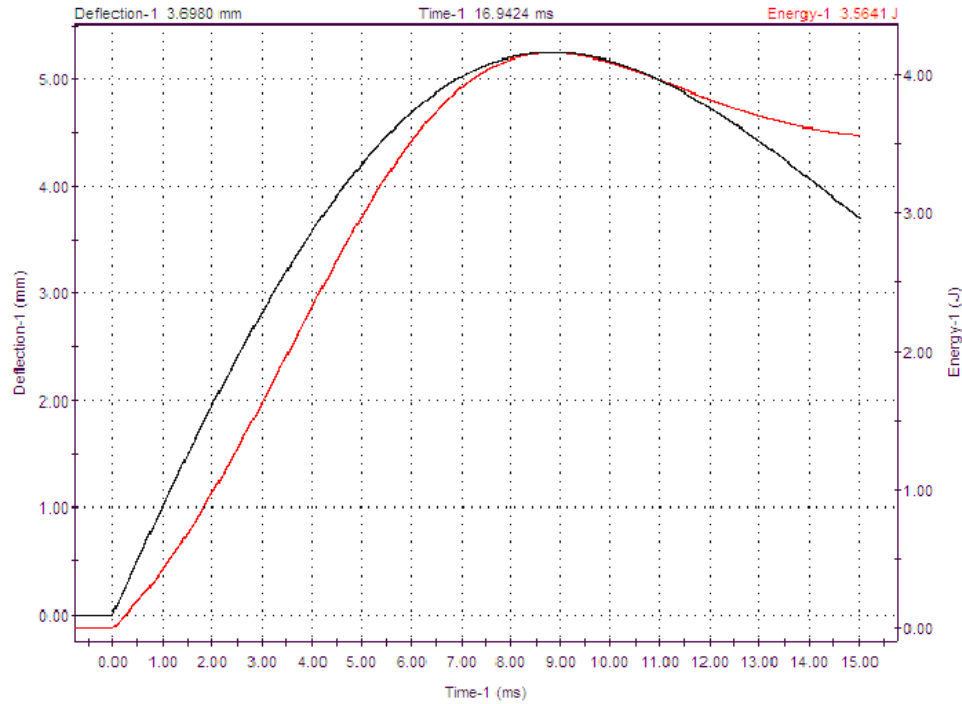


Figure 5-18 Deflection and energy curve for 5 J impact. Black curve: deflection. Red curve: energy.

For this impact with impact energy of 4 J, Figure 5-19 shows the output of the carbon fiber sensor in percentage change in resistance when plotted along with the deflection curve versus time. The results show that the change in resistance of the carbon fiber sensor closely follows that of deflection. The curve for the resistance has a peak that leads the peak of the deformation. This can be attributed to the nature of deformation that occurs at the impact point. Since the sensor is placed at the bottom surface, it cannot detect the crushing of the plate (plastic deformation) relative to the bottom surface. However, the results show that the sensor can detect the induced strains on the plate due to impact damage. From each

impact damage inflicted on the plate, the maximum value of the deflection is of interest, as the damage will depend on the highest value of the impact load. Therefore, from the impact tests with different impact energies, the highest deflection of the plate and the corresponding output of the carbon fiber sensor were noted in Table 5-1.

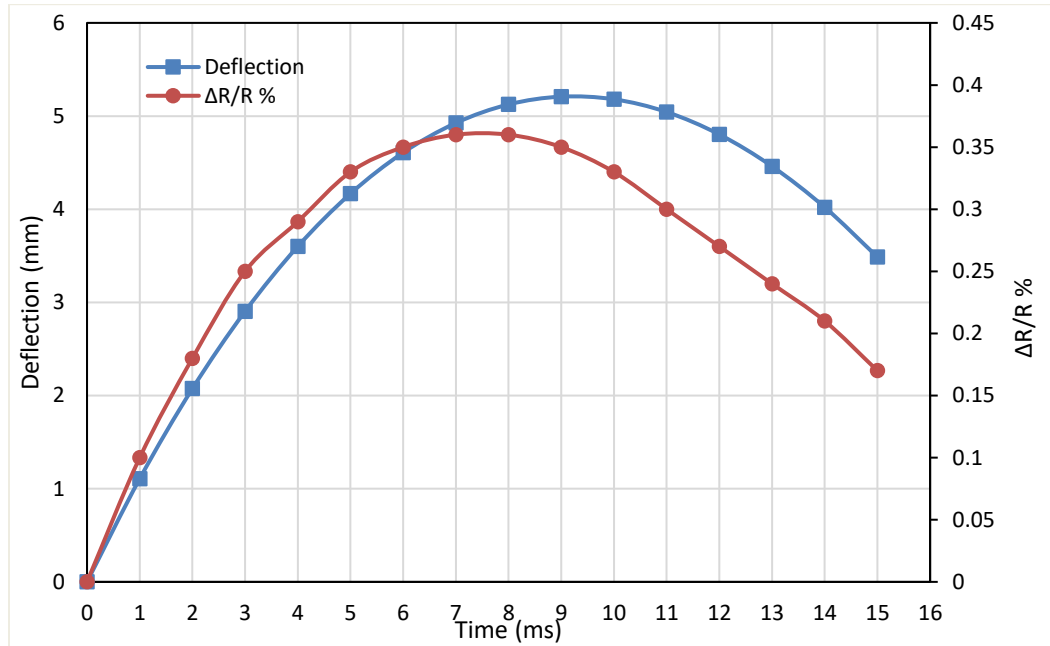


Figure 5-19 Plot of deflection vs time vs $\Delta R/R_o$ %.

Similarly, experiments were carried out on plates with carbon fiber sensor with different impact energies. Five experiments were performed with impact energies of 5J, 6J, 7J, 8J and 10J. It was noted that if the impact energy was increased beyond 15 J, a through hole was inflicted on the plate, which means that the plate is completely penetrated. However, the sensor did not breakdown. Comparing the level of strain attained in the impact test with tensile test results of carbon fibers, the range of strain that causes permanent damage to the plate is relatively small and within the linear range of the carbon

fiber sensors. Moreover, the change in resistance is also within the measurable range of used sensors. This demonstrate the capability of the carbon fiber sensors to detect impact damages.

The deflection of the plates due to different impact energies is plotted in a single graph in Figure 5-20. The 10 J was chosen to ensure enough impact damage is inflicted to the plate to see visible and permanent results. It is seen that 10 J causes a comparatively high deflection compared to other impact energies. A visible deep indent was observed at the location where impactor struck the plate. This is the cause of the higher deflection value as the impactor had penetrated few millimeters deep into the plate upon striking it.

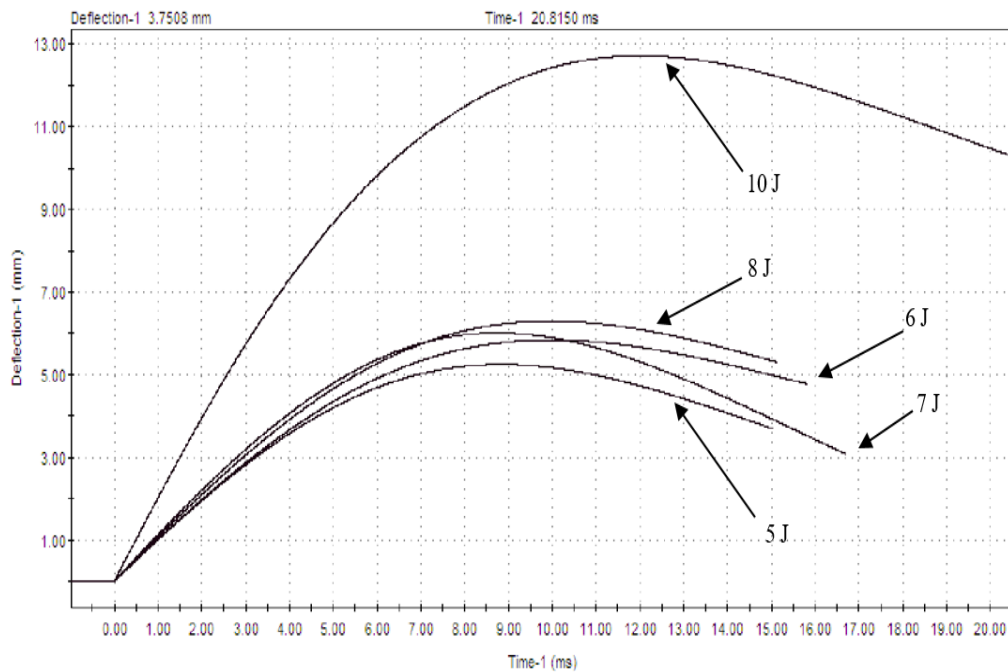


Figure 5-20 Deflection plots of all five impact tests

The corresponding response of the carbon fiber sensor for the mentioned impact energies was recorded and is plotted in Figure 5-21. It is observed that the output curves match those of the deflection and thus giving us confidence in sensors ability to predict impact damage. The maximum damage caused by any impact energy would be at the maximum value of the sensor output for that impact energy. From the performed experiments, the maximum deflection and the corresponding sensor's output are noted in Table 5-1, it was found that 10J impact energy caused visible damage to the plate in form of an indent while other impacts did not have any significant visible damage. Thus, the maximum value of the sensor output at 10J can be correlated with damage; meaning whenever the sensor output reaches that value (0.895 in this case), it can be known that damage has occurred in the plates.

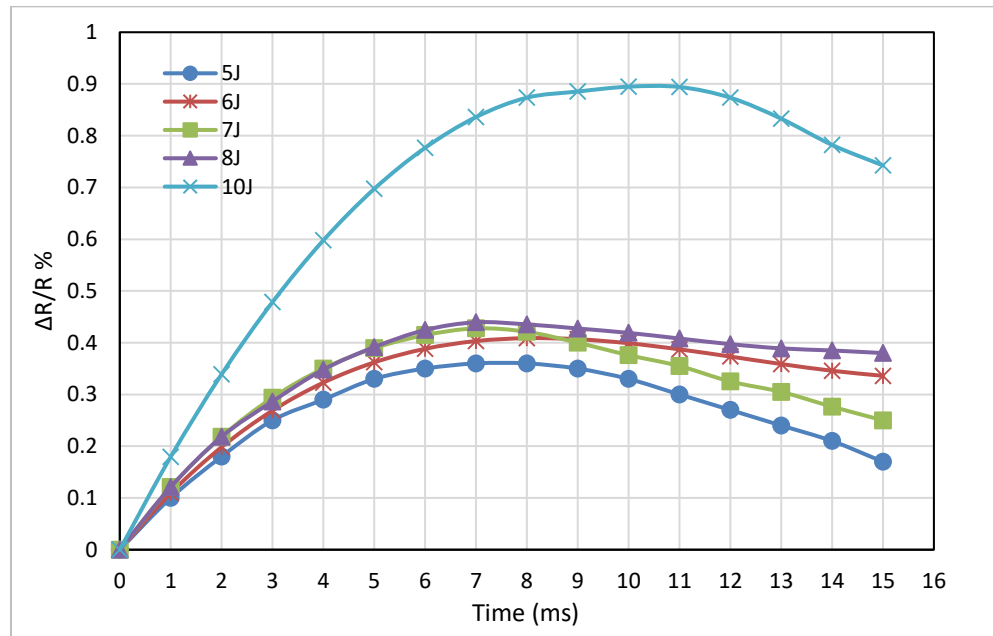


Figure 5-21 Carbon fiber sensor output for five different impact energies

Table 5-1 Max deflection and sensor's output

	5J	6J	7J	8J	10J
Max deflection(mm)	5.1354	5.8762	6.0738	6.4725	12.8114
Corresponding sensor output ($\Delta R/R$ %)	0.3654	0.4088	0.4277	0.4395	0.89478

Figure 5-22 shows the plate after it was hit by the impactor at the impact energy of 5J. Though the plate becomes discolored at the hit location, no dents were found on either side of the plate. However, when the plate is hit with impact energy of 10J, a dent is clearly visible as shown in Figure 5-23.

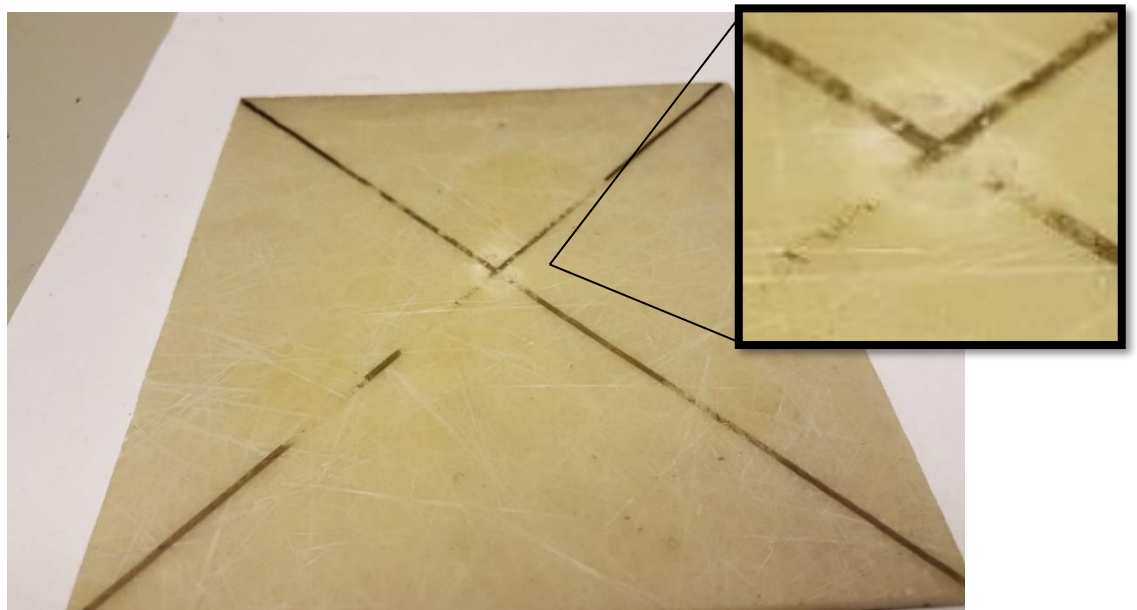


Figure 5-22 impactor damage mark when using impact energy of 5J.

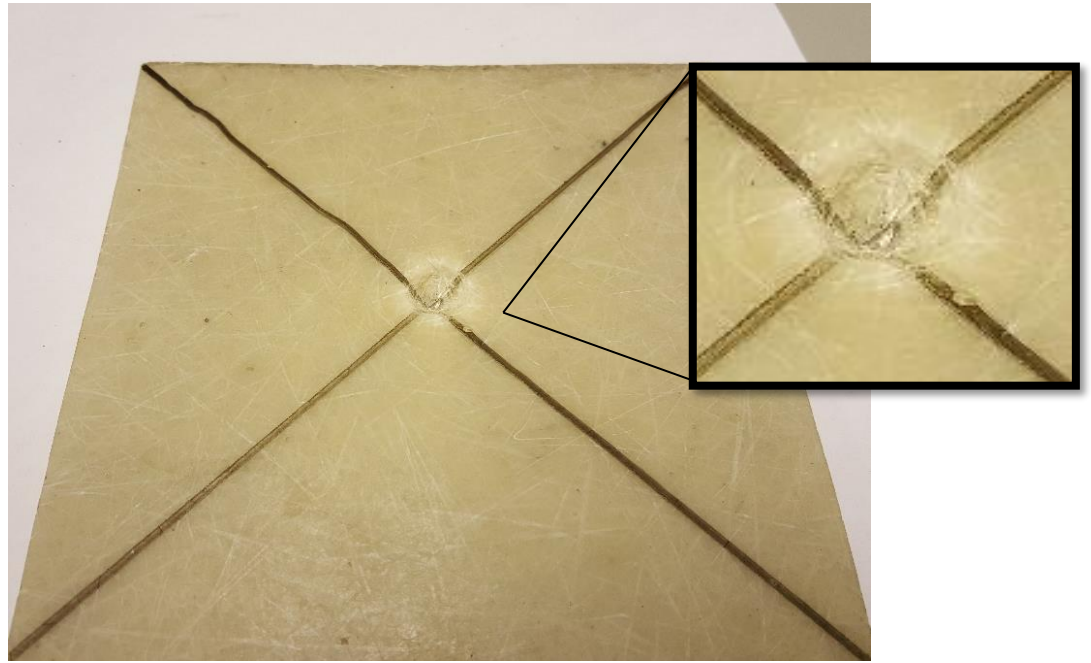


Figure 5-23 Dent left from the strike using impact energy of 10J

5.3 Computational Results

5.3.1 Computational model of carbon fiber sensor

In this section, results of the computational model of the carbon fiber sensor is presented. The model was calibrated using the experimental data. Strains were applied on the COMSOL model by fixing one end and having a gradual increase in applied force to the other end. Figure 5-24 shows the carbon fiber sensor model when strain is applied. It can be noted that maximum displacement occurs at the free end which is the top end in the figure. Stress and strain distribution contours can be seen in Figure 5-25. Since only constant stress is applied, it is seen that only a constant stress can be observed. Also for a constant value of stress, the value of strain will also remain constant.

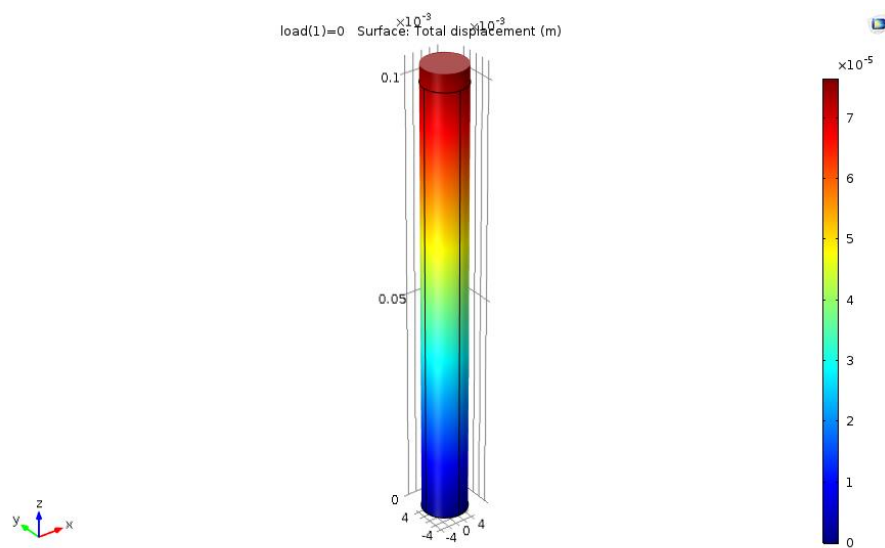


Figure 5-24 Displacement Contours on the carbon fiber sensor

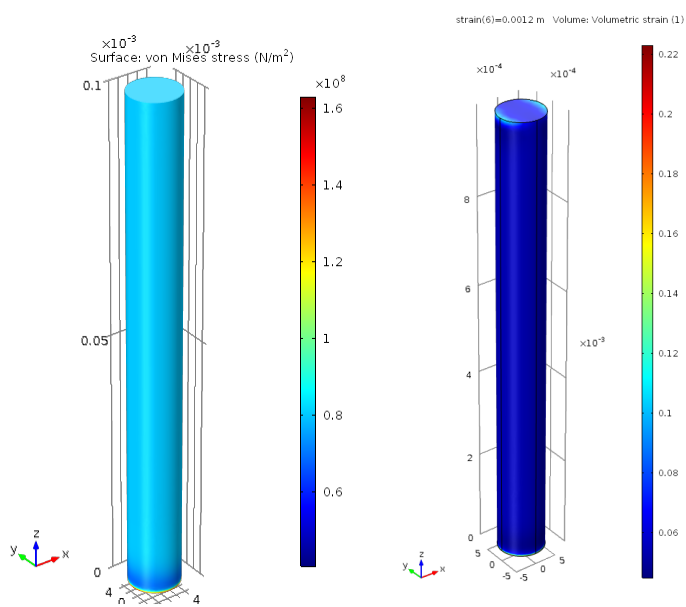


Figure 5-25 Left: Von Mises Stress. Right: Strain distribution.

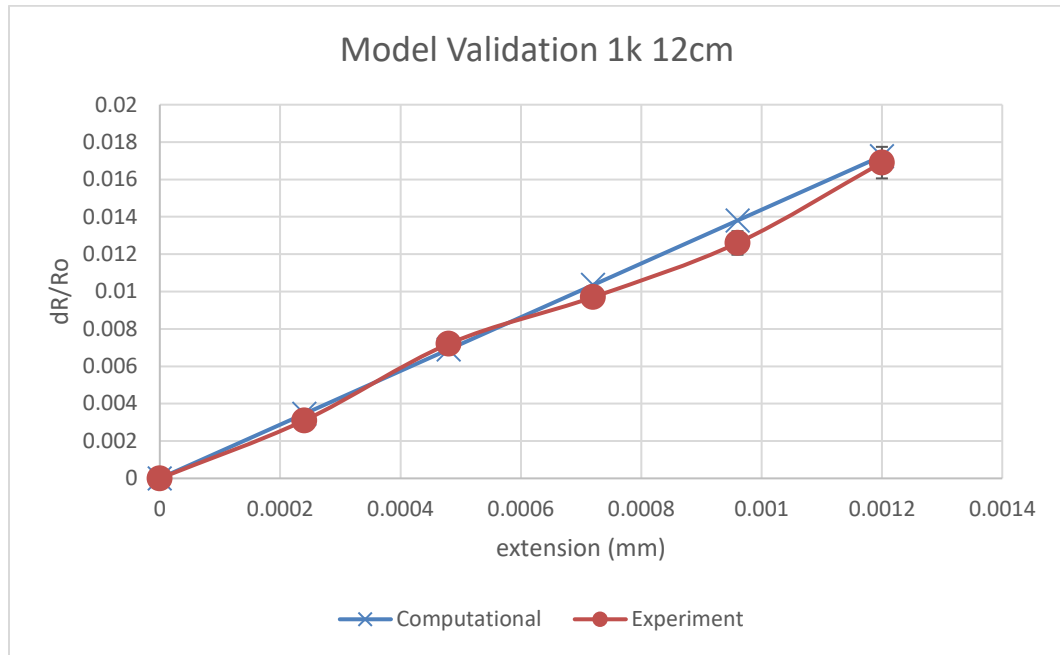


Figure 5-26 Comparison of experiment and COMSOL results

The numerical model requires the piezoresistive coefficients to be entered in order to solve the differential equations as explained in chapter 4. Then the model was calibrated to fit the experimental data. Parameter estimation was performed on piezoresistive coefficients till the computational results agreed with the experimental ones. As can be observed in Figure 5-26, both graphs have good agreements with maximum error of 7.03% and average error of 6.04%.

The piezoresistive coefficients of the carbon fiber sensor obtained after calibrating the model with the experiments are shown in Table 5-2, with Silicon's to show the comparison between the two materials.

Table 5-2 Comparison of CFS and Si piezoresistive coefficients

Carbon fiber sensor	Silicon
$\pi_{11} = 6.530 \times 10^{-5} \text{ MPa}^{-1}$	$\pi_{11} = -102.2 \times 10^{-5} \text{ MPa}^{-1}$
$\pi_{12} = -1.0801 \times 10^{-5} \text{ MPa}^{-1}$	$\pi_{12} = 53.4 \times 10^{-5} \text{ MPa}^{-1}$
$\pi_{44} = 69.05 \times 10^{-5} \text{ MPa}^{-1}$	$\pi_{44} = 13.6 \times 10^{-5} \text{ MPa}^{-1}$

To ensure the accuracy of the estimated coefficients, the model was tested with different lengths: 8 cm and 4 cm of the same model. Since the material is same, the models with different lengths would have same piezoresistive coefficients and the obtained results should match with those obtained from the experimental data.

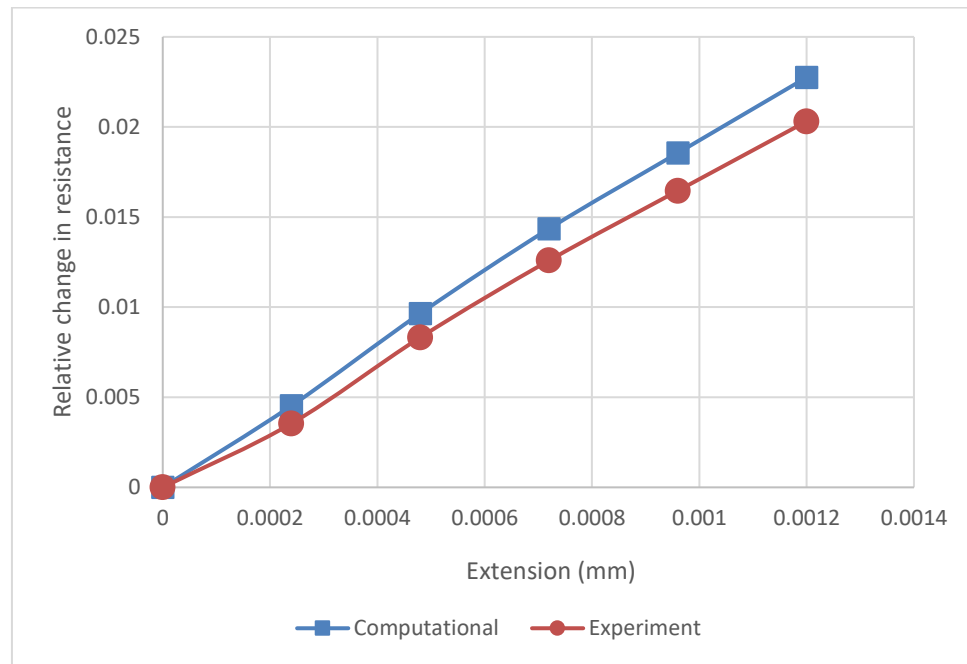


Figure 5-27 Model validation of computational and experimental data for 1K 8cm

Figure 5-27 shows the validation of computational and experimental data for the 1K 8cm sample. The results show that model agrees fairly with the results of experiments. The

maximum error obtained is 11.8%. Thus, by changing the length to 8cm, the model still gives results that can be compared to the results obtained by the experiments.

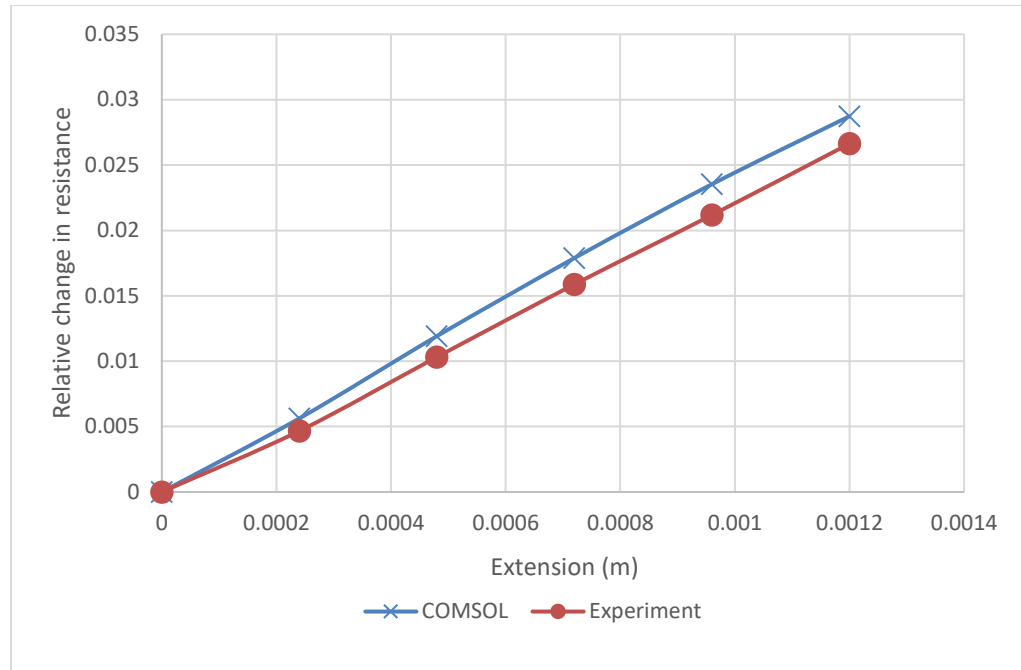


Figure 5-28 Model validation of computational and experimental data for 1K 4cm.

Figure 5-28 shows the model validation of computational and experimental data for 1K 4cm sample. It is shown that the graphs are close and maximum error obtained is 7.89% and the average error is 11.4%. it can be seen from the results that even if the length is changed in the model, the results obtained does agree with the results of the experiment. Hence, this gives us confidence in the validity of the computational model.

5.3.2 Model Validation using different piezoresistive coefficients

In previous subsection, 1K model of carbon fiber sensor was calibrated using experimental data and validated by observing the accuracy of the model when length is changed. In this section, it was desired to see how model would behave when piezoresistive parameters from one carbon fiber is used in the model of another carbon fiber with different diameter (or number of filaments). For example, observing the output of models of 3K, 6K and 12K when piezoresistive coefficients estimated from 1K experiment and then similar analysis was performed using the parameters of 3K, 6K and 12K experiments. The piezoresistive coefficients are shown in Table 5-3.

Table 5-3 Piezoresistive coefficients of 1K, 3K, 6K and 12 K carbon fiber sensors.

Carbon fiber sensors	π_{11}	π_{12}	π_{44}
1K	6.53×10^{-5}	-1.0801×10^{-5}	69.05×10^{-5}
3K	9.154×10^{-5}	-5.0641×10^{-5}	69.05×10^{-5}
6K	34.55×10^{-5}	-15.7285×10^{-5}	69.05×10^{-5}
12K	41.79×10^{-5}	-20.6247×10^{-5}	69.05×10^{-5}

Using the estimated parameters for 1K (from Table 5-2), it can be observed from the graphs in Figure 5-29 that the model can predict the experimental data of 3K carbon fiber sensor but is not accurate in predicting 6K and 12K. This is due to the 6K and 12K experiments giving us different results due to fiber breakage and internal resistance between the fibers.

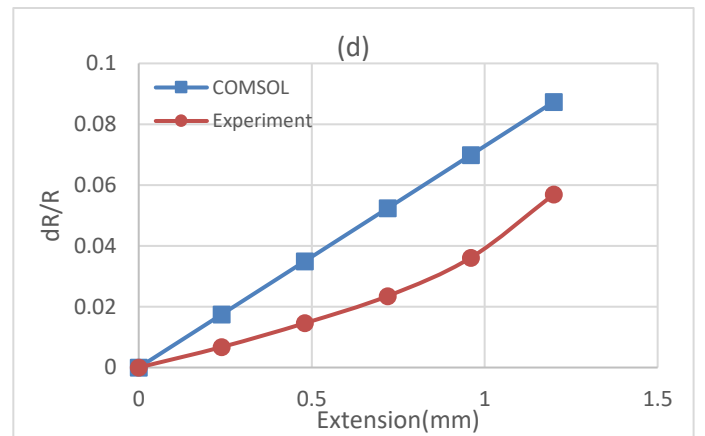
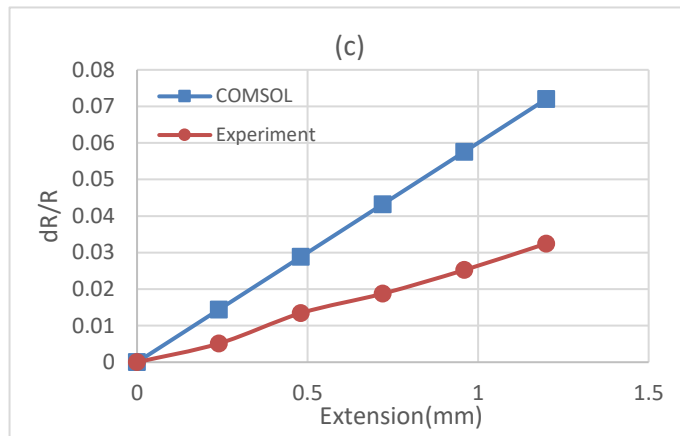
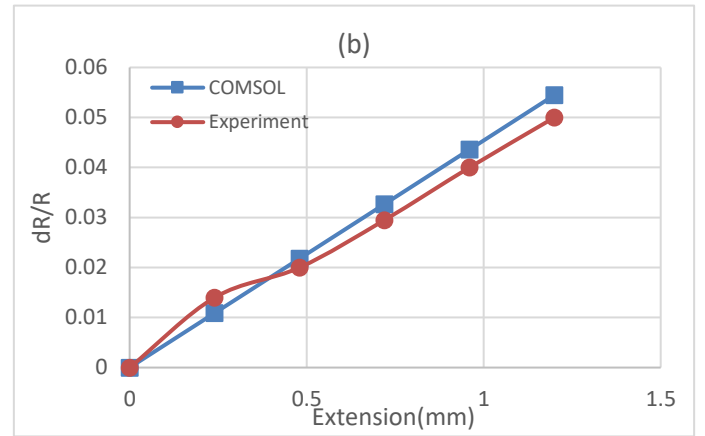
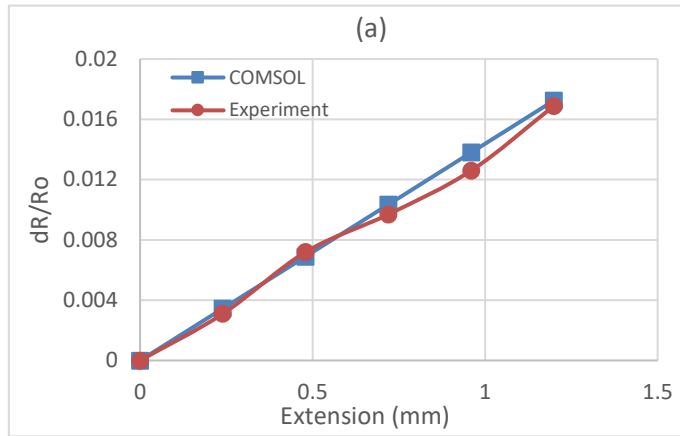


Figure 5-29 Model validation using 1K parameters for (a) 1K Model, (b) 3K Model, (c) 6K Model, (d) 12K Model.

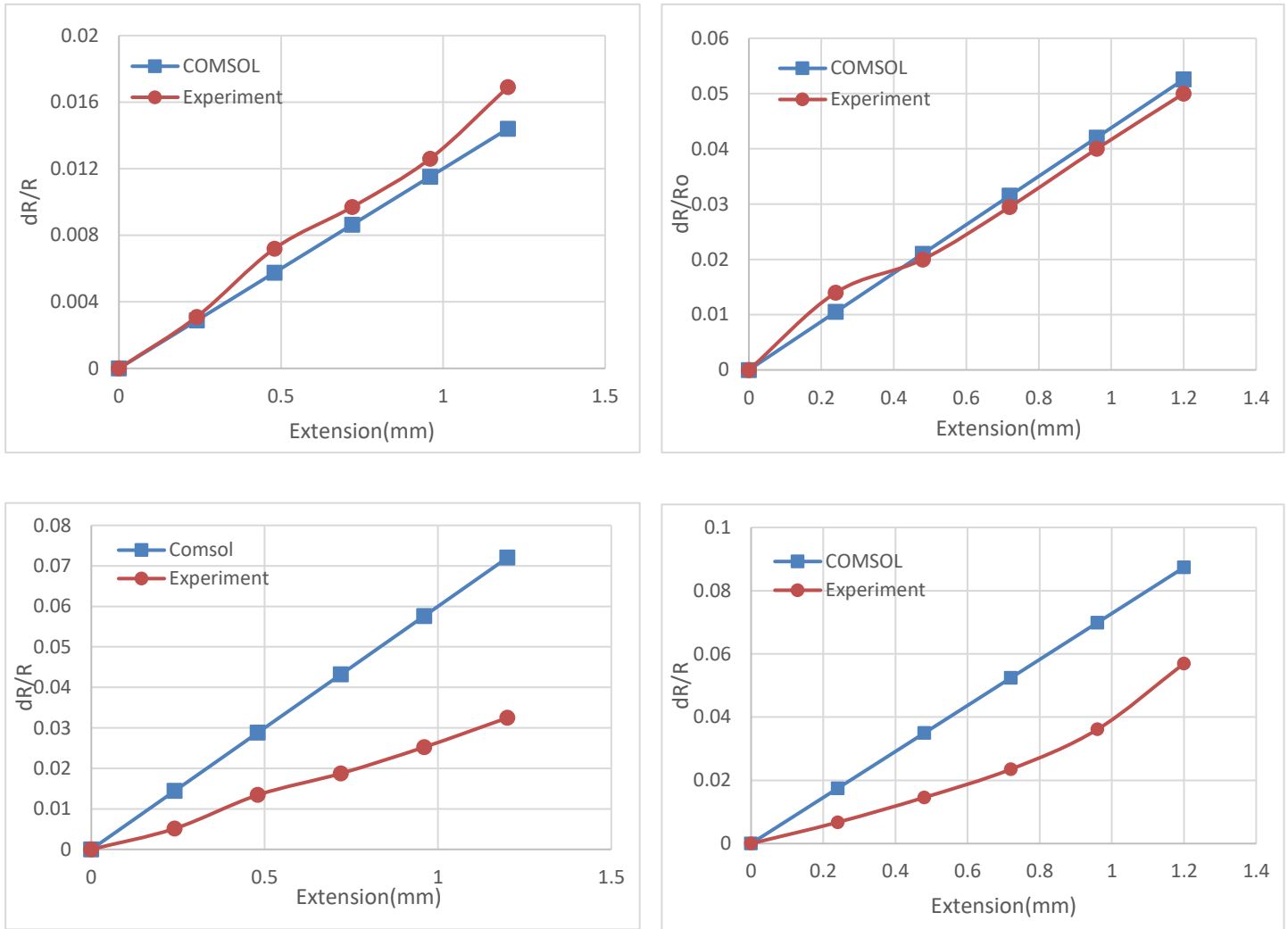


Figure 5-30 Model Validation using 3K parameters for (a) 1K Model, (b) 3K Model, (c) 6K Model, (d) 12K Model.

Figure 5-30 shows the response of the models using piezoresistive parameters estimated using the experimental test of 3K carbon fiber. similar observation can be made that again 1K and 3K are predicted fairly but 6K and 12K are not because of experimental results been different due to output been affected by resistance changes due to internal connections of fibers and fiber breakage.

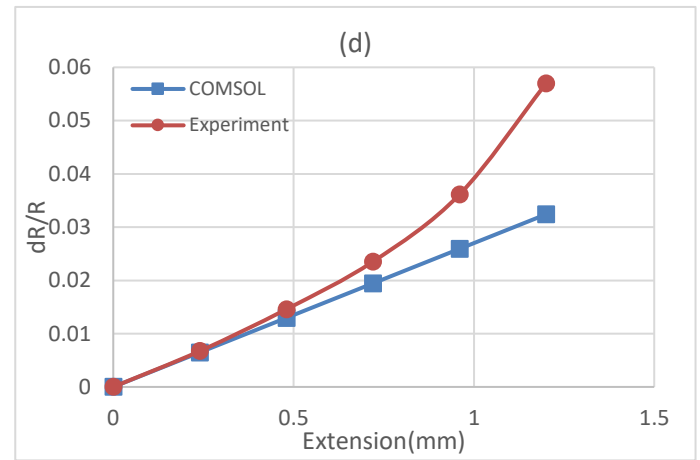
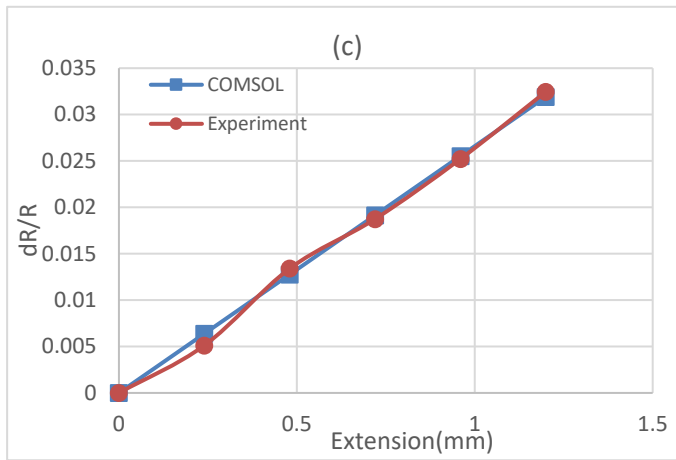
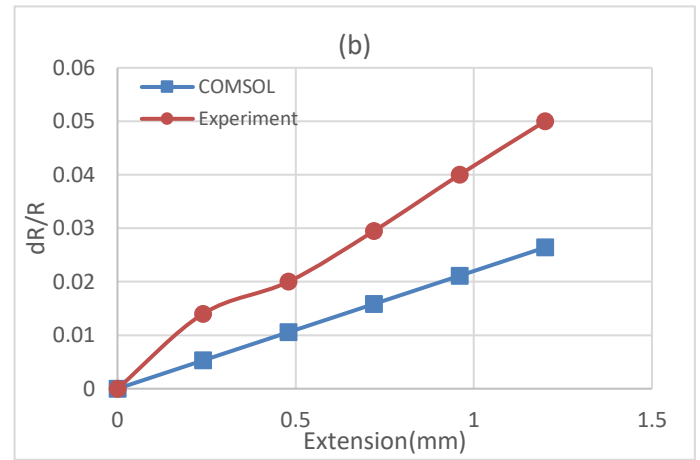
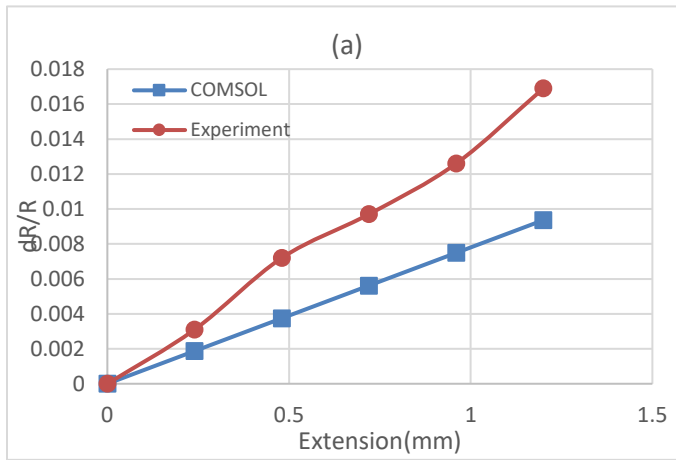


Figure 5-31 Model Validation using 6K parameters for (a) 1K Model, (b) 3K Model, (c) 6K Model, (d) 12K Model.

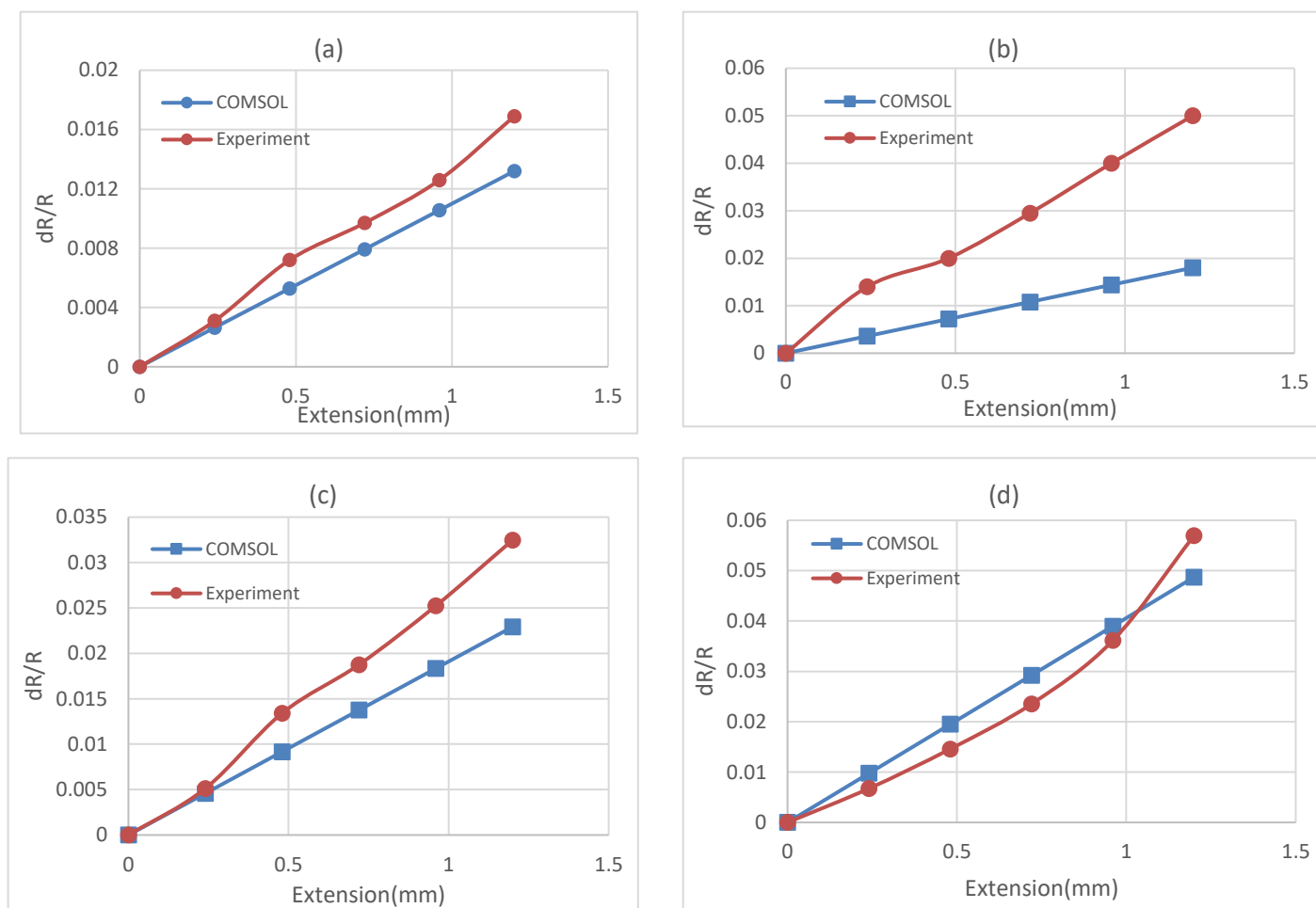


Figure 5-32 Model Validation using 12K parameters for(a) 1K Model, (b) 3K Model, (c) 6K Model, (d) 12K Model.

In Figure 5-31 and Figure 5-32, the parameters from 6K and 12K experiments were used to estimate the resistance variations for other fibers, respectively. As noted previously, 6K and 12K had a non-linear behaviour due to combination of reasons discussed such as transverse resistance and fiber breakages in the experiment. Therefore, when using the developed model, the results of 12K sensor was a linear line instead of a curved line because the model assumes linear relations. With these parameters, closer results of 1K

model are achieved but still results of 3K are inaccurate. The results show significant effect of nonlinearity, which cannot be ignored while comparing carbon fibers with different filaments.

5.3.3 Application of carbon fiber sensor model

After the development and validation of the model, the next task is to embed the sensor to a structure and observe the variation of both strain and resistance. A cantilever beam with an embedded carbon fiber sensor on its surface is modeled, as shown in Figure 5-33. The cantilever provides a good example to test the capability of the carbon fiber to detect strains as the displacements of a cantilever can be calculated using analytical formulas.

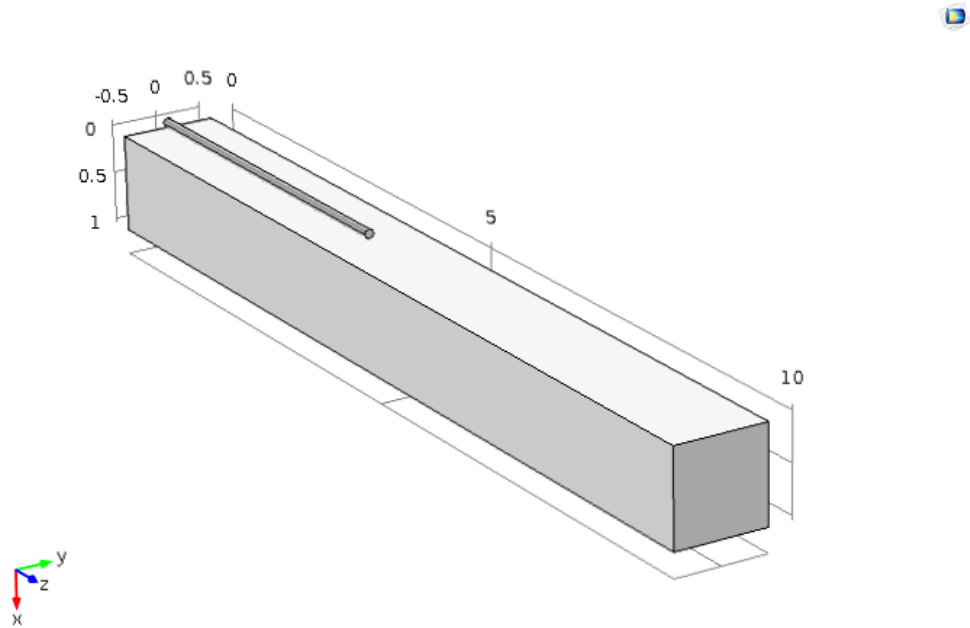


Figure 5-33 Geometric model of the cantilever and carbon fiber sensor.

The geometric model is shown in Figure 5-33. Similar to the model of the microcantilever beam presented in section 4.1, the 1K sensor is attached close to the fixed end where the maximum bending strain occurs. The displacement contours are shown in Figure 5-34. It can be observed that the maximum displacement occurs at the free end but the maximum stresses and strains are developed near the fixed end as shown in Figure 5-35 and Figure 5-36, respectively.

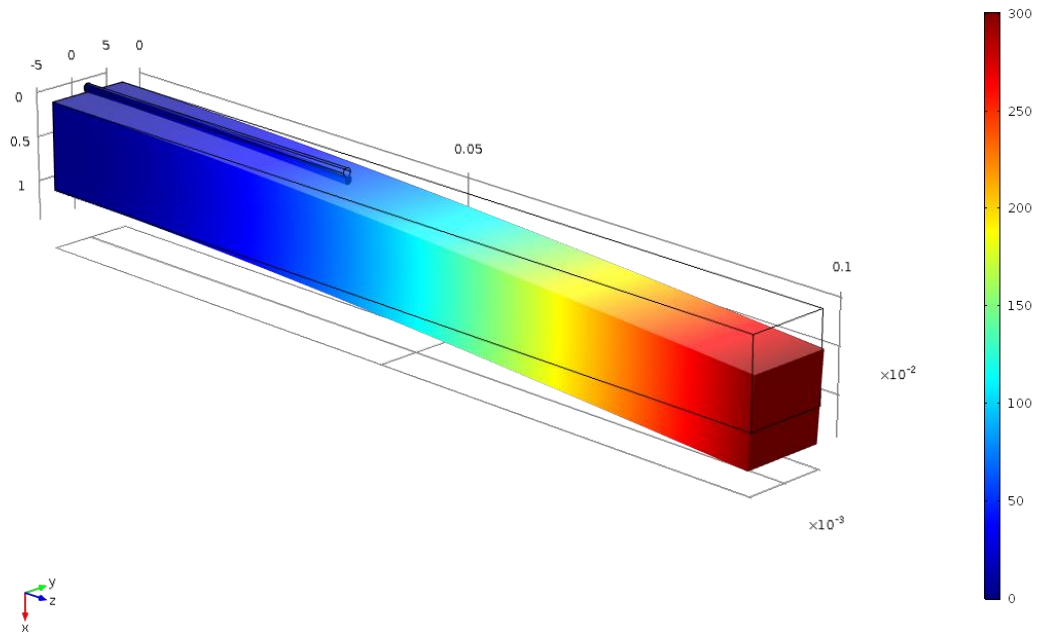


Figure 5-34 Displacement contours of the cantilever beam.

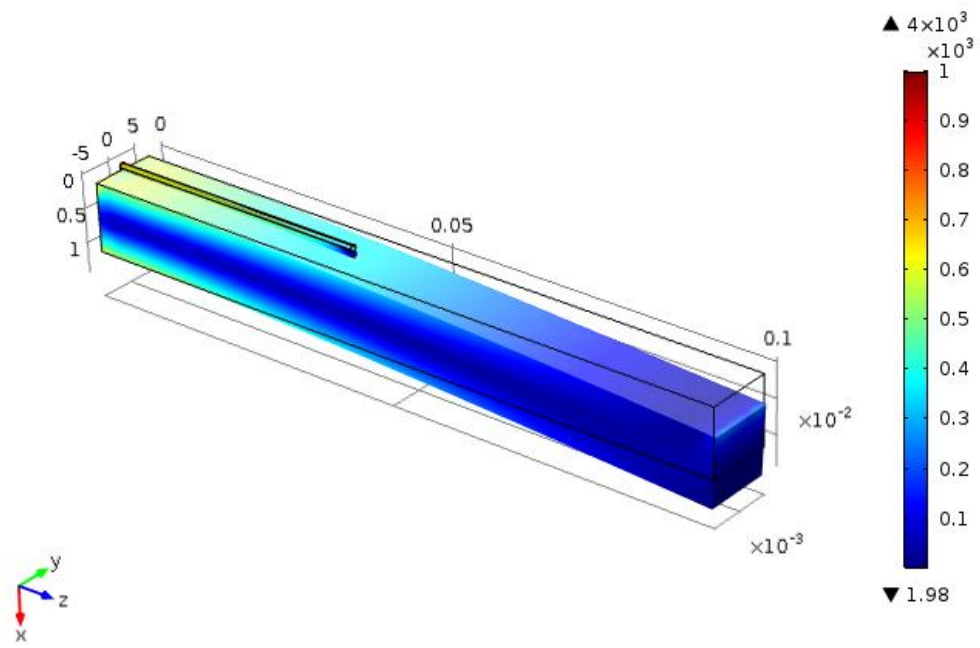


Figure 5-35 Von Mises Stresses on the cantilever beam.

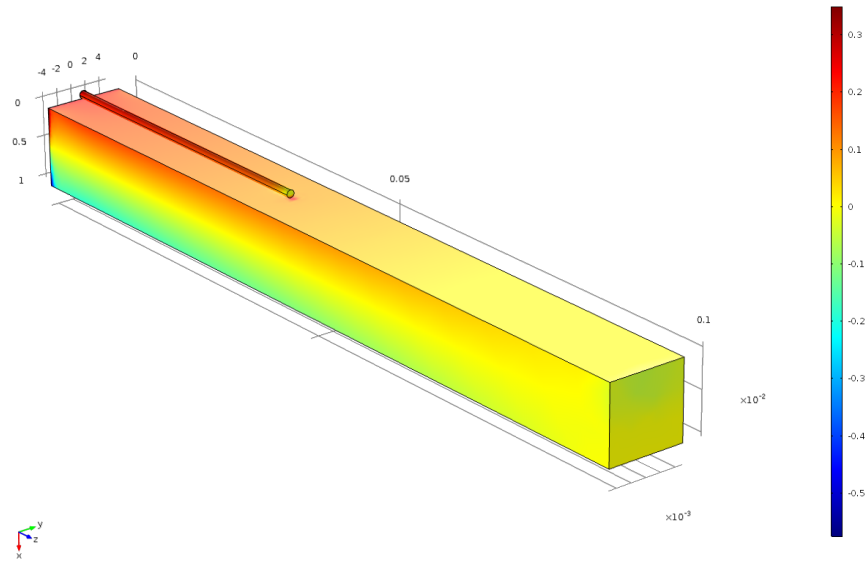


Figure 5-36 Strain distribution on the cantilever beam.

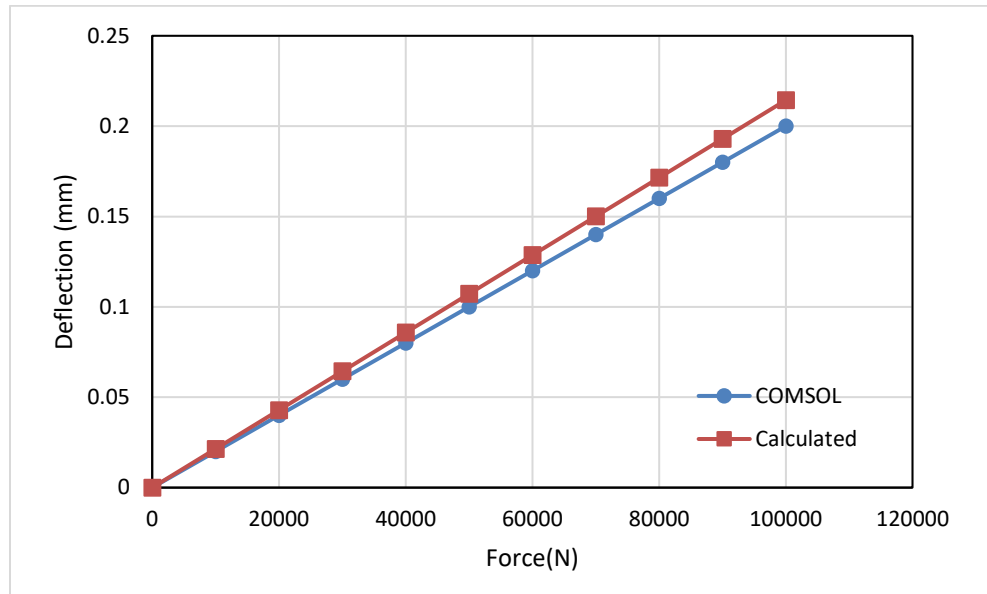


Figure 5-37 Comparison of COMSOL and analytical results of deflection of beam.

Figure 5-37 shows the results of the deflection of the cantilever beam with changing applied loads. Analytical results are also calculated and shown in the graph to compare the two deflections. It is noted that the results are very accurate and the maximum error between the two results is 3.73%. The mesh was refined until a convergence was achieved in the displacement results.

The output response of the sensor in the computational model is plotted against applied force in Figure 5-38. It is observed that the response of the carbon fiber sensor is linear and increases with the applied force. This application shows that carbon fiber sensor can detect bending in a cantilever beam when embedded on the surface.

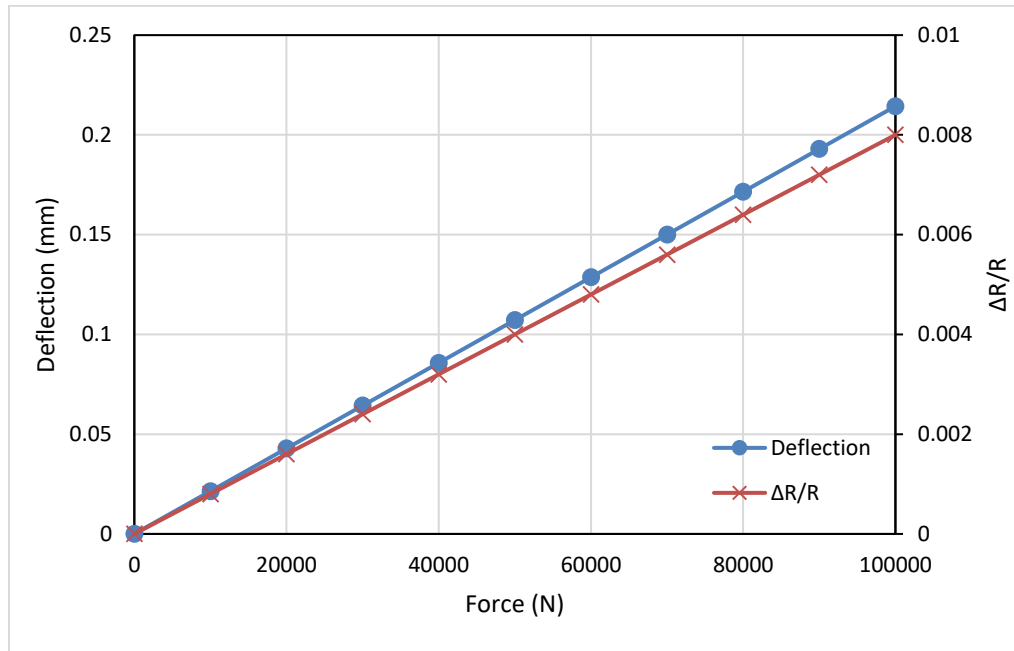


Figure 5-38 Output of the carbon fiber sensor against applied force and deflection.

5. 4 Conclusion

In conclusion, experimental and computational results were presented. Various effects of different parameters were shown and discussed. The effects shown in the experiments were the effect of diameter, length and treatment. Impact results were also discussed and it was shown that the carbon fiber sensor can detect the strains induced on the composite plates.

Computational results were also presented in this chapter. Parametric study was performed and the results were discussed. Then computational model of the carbon fiber sensor was also developed and presented. The model was calibrated using the experimental results so that results as agree with the experimental ones. This model was then validated

by varying the lengths and results were plotted with the experimental ones. The results obtained were close and agree with a fair degree of precision. A parametric study was then performed to see the response of different fibers when different piezoresistive coefficients are used. It was found that 1K and 3K's results can be fairly estimated but 6K and 12K cannot be estimated accurately. The reason being the transverse resistance between the fibers and the fiber breakage that occurs in the experiments. A FEA model of an application of a carbon fiber sensor was made. The model showed a carbon fiber sensor embedded on a cantilever beam.

CHAPTER 6

CONCLUSIONS AND RECOMMENDATIONS

6.1 Conclusions

Both experimental and numerical studies have been carried out to thoroughly understand the piezoresistivity of carbon fiber sensors. One application of carbon fiber sensor was also carried out where the sensor is used to measure strain due to low velocity impact.

Carbon fiber sensors were examined experimentally and their piezoresistivity was characterized. Relation between changes in resistance with applied strains was obtained. A parametric study was performed in which some parameters that affect the performance of the sensors were varied and the behavior of the sensor was studied to observe any change.

The results of the experiments showed that if the number of fibers are increased, hence diameter is increased, the performance of the sensor generally decreased for 6K and 12K samples with 12K sample displaying obvious non-linear behavior. Carbon fiber samples of 1K displayed the least change in resistance and 3K sample showed the largest change in resistance in the low strain level.

The study of change in length was carried out on 1K, 3K and 6K samples. Three different lengths were selected: 4 cm, 8 cm and 12 cm. It was found that sensors with shorter lengths performed better. This is because shorter lengths mean less initial resistance of the sensor which will increase the change of resistance over initial resistance.

Final experiments in the parametric study were performed to study the effect of epoxy treatment of the carbon fiber sensors. In the fabrication process, the epoxy resin is applied to the sensors to hold the fibers together. The fibers are then heat-treated for 90 minutes at 180°C in order to cure the epoxy resin. The mixture uses 5-parts epoxy resin and 1-part hardener. For this study, three different mixtures were used while all other parameters were the same. It was found that there was no significant change in the behavior of the fibers. This can be explained by the fact that carbon fiber of the composite are responsible for the tensile properties of the composite and the function of the matrix is to hold the fibers together. Therefore, it is expected that the epoxy treatment of the carbon fiber does not affect its tensile properties as the study shows.

An application of the carbon fiber sensor is its use in structures to detect damage. Therefore, impact tests were carried out on composite plates in which the carbon fiber sensors were embedded. Experiments were carried out with different impact energies and the results show that carbon fiber sensor can successfully predict the damage based on the resulting strains developed in the composite plate. Hence, carbon fiber sensors can be used in structural health monitoring of composite materials.

Computational study was also carried out in which electrical and structural mechanics modules were coupled to understand piezoresistivity in carbon fibers. The model was developed using FEA package ANSYS in which geometrical characterization of a microcantilever beam was carried out. The microcantilever beam was embedded with piezoresistors which detect changes in strains when the microbeam is disturbed. The length and width of the microbeam was varied as well as the length of the embedded piezoresistors. It was observed that the thickness of the microcantilever beam caused the most change in results.

Carbon fiber sensor's model was created in COMSOL. The model was calibrated using the data obtained from the experiments and it was shown that both the computational and experimental results were close. A parametric study was performed to understand the effects of piezoresistive coefficients on different fibers. Finally, a computational model of an application of a carbon fiber sensor was done. A cantilever beam was considered and the carbon fiber sensor was placed near the fixed end. Various forces were applied and it was shown that the sensor could detect the changes in strains in the beam.

6.2 Recommendations

This work has potential for further research on the behavior of the carbon fiber sensors and their applications. Some of the suggested future work can be as follows:

- To study the effect of temperature on the performance of the carbon fiber sensors as studies have shown that temperature affects the performance of these sensors.

- Carry out experiments with long carbon fiber sensors with lengths up to 100 cm which can be used in pipes and bridges as shown in literature.
- To study the damage detection capabilities of the sensor when embedded inside a composite structure.
- Study the performance of carbon fiber sensors on composite pipes.
- To explore further applications of carbon fiber sensors in structural health monitoring in airplanes, building and bridges, etc.
- Study behavior of carbon fiber sensors in real working conditions such as pipes with flowing liquid inside to observe any effect of flowing materials on the sensors performance.
- Test wireless communications of sensor networks when used in big scale applications.
- Better estimation of 6K and 12K behaviour using computational model of carbon fiber sensor.

REFERENCES

- [1] A. K. Kaw, *Mechanics of Composite Materials*. CRC press, 2006.
- [2] N. Hu, *Composites and Their Applications*. Intech, 2012.
- [3] R. Smith, “Composite Defects and Their Detection,” *Mater. Sci. Eng.*, vol. III, 1997.
- [4] Varvani-Farahani A. and T. H. Topper, “<http://www.ryerson.ca/~avarvani/Mechanism.htm>.”
- [5] A. Chib, “Parametric study of low velocity impact analysis on composite tubes,” M.S. thesis, Dept. Mech., University of Pune, India, 2006.
- [6] S. Abrate, *Impact on composite structures*. Cambridge University Press, 1998.
- [7] H. Sohn, C. R. Farrar, F. M. Hemez, D. D. Shunk, D. W. Stinemates, B. R. Nadler, and J. J. Czarnecki, “A Review of Structural Health Monitoring Literature : 1996 – 2001,” pp. 1996–2001, 2004.
- [8] S. Takeda, S. Minakuchi, Y. Okabe, and N. Takeda, “Delamination monitoring of laminated composites subjected to low-velocity impact using small-diameter FBG sensors,” *Compos. Part A Appl. Sci. Manuf.*, vol. 36, no. 7, pp. 903–908, 2005.
- [9] M. a. Hamstad, “A review: Acoustic emission, a tool for composite-materials studies,” *Exp. Mech.*, vol. 26, no. 1, pp. 7–13, 1986.
- [10] M. Lin and F.-K. Chang, “Composite structures with built-in diagnostics,” *Mater. Today*, vol. 2, no. 2, pp. 18–22, 1999.
- [11] M. F. Anderson, “Parametric investigation of strain gauges in structural damage

- detection,” M.S. thesis, Dept. Civil Eng., University of Iowa, IA, 2013.
- [12] M. Santos, F. Luis, B. Peeters, J. Lau, W. Desmet, and L. C. S. Goes, “The use of strain gauges in vibration-based damage detection,” *J. Phys. Conf. Ser.*, vol. 628, p. 12119, 2015.
 - [13] V. Giurgiutiu, *Structural Health Monitoring with Piezoelectric Wafer Active Sensors*. 2008.
 - [14] B. L. and V Giurgiutiu, “Modeling and testing of PZT and PVDF piezoelectric wafer active sensors,” *Smart Mater. Struct.*, 2013.
 - [15] S. Vashist, “A review of microcantilevers for sensing applications,” *J. Nanotechnol.*, vol. 3, no. June, pp. 1–15, 2007.
 - [16] L. Cao, T. S. Kim, S. C. Mantell, and D. L. Polla, “Simulation and fabrication of piezoresistive membrane type MEMS strain sensors,” *Sensors Actuators, A Phys.*, vol. 80, no. 3, pp. 273–279, 2000.
 - [17] D Huston, *Structural sensing, health monitoring, and performance evaluation*. CRC press, 2011.
 - [18] H. N. Li, D. S. Li, and G. B. Song, “Recent applications of fiber optic sensors to health monitoring in civil engineering,” *Eng. Struct.*, vol. 26, no. 11, pp. 1647–1657, 2004.
 - [19] Seth S. Kessler, S. M. Spearing, and C. Soutis, “Structural Health Monitoring in Composite Materials Using Lamb Wave Methods Seth S . Kessler ,” *Technol. Lab. Adv. Compos. Dep. Aeronaut. Astronaut. MIT*, 2001.
 - [20] L. Mescia and F. Prudenizano, “Advances on Optical Fiber Sensors,” *Fibers*, vol. 2,

no. 1, pp. 1–23, 2013.

- [21] Y. Xu, P. Lu, L. Chen, and X. Bao, “Recent Developments in Micro-Structured Fiber Optic Sensors,” *Fibers*, vol. 5, no. 1, p. 3, 2017.
- [22] Y. J. Rao and Z. L. Ran, “Optic fiber sensors fabricated by laser-micromachining,” *Opt. Fiber Technol.*, vol. 19, no. 6 PART B, pp. 808–821, 2013.
- [23] M. Ramakrishnan, G. Rajan, Y. Semenova, and G. Farrell, “Overview of Fiber Optic Sensor Technologies for Strain/Temperature Sensing Applications in Composite Materials,” *Sensors (Basel)*, vol. 16, no. 1, p. 99, 2015.
- [24] M. Valinejadshoubi, A. Bagchi, and O. Moselhi, “Structural Health Monitoring of Buildings and Infrastructure,” *J. civil, Environ. Struct. Constr. Archit. Eng.*, vol. 10, no. 6, pp. 694–701, 2016.
- [25] J. Wang, H.-J. Su, C.-I. Hsu, and Y.-C. Su, “Composite Piezoelectric Rubber Band for Energy Harvesting from Breathing and Limb Motion,” *J. Phys. Conf. Ser.*, vol. 557, p. 12022, 2014.
- [26] M. C. Koecher, J. H. Pande, S. Merkley, S. Henderson, D. T. Fullwood, and A. E. Bowden, “Piezoresistive in-situ strain sensing of composite laminate structures,” *Compos. Part B Eng.*, vol. 69, pp. 534–541, 2015.
- [27] L. M. Castano and A. B. Flatau, “Smart fabric sensors and e-textile technologies: a review,” *Smart Mater. Struct.*, vol. 23, no. 5, p. 53001, 2014.
- [28] X. Wang and D. D. L. Chung, “Continuous carbon fiber epoxy-matrix composite,” *Smart Mater Structure*, vol. 5, p. 796, 1996.
- [29] X. Wang and D. D. L. Chung, “Short-carbon-fiber-reinforced epoxy as a

- piezoresistive strain sensor,” *Smart Mater. Struct.*, vol. 4, no. 4, pp. 363–367, 1995.
- [30] X. Wang, X. Fu, and D. D. L. Chung, “Strain sensing using carbon fiber,” *Journal of materials research*, vol. 14, no. No 3. pp. 790–802, 1997.
- [31] S. Blazewicz, B. Patalita, and P. Touzain, “Study of piezoresistance effect in carbon fibers,” *Carbon N. Y.*, vol. 35, no. 10–11, pp. 1613–1618, 1997.
- [32] H. Huang, C. Yang, and Z. Wu, “Electrical sensing properties of carbon fiber reinforced plastic strips for detecting low-level strains,” *Smart Mater. Struct.*, vol. 21, no. 3, p. 35013, 2012.
- [33] D. D. L. Chung, “Processing-structure-property relationships of continuous carbon fiber polymer-matrix composites,” *Mater. Sci. Eng. R Reports*, vol. 113, pp. 1–29, 2017.
- [34] A. Todoroki, M. Ueda, and Y. Hirano, “Strain and Damage Monitoring of CFRP Laminates by Means of Electrical Resistance Measurement,” *J. Solid Mech. Mater. Eng.*, vol. 1, no. 8, pp. 947–974, 2007.
- [35] K. Schulte and C. Baron, “Load and Failure Analyses of CFRP Laminates by Means of Electrical Resistivity Measurements,” vol. 36, pp. 63–76, 1989.
- [36] N. Muto, H. Yanagida, T. Nakatsuji, M. Sugita, and Y. Ohtsuka, “Preventing Fatal Fractures in Carbon-Fiber–Glass-Fiber-Reinforced Plastic Composites by Monitoring Change in Electrical Resistance,” *J. Am. Ceram. Soc.*, 1993.
- [37] A. Kaddour, F. Al-Salehi, S. Al-Hassani, and M. Hinton, “Electrical resistance measurement technique for detecting failure in CFRP materials at high strain rates,” *Compos. Sci. Technol.*, vol. 51, pp. 377–385, 1994.

- [38] X. Xu, G. Liu, X. Gao, and P. Fang, “Correlation of change in electrical resistance with strain of carbon fiber-reinforced plastic in tension,” *J. Appl. Polym. Sci.*, vol. 60, pp. 1595–1599, 1996.
- [39] S. Wen, S. Wang, and D. D. L. Chung, “Piezoresistivity in continuous carbon fiber polymer-matrix composite.” 2000.
- [40] N. Angelidis, C. Y. Wei, and P. E. Irving, “The electrical resistance response of continuous carbon fibre composite laminates to mechanical strain,” vol. 35, pp. 1135–1147, 2004.
- [41] A. Todoroki and J. Yoshida, “Electrical Resistance Change of Unidirectional CFRP Due to Applied Load,” *JSME Int. J. Ser. A*, vol. 47, no. 3, pp. 357–364, 2004.
- [42] A. Horoschenkoff, T. Mueller, and A. Kroell, “On the Characterization of the Piezoresistivity of Embedded Carbon Fibres,” 2012.
- [43] A. Horoschenkoff and C. Christner, “Carbon Fibre Sensor: Theory and Application,” *In-Tech*, pp. 1–20, 2012.
- [44] A. Horoschenkoff, T. Müller, C. Strössner, and K. Farmbauer, “Use of Carbon-Fibre Sensors To Determine the Deflection of Composite Beams,” pp. 0–3, 2011.
- [45] A. Horoschenkoff, H. Rapp, and T. Muller, “Carbon Fiber Sensor for Crack Monitoring of Composite Materials,” pp. 4193–4204, 2013.
- [46] Y. Goldfeld, O. Rabinovitch, B. Fishbain, T. Quadflieg, and T. Gries, “Sensory carbon fiber based textile-reinforced concrete for smart structures,” *J. Intell. Mater. Syst. Struct.*, 2015.
- [47] T. Matzies, C. Christner, A. Horoschenkoff, and H. Rapp, “Carbon fibre sensor

- meshes: Simulation and experiment,” *Comput. Mater. Sci.*, vol. 64, pp. 122–125, 2012.
- [48] L. Hou and S. A. Hayes, “A resistance-based damage location sensor for carbon-fibre composites,” *Smart Mater. Struct.*, vol. 11, no. 6, pp. 966–969, 2002.
 - [49] C. Q. Yang, Z. S. Wu, and H. Huang, “Electrical properties of different types of carbon fiber reinforced plastics (CFRPs) and hybrid CFRPs,” *Carbon N. Y.*, vol. 45, no. 15, pp. 3027–3035, 2007.
 - [50] H. Huang and Z. S. Wu, “Static and dynamic measurement of low-level strains with carbon fibers,” *Sensors Actuators A Phys.*, vol. 183, pp. 140–147, 2012.
 - [51] M. A. Saifeldeen, N. Fouad, H. Huang, and Z. Wu, “Advancement of long-gauge carbon fiber line sensors for strain measurements in structures,” *J. Intell. Mater. Syst. Struct.*, 2016.
 - [52] A. Todoroki, Y. Samejima, Y. Hirano, and R. Matsuzaki, “Piezoresistivity of unidirectional carbon/epoxy composites for multiaxial loading,” *Compos. Sci. Technol.*, vol. 69, no. 11–12, pp. 1841–1846, 2009.
 - [53] E. Häntzsche, A. Matthes, A. Nocke, and C. Cherif, “Characteristics of carbon fiber based strain sensors for structural-health monitoring of textile-reinforced thermoplastic composites depending on the textile technological integration process,” *Sensors Actuators A Phys.*, vol. 203, pp. 189–203, 2013.
 - [54] Instron, “3360 Series - Dual Column Tabletop Models.” pp. 1–3, 2010.
 - [55] Y. Zhou, D. Jiang, and Y. Xia, “Tensile mechanical behavior of T300 and M40J fiber bundles at different strain rate,” *J. Mater. Sci.*, vol. 36, no. 4, pp. 919–922,

2001.

- [56] R. A. Rahim, B. Bais, and B. Y. Majlis, “Design and analysis of MEMS piezoresistive SiO₂ cantilever-based sensor with stress concentration region for biosensing applications,” *IEEE Int. Conf. Semicond. Electron. Proceedings, ICSE*, pp. 211–215, 2008.

VITAE

Name: Mohammad Abdullah Siddiqui

Date of Birth: July 29, 1991

Present Address: KFUPM P. O. Box 8642, King Fahd University of Petroleum and Mineral, Dhahran, 31261, Saudi Arabia

Permanent Address: KFUPM P. O. Box 8642, King Fahd University of Petroleum and Mineral, Dhahran, 31261, Saudi Arabia

Email Address: masiddiqui@kfupm.edu.sa
abdullahsiddiqui12@gmail.com

Educational Qualification: **M.S (Mechanical Engineering)**
December, 2016
King Fahd University of Petroleum & Minerals,
Dhahran, Saudi Arabia.

B.E. (Mechatronics Engineering)
June, 2013
Air University
Islamabad, Pakistan.